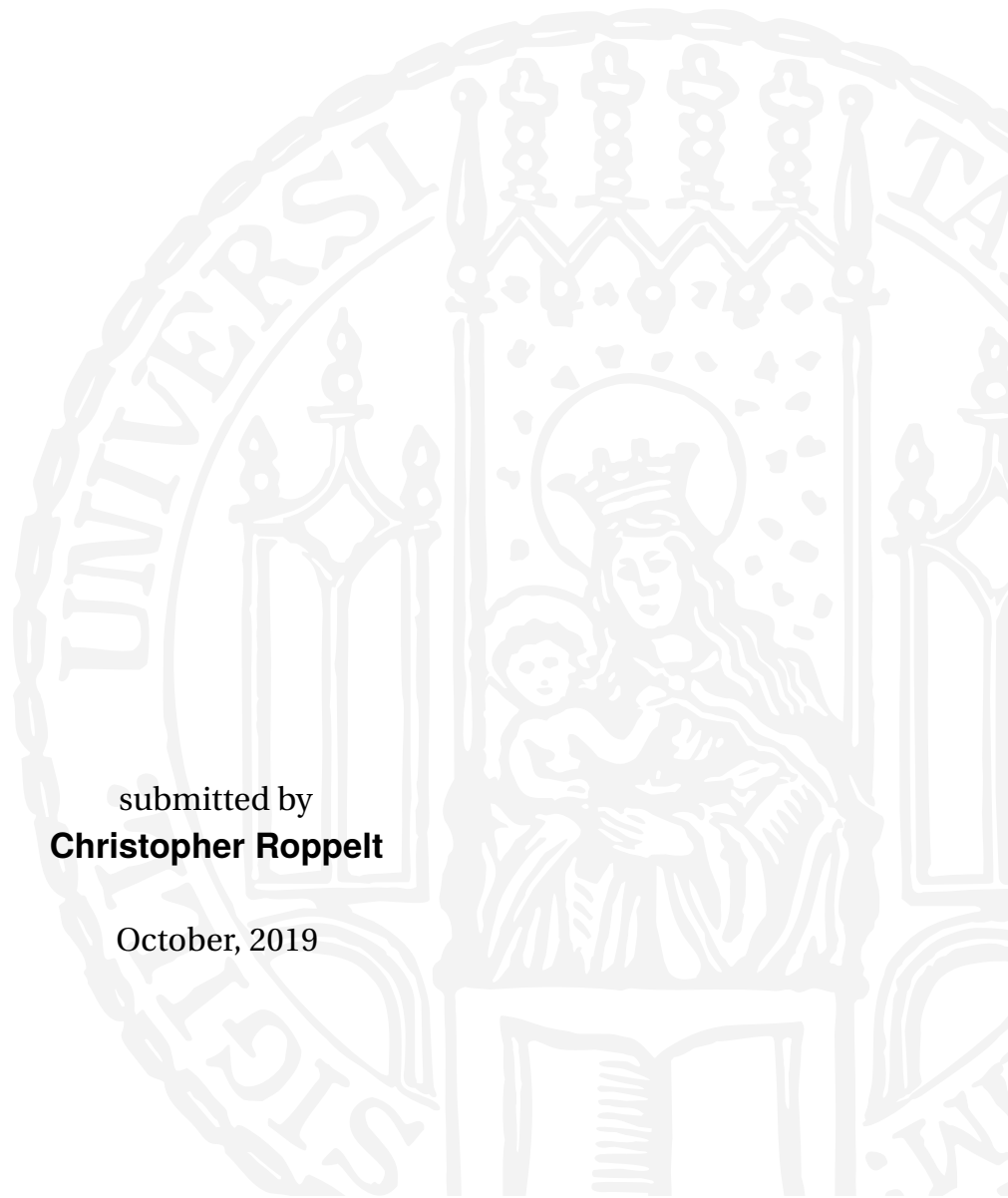


Maps and Memories of Space in the Human Brain

Dissertation at the
Graduate School of Systemic Neurosciences
Ludwig-Maximilians-Universität München

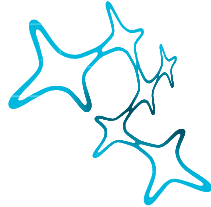
submitted by
Christopher Roppelt

October, 2019



Maps and Memories of Space in the Human Brain

Dissertation der
Graduate School of Systemic Neurosciences der
Ludwig-Maximilians-Universität München



Graduate School of
Systemic Neurosciences
LMU Munich



eingereicht von
Christopher Roppelt

München, im Oktober 2019

Christopher Roppelt

Maps and Memories of Space in the Human Brain

Date of Submission: 25th of October 2019

Date of Defense: 15th of July 2020

Supervisor and 1st Reviewer:

Dr. Virginia L. Flanagin

Department of Neurology, Ludwig-Maximilians-Universität München

2nd Reviewer: **Prof. Andreas V. Herz**

3rd Reviewer: **Prof. Oliver Baumann**

Abstract

Mammalian navigation is mostly studied in rodents and humans. Due to ethical and methodological constraints, rodent research so far primarily targeted the neurophysiological mechanisms of navigation, while navigation studies in humans predominantly focused on navigational behavior and the cognitive processes involved in it. Although basic mechanisms of navigation seem well preserved across rodents and humans in general, human and rodent navigation also differ substantially in several aspects and it is not obvious how particular findings translate across both species. As a consequence, for many aspects of navigation, we do not know how processes on the cognitive level can be attributed to those on the cellular level, and, eventually, how particular navigation behavior can be causally related to neural activity. This knowledge gap is addressed in this thesis with two studies that extend our understanding of how findings from rodents and humans translate across both species. To this end, a framework was developed that combines human navigation in landmark-sparse virtual environments that resemble the open-field setups typically used to study spatially tuned neurons in rodents. Applying this framework, the first study presented in this thesis separates passive and active components during navigation, and investigates how varying navigational and spatial memory demands impact participants' brain activity. The results suggest that, first, certain brain regions primarily known for perception of static scenes are recruited during passive navigation, and also contribute information processing specifically relevant for active navigation; and that, second, the anterior medial hippocampus provides a coherent spatial representation of the current environment that is dependent on spatial memory. Using a similar setup, the second study investigates participants' spatial representation in more detail. The results show that, first, a model inspired by electrophysiological findings in rodents that explains location memory as a function of proximity to the environment's boundaries generally matches participants' behavior in a similar open-field environment; that, second, the model's explanatory power may be further improved when, in addition to the precision, also the accuracy of participants' location memory is considered; and that, finally, in a quadratic open-field environment, the diagonals also impact participant's spatial orientation and location memory. The findings reported in this thesis demonstrate that the framework applied in both studies allows for a detailed investigation of human navigation behavior, and the cognitive processes associated with it. It furthermore increases comparability of findings between human and rodent navigation, and may eventually help to better understand how neurophysiological processes are transformed into navigation behavior.

Contents

1 Introduction	1
1.1 Evidence from rodents	2
1.1.1 Place cells	2
1.1.2 Head-direction cells	4
1.1.3 Grid cells	5
1.1.4 Boundary-modulated cells	6
1.1.5 Other types of neurons supporting navigation	7
1.2 Evidence from humans	8
1.2.1 Memory and the hippocampus	8
1.2.2 Theories of hippocampal function	9
1.2.3 Navigation beyond the hippocampal system	11
1.3 Aim of this thesis	13
1.4 References	15
2 The Impact of Varying Navigational and Spatial Memory Demands on Human Brain Activity during Spatial Exploration	25
3 Human Spatial Accuracy in an Open-Field Virtual Environment	65
4 General Discussion	93
4.1 Human scene-selective regions contribute to active navigation	94
4.2 The human hippocampus' role in spatial memory	97
4.3 Spatial memory in an open-field environment	98
4.4 Concluding remarks	102
4.5 References	104
List of publications	109
Curriculum Vitae	111
Eidesstattliche Versicherung/Affidavit	113
Author contributions	115

Introduction

“How do we know where we are? How can we find the way from one place to another? And how can we store this information in such a way that we can immediately find the way the next time we trace the same path? This year’s Nobel Laureates have discovered a positioning system, an ‘inner GPS’ in the brain that makes it possible to orient ourselves in space, demonstrating a cellular basis for higher cognitive function.”¹

With these sentences opens the press release issued on the 2014 Nobel Prize in Physiology or Medicine that has been awarded to John O’Keefe, May-Britt Moser, and Edvard I. Moser. The three laureates were instrumental in the discovery and characterization of two types of neurons in the rat brain which show very distinct activation patterns dependent on a rat’s location in its environment. In fact, it has been shown that a rat’s location anywhere in its environment can be decoded based on an ensemble of these neurons, and, moreover, that these cells also provide a robust distance measure across space (Fiete et al., 2008; Keinath et al., 2014; Stemmler et al., 2015; Wilson and McNaughton, 1993). Both are crucial features relevant for most forms of effective navigation, an essential ability common to all motile animals.² It is thus not surprising that the discovery of these neurons in the rat brain has inspired researchers across all fields of neuroscience who, together, contributed greatly to our understanding of the mammalian brain in general, and the neural mechanics underlying navigation in particular.

Yet, two important limitations apply. First, these neurons were discovered, and still are predominantly studied in the rat brain. Though there is evidence that similar neurons also exist in the human brain (Doeller et al., 2010; Ekstrom et al., 2003; Jacobs et al., 2013; Miller et al., 2013; Nadasdy et al., 2017), it is not clear to which extent these neurons share similar firing properties across species, and thus, how the neural mechanics underlying the processing of spatial information by these cells, when studied in rats, ultimately translate to humans. Second, we already know many details about the striking activity patterns of these neurons, and meanwhile also several other types of spatially tuned neurons have been recorded in the rat brain that, together, provide all sorts of spatial information processing (see Chpt. 1.1). But we are only beginning to understand how all these types of neurons interact with each other. How these neurons’ firing patterns relate to cognitive processes, shape an internal representation of space, and eventually enable behavior such as effective navigation through the environment, remain unresolved questions.

¹Source: https://www.nobelprize.org/nobel_prizes/medicine/laureates/2014/press.html

²Note that several different definitions of navigation have been proposed, and further, that not every form of navigation necessarily requires a distance measure or even knowledge of oneself in the environment (for a review see, e.g., Franz and Mallot, 2000).

These two issues are interconnected. Most of what we know about the firing patterns of spatially tuned neurons stems from electrophysiological recordings in rodents, particularly in rats. Such recordings allow to analyze the activity of single cells with high temporal resolution, but are currently restricted to few parallel recording sites and are not well suited to understand the interaction of different brain regions during a particular navigation task (Buzsáki, 2004). This is instead the domain of non-invasive recording methods such as functional magnetic resonance imaging (fMRI) which, for ethical considerations, are primarily used when studying brain activity during navigation in humans. These techniques, on the other hand, provide only indirect and spatially coarse information about the underlying neural activity. Electrophysiological recordings that reveal neural firing properties of spatially tuned neurons in humans are scarce and currently limited to studies in hospitalized epilepsy patients (see Jacobs and Kahana, 2010). In other words: our knowledge of the neural mechanisms in service of navigation is predominantly based on evidence from rodents, whereas our understanding of the cognitive processes involved in different aspects of navigation stems primarily from investigations in humans. How neural and cognitive processes relate to each other, and lead to navigation behavior is therefore often not clear. Bridging this gap is challenging due to the different methodological and ethical constraints that apply to human and rodent research.

The studies presented in this thesis focus on this gap and aim to bring findings from rodent and human navigation literature closer together in order to better understand what we can learn about navigation from both species. In the following sections of this chapter, I first summarize the most relevant properties of spatially modulated neurons in the rat brain and how they are believed to interact in the service of navigation (Chpt. 1.1). I then summarize the findings from humans that have helped establishing our understanding of cognitive processes and brain regions involved in navigation behavior (Chpt. 1.2). Finally, I outline gaps in our understanding of the mechanisms that enable successful navigation and how this motivates the questions addressed in this thesis (Chpt. 1.3).

1.1 Evidence from rodents

The following sections introduce the most well-investigated types of neurons in the rodent brain that, together, are commonly believed to form the basis of a mental positioning system – the ‘inner GPS’. The sections focus on the neurons’ features and firing patterns that suggest a role for these cells in spatial information processing and, eventually, the mechanisms underlying successful navigation.

1.1.1 Place cells

The first of the two types of neurons for which the 2014 Nobel Prize in Physiology or Medicine was awarded to John O’Keefe are the so-called ‘place cells’. These cells are pyramidal neurons that were first reported in the rat hippocampus by John O’Keefe and

John Dostrovsky in 1971 (O'Keefe and Dostrovsky, 1971). Their name derives from their characteristic firing behavior: a particular hippocampal place cell tends to fire only when the rat is in a specific location of its environment: its firing field, later termed 'place field' (O'Keefe and Nadel, 1978). Note that neurons resembling certain properties of hippocampal place cells have meanwhile also been recorded outside the hippocampus (see, e.g., Mao et al., 2017), but in this thesis, the term 'place cell' refers only to hippocampal place cells.

In open-field environments³, place cells fire independent of an animal's orientation in space, and typically not outside their place field (O'Keefe, 1976). What makes it so tempting to compare these neurons to an 'inner GPS' is the observation that a rat's position anywhere in its environment can be accurately predicted from a sufficiently large ensemble of simultaneously recorded place cells (Keinath et al., 2014; Wilson and McNaughton, 1993). Furthermore, the representation of space coded by a population of place cells is persistent across time: in a constant environment, most place cells' firing fields are usually stable for days or weeks (Muller et al., 1987; Thompson and Best, 1990).

When a rat is moved from one environment to another, place cells change the location (and firing rates) of their place fields in a manner seemingly unpredictable from their previous configuration, a phenomenon termed 'global remapping' (Leutgeb, 2005). This effect can be differentiated from 'rate remapping' where place cells change their firing rate, but not their firing field, in response to subtle changes in the environment (Leutgeb, 2005; Muller et al., 1987), and it raises the question how place cells are anchored to a particular environment.

In a typical recording setup, where the rat is placed inside an empty cylindrical apparatus that has a cue card occupying 100° of arc attached on the inside, place fields rotated accordingly when the cue card was rotated (Muller and Kubie, 1987). This suggests that salient environmental cues anchor the place cells' topographic representation, probably much like what one would expect from a neural substrate of an 'inner GPS'. However, it has been also been shown that place cells can encode the same environment differently, depending on a rat's previous experience in that environment (e.g., Quirk et al., 1990), or its future goal (e.g., Ainge et al., 2007; Markus et al., 1995; Wood et al., 2000). Furthermore, during resting periods, place cells have been shown not to encode the animal's current location, but to 'preplay' sequences of place fields along the animal's future trajectory (Dragoi and Tonegawa, 2011).

Taken together, hippocampal place cells, when recorded as a sufficiently large population, show characteristics expected from a topographic map of an animal's environment, thus

³This is different on linear tracks such as an arm of a maze, where rat place cells have been recorded that express place fields only when the animal is running along the track in one direction but not the other. Thus, on linear tracks, place cells can show unidirectional firing behavior that differs from the omnidirectional firing pattern of place cells typically observed in open-field environments (McNaughton et al., 1983; Muller et al., 1994).

in fact akin to an ‘inner GPS’. Moreover, there is also ample evidence for a role of place cells beyond just mapping physical space (for a recent review, see [Epstein et al., 2017](#)).

1.1.2 Head-direction cells

For successful navigation it is important to know one’s own position in space, as encoded by place cells. But it also requires to determine oneself’s orientation in space. This information is commonly considered to be provided by a type of neurons termed ‘head-direction cells’.

Head-direction cells were first reported in the mid-eighties, and described in detail in [Taube et al. \(1990a,b\)](#) (for a detailed review see [Taube, 2007](#)). Their name derives from their characteristic firing behavior which is a function of an animal’s directional heading in the horizontal plane. Importantly, head-direction cells’ firing properties are independent of an animal’s position in space or its current behavior, and therefore are believed to be a pure reflection of the animal’s perceived orientation in the environment.

Head-direction cells are found in several brain areas, most of which are considered structures part of the classic Papez circuit. These regions include the lateral mammillary nucleus, thalamus, presubiculum, postsubiculum, entorhinal cortex, and retrosplenial cortex ([Grieves and Jeffery \(2017\)](#); for reviews see [Yoder et al. \(2011a,b\)](#)).

Each head-direction cell has a ‘preferred firing direction’ that indicates the heading direction at which it fires maximally. The range around a cell’s preferred firing direction at which it fires above baseline has been termed the cell’s ‘directional firing range’ and is approx. 90 degrees on average; outside this range, the cell’s firing rate is at or near zero ([Taube, 2007](#)). Head-direction cells’ preferred firing directions are distributed evenly around angular space such that all heading directions are represented within a population ([Taube et al., 1990b](#)). Neural networks downstream of head-direction cells therefore can, theoretically, precisely read out an animal’s perceived orientation in space ([Moser et al., 2017](#)).

What determines the head-direction cell system’s perceived orientation? Similar to place cells, head-direction cells’ firing is anchored to the environment. It has been shown that environmental cues such as landmarks, be they stable over time or not, act as external reference points to which the head-direction cell system is aligned. When such cues are rotated or the animal is moved between environments, head-direction cells’ preferred firing directions rotate or realign accordingly and coherently (reviewed in [Grieves and Jeffery, 2017](#)).

Head-direction cells can thus be thought of as a compass: a sufficiently large population of head-direction cells encodes any possible heading direction of an animal in its environment. Yet, rather than to the Earth’s geomagnetic field, they instead depend on environmental cues.

1.1.3 Grid cells

The second of the two types of neurons for which the Nobel Prize in Physiology or Medicine was awarded in 2014 is the so-called 'grid cell'. These neurons were first described in 2004 by the group of May-Britt and Edvard Moser (who, together with John O'Keefe, share the 2014 Nobel Prize) and reported in the rat's medial entorhinal cortex (mEC), and the pre- and parasubiculum (Boccaro et al., 2010; Fyhn, 2004; Hafting et al., 2005). Evidence for their existence has since been reported also for mice (Fyhn et al., 2007), bats (Yartsev et al., 2011), and humans (Doeller et al., 2010; Jacobs et al., 2013).

Grid cells are also characterized by their firing properties. Much like a place cell, a grid cell also encodes an animal's location in the environment. But, contrary to a place cell, a grid cell has several place fields that cover the whole physical space accessible to the animal with a regular periodic hexagonal grid; the striking regularity of that grid is what gave grid cells their name. Importantly, grid cells' firing patterns are robust to changes in an animal's speed and direction of movement (Fyhn, 2004; Hafting et al., 2005; Rowland et al., 2016).

The grid expressed by a particular grid cell can be described by three parameters: wavelength (or spacing; the distance between the grid's vertices); orientation (the grid's tilting relative to an external reference line); and spatial phase (the offset in the *X* and *Y* axes of the grid's vertices relative to an external reference point). In neighboring cells, both orientation and spatial phase are maintained across differing environments (Fyhn et al., 2007; Hafting et al., 2005). It has been shown that grid cells are furthermore organized in discrete functional modules along the mEC's dorso-ventral axis. These modules are characterized by the spatial arrangement of grid cells' firing fields: grids expressed by cells in the same module all share similar orientation and wavelength. Grid cells in modules that are located towards the ventral end of the mEC tend to express grids of larger wavelengths, thus tiling the space with a more coarse resolution than grid cells in more dorsal areas of the mEC (Stensola et al., 2012).

This modular arrangement of grid scales has important implications on grid cells' potential contribution to navigation. A single grid cell provides merely an ambiguous representation of an animal's location in space. A sufficiently large population of grid cells from different modules – whose grids thus span multiple orientations and wavelengths – however, could theoretically be used to efficiently decode an animal's position in space. Fine grids in the dorsal mEC may provide precise location estimates whereas coarser grids in the dorsal mEC regions would resolve location ambiguity (Mathis et al., 2012; Stemmler et al., 2015; Wei et al., 2015). Furthermore, it has been shown that such population activity would, in theory, provide the animal with an accurate distance measure (Stemmler et al., 2015).

Grid cells' regular, speed- and direction-invariant firing patterns, together with their potential to provide a robust metric of an animal's environment, suggests they play an important role in the computations underlying self-motion calculation (Fuhs, 2006; Mc-

Naughton et al., 2006). Contrary to place cells, grid cells are therefore thought to provide a position estimation system that is independent of an animal's current environment and behavioral context, much like a universal coordinate system of space (Moser et al., 2017; Rowland et al., 2016).

1.1.4 Boundary-modulated cells

For all the spatially modulated cell types introduced so far, a significant role of environment cues or boundaries has been shown. Anchoring of head-direction cells is modulated by the position of salient visual cues in an animal's environment (Grieves and Jeffery, 2017, and see Chpt. 1.1.2). Similarly, the orientation of grid cells' firing fields has been shown to rotate with respect to landmarks in the environment (Hafting et al., 2005). For grid cells it has furthermore been shown that their firing fields are distorted depending on the proximity and geometry of an environment's boundaries (Krupic et al., 2015, 2018). Finally, place cells' place fields have been reported to become elongated or compressed relative to the displacement of a familiar environment's boundary (Lever et al., 1999; O'Keefe and Burgess, 1996).

The observation that place cells firing is modulated by an environment's boundaries has led to the suggestion that a specific type of neuron must exist that is tuned exclusively to extended spatial boundaries. Such neurons were hypothesized to fire optimally when an animal perceives a boundary at a specific allocentric direction and distance, and therefore termed 'boundary vector cells' (BVC). A particular boundary vector cell might, for instance, fire whenever the animal perceives a barrier to the north-east and approximately 20 centimeters away. According to the boundary vector cell model, place cells activity is driven by feed-forward connections from BVCs: firing fields are then expressed as the thresholded sum of few putative BVCs (Barry et al., 2006; Hartley et al., 2000).

A number of cell types have since then been reported that at least partially fit the hypothesized properties of boundary vector cells. First revealed were so-called 'border cells', found in the mEC of rats, that exclusively fire along one or more of the environment's border (Savelli et al., 2008; Solstad et al., 2008). These cells seem to fire never more than 10 centimeters away from a boundary though (Bjerknes et al., 2014). Subsequently, the existence of cells that show boundary vector cell-like firing has been demonstrated in the rat dorsal subiculum (Lever et al., 2009). Due to the hippocampal circuit's unidirectional wiring, however, it seems unlikely that these cells provide a major input to upstream hippocampal place cells (Moser et al., 2017). Furthermore, cells have been reported that show just the opposite behavior of border cells: they fire everywhere in the environment except close to a particular border (Stewart et al., 2014). Yet other cells fire close to every environmental boundary and might serve as a precursor to other types of more specific boundary-modulated neurons (Grieves and Jeffery, 2017; Jankowski and O'Mara, 2015; Weible et al., 2012). Finally, in addition to the cells described so far, even more types of neurons with even more distinct boundary-dependent firing behavior seem to exist in the brain; for a summary see Grieves and Jeffery (2017).

Several models have been suggested how firing of boundary cells might inform place and grid cell activity (e.g. Barry et al., 2006; Bicanski and Burgess, 2018; Krupic et al., 2014; Widloski and Fiete, 2014). However, which features actually define a boundary, and whether this might also differ between different types of boundary-modulated neurons is still unclear. It is also not well understood how exactly these cells interact with grid cells, place cells, and, potentially, other spatially modulated neurons (Poulter et al., 2018). However, knowing the spatial locations of boundaries in an environment intuitively appears to be a valuable information in the context of navigation, particularly for route planning and orientation in an environment (Cheng et al., 2013).

1.1.5 Other types of neurons supporting navigation

Place cells, head-direction cells, and grid cells are arguably the most prominent types of spatially tuned neurons that have been discovered so far. Yet, beyond these, there exists a variety of cell types that show all sorts of potentially navigation-relevant firing properties.

To begin with, so-called ‘object cells’ have been reported in the rodent lateral EC (Deshmukh and Knierim, 2011). These cells exhibit firing properties similar to place cells when an object is present at a particular location in the environment. In the absence of this object, however, such an object cell shows only weak spatial tuning to the environment. Object cells could potentially provide place cells with non-spatial object information of an environment (Deshmukh and Knierim, 2011).

Object cells are also an example of cells termed ‘conjunctive cells’. However, contrary to cell types described so far, conjunctive cells are *not* a specific type of spatially tuned neurons themselves. Rather, conjunctive cells are a *class* of cell types which combine several types of information and whose firing behavior therefore expresses a conjunction of the firing properties of two or more different cell types. Speed-modulated cells with conjunctive grid and head-direction properties, for instance, have been recorded in the rat presubiculum (Cacucci, 2004) and the deeper layers of the rat mEC (Sargolini et al., 2006). More recently, cells that fire as a conjunction of direction and border, and neurons that are a conjunction of direction and place have also been reported (for a review see Grieves and Jeffery, 2017). Conjunctive cells may play an important role in navigation (Kubie and Fenton, 2012; Milford et al., 2010; Sargolini et al., 2006), and a wide range of conjunctive cells is believed to exist.⁴

Finally, there are ‘time cells’ and ‘speed cells’. These two types of neurons differ from all the aforementioned ones in that they are not directly tuned to specific spatial features of an environment. Hippocampal time cells show temporally tuned firing behavior, with a particular time cell reliably indicating a distinct time point in a repeating temporal sequence, and a population of time cells showing varying temporal tuning curves in the

⁴Due to conjunction cells’ potentially complex firing patterns, currently unknown types of conjunctive cells may be hard to detect experimentally, and we might thus only know the ‘tip of the ice berg’ of conjunctive cells yet.

range of a few seconds (Kraus et al., 2013; MacDonald et al., 2011; Pastalkova et al., 2008). Time cells have been attributed a role particularly in episodic memory (MacDonald et al., 2013, 2011), but also in estimating travelled distance (Kraus et al., 2013; Poulter et al., 2018). Similar to time cells, speed cells found in the rat mEC and hippocampus could also enable calculation of travelled distance. This type of neuron is tuned to an animal's locomotion speed in a context-invariant, linear, and positive manner. That is, a speed cell's firing rate increases linearly with the animal's running speed, independent of environment, visual stimuli, or behavioral conditions (Hinman et al., 2016; Kropff et al., 2015). Several computational models assume neurons with speed cell-like firing properties required to dynamically update the grid cell signal (e.g. Couey et al., 2013; Fuhs, 2006; McNaughton et al., 2006).

1.2 Evidence from humans

The previous chapter featured a range of neurons located in rodents' hippocampal formation – comprising the hippocampus proper with its subfields (CA1, CA2, CA3), dentate gyrus, subiculum, presubiculum, parasubiculum, and entorhinal cortex – that are all characterized by their spatially modulated firing properties. A number of mechanistic models have been proposed throughout the last decades that aim to explain various aspects of spatial information processing and, eventually, effective navigation through the environment. The common centerpiece of all these models is the hippocampal system with its variety of spatially tuned cell types. Yet, while navigational processes have been the focus of hippocampal research in rodents, an entirely different field of research has long dominated the view on hippocampal function in the human literature: the hippocampus' role in autobiographical memory.

1.2.1 Memory and the hippocampus

Autobiographical memory describes “episodes recollected from an individual's life” (Williams et al., 2008, p. 22), and is considered a form of explicit memory that combines aspects of both semantic (conceptual and factual knowledge) and episodic (personal experiences at a particular time and place) memory (Tulving, 1972; Williams et al., 2008). Research on the connection between the human hippocampus and autobiographical memory was inspired by a seminal case study in the 1950s. In 1953, Henry G. Molaison – later known as patient H.M. throughout the neuroscience literature – had large parts of his hippocampus and adjacent medial temporal lobes (MTL) structures bilaterally resected in an attempt to cure his medically intractable epilepsy (Scoville and Milner, 1957)⁵. As intended, the frequency of his epileptic seizures markedly decreased. However, as an unexpected and quite severe side effect of this operation, H.M. also suffered from a persistent and profound anterograde amnesia for the rest of his life. Having recovered from the surgery, he was no longer able to recognize the hospital staff, to recollect events

⁵For a detailed post mortem examination of H.M.'s brain see Annese et al. (2014).

of his daily life, or to form any sort of semantic long-term memory (Annese et al., 2014; Corkin, 2002; Scoville and Milner, 1957). Following the bilateral MTL resection, H.M. had lost the ability to acquire episodic and semantic knowledge, hence his ability to form autobiographical memories.

The case of patient H.M. inspired decades of research on different kinds of memory processes and the hippocampal formation became the center of many theories that seek to explain the mechanisms underlying memory formation and recollection (Corkin, 2002; Squire and Zola-Morgan, 2011). In rodents, on the other hand, with the discovery of place cells, O'Keefe and Nadel's influential proposal of the hippocampus as a cognitive map (O'Keefe and Nadel, 1978), and subsequent findings of further spatially tuned neurons in close proximity to the hippocampus, the hippocampus became the centerpiece of research on spatial navigation and the processes related to it. Many attempts have been made in the last two decades to reconcile this seemingly disparate functional roles of the hippocampus in a consistent mechanistic framework of the hippocampal system (e.g. Buzsáki and Moser, 2013; Clark et al., 2019; Eichenbaum, 2017; Eichenbaum and Cohen, 2014; Ekstrom and Ranganath, 2017; Epstein et al., 2017; Maguire and Mullally, 2013; Milivojevic and Doeller, 2013; Redish, 1999; Robin, 2018; Schiller et al., 2015).

1.2.2 Theories of hippocampal function

Some researchers propose the hippocampal formation's mnemonic functions derive from its mechanisms in spatial information processing (e.g. Buzsáki and Moser, 2013; Epstein et al., 2017). Buzsáki and Moser (2013), for instance, note that semantic memory, which defines knowledge independent of a temporal context, functions much like an allocentric map that also provides information independent of the context in which it was acquired. Episodic memory, on the other hand, defines experiences in the context of a particular time and space, and from a self-centered ('egocentric') perspective. This information can be used to plan actions similarly to a neural path integrator that links sequences of locations in the service of navigation. They hypothesize that mechanisms defining positions in space and their relationships in a map could be applied analogously to define objects or events in order to categorize or represent semantic knowledge. Stating "clear parallels between allocentric navigation and semantic memory, on one hand, and path integration and episodic memory, on the other," Buzsáki and Moser suggest "that the same networks and algorithms support both physical and mental forms of travel" and propose that, eventually, "mechanisms of memory and planning have evolved from mechanisms of navigation in the physical world." (Buzsáki and Moser, 2013, p. 130)

Other researches hold quite the contrary view, whereby the hippocampus' role in spatial navigation is just a prominent application of its more general role in the organization of memories (Eichenbaum, 2017; Eichenbaum and Cohen, 2004; Kim et al., 2015). One of the most prominent proponents of this idea was Howard Eichenbaum, who argued that a cognitive map represents a relational organization of memories, and that this concept is a general principle of memory organization beyond just the spatial domain.

In his view, “the role of the hippocampal system in navigation is to support a particular form of memory organization characterized by Tolman’s broader view of a mapping of memories into a cognitive space of the navigational task, and therein the contribution of the hippocampus to navigation is memory.” (Eichenbaum, 2017, p. 1793)

The concepts outlined above mark opposite ends of a spectrum of theories that aim to explain the role of the hippocampal system by either its mnemonic or its spatial functions. Arguing that, until now, this traditional dichotomy has fallen short of providing a comprehensive framework of the hippocampal system, several researches suggested instead to focus on processes that spatial and nonspatial hippocampal functions have in common, and from them to deduce the underlying processes mediated by the hippocampal system (e.g. Ekstrom and Ranganath, 2017; Lisman et al., 2017; Maguire and Mullally, 2013; Milivojevic and Doeller, 2013).

A prominent example is the ‘scene construction theory’ (SCT), originally formulated by Hassabis and Maguire in 2007, and repeatedly refined over the past decade (Barry and Maguire, 2019; Dalton and Maguire, 2017; Hassabis and Maguire, 2007, 2009; Maguire and Mullally, 2013; Zeidman and Maguire, 2016). SCT considers the hippocampus’ contributions beyond the spatial and mnemonic domains, and emphasizes particularly its importance for processing of scene-related information and scene construction⁶. Accounting for evidence from neuroimaging studies and reports of scene construction and scene-processing impairments in patients with hippocampal damage, the SCT posits that the hippocampus’ key contribution to these functions is to provide spatially coherent scenes. Hassabis and Maguire argue that, whenever we require autobiographical memory, plan how to navigate towards a particular goal, or imagine fictitious events, the construction of a coherent scene is the key underlying process common to all these tasks (Hassabis and Maguire, 2007). Hence, rather than focusing solely on the spatial information processing observed during navigation, or aiming to derive the hippocampal system’s functional contributions purely from its role in mnemonic processes, the SCT instead puts the concept of coherent spatial scenes in the center of hippocampal information processing. Notably, SCT proposes scene construction to be the hippocampus’ key contribution to cognitive functions also beyond episodic memory and spatial navigation, including imagining the future, fictitious events, and possibly even mind wandering and dreaming (Maguire and Mullally, 2013). It does, however, not state that these functions are provided by the hippocampus alone, nor that scene construction is the sole mechanism provided by the hippocampus. The bottom line of Maguire and colleagues’ scene construction theory being that neither cognitive maps nor autobiographical memory but “scenes are the primary currency of the hippocampus. For many of us, scenes are the language of thought, and we argue that the hippocampus actively and automatically predicts and constructs the scenes we need to fuel our cognition.” (Maguire and Mullally, 2013, p. 1187)

⁶Hassabis and Maguire define scene construction as “the process of mentally generating and maintaining a complex and coherent scene or event.” (Hassabis and Maguire, 2007, p. 299)

In recent years, with the advent of high-resolution functional neuroimaging techniques, mechanistic concepts of the hippocampus also became more fine-grained. The hippocampal formation's functional and morphological differences along its dorso-ventral axis, its subfields, and the heterogeneity in the neural connections of different parts of the hippocampal system receive increasing attention (reviewed in [Poppenk et al., 2013](#); [Strange et al., 2014](#)). Yet, despite vivid research and great technical advances throughout the recent decades, still no unifying framework of the hippocampal system's contribution to episodic memory and spatial cognition exists that is commonly agreed on. The debate on how to reconcile the hippocampus' different functions continues (see [Lisman et al., 2017](#)).

1.2.3 Navigation beyond the hippocampal system

Unlike research in rodents, electrophysiological investigation of the human brain is restricted to patients with medically intractable epilepsy, and therefore evidence on single-cell level in humans is scarce. Instead, neuroimaging techniques are usually the method of choice when investigating human brain functions. Functional neuroimaging techniques have much coarser spatial and temporal resolution than electrophysiological single-unit recording. On the other hand, they operate on a much larger spatial scale and so allow to simultaneously record activity in multiple brain regions. Functional neuroimaging techniques are therefore important and frequently applied tools to understand how different brain regions interact in the service of particular cognitive processes.

This is also the case for navigation-related cognitive processes in humans, where particularly functional magnetic resonance imaging (fMRI) has helped to reveal a number of brain regions relevant for navigation beyond the hippocampal formation. Of these areas, the posterior parietal cortex, retrosplenial cortex, and parahippocampal cortex are amongst the most frequently reported ones ([Boccia et al., 2014](#); [Ekstrom et al., 2017](#); [Hunsaker and Kesner, 2018](#); [O'Mara and Aggleton, 2019](#); [Qiu et al., 2019](#)).

The posterior parietal cortex' (PPC) is considered to integrate the input from different sensory systems into a consistent body-centered (egocentric) representation suitable for movement and action planning ([Andersen et al., 1997](#); [King and Andersen, 2000](#)). In humans it has been shown that damage to the PPC leads to an impaired understanding of egocentric object locations ([Aguirre and D'Esposito, 1999](#)). In the context of navigation tasks, neuroimaging studies have also reported the human PPC to code for egocentric target direction ([Howard et al., 2014](#); [Spiers and Maguire, 2007](#)), and to contribute to successful first-person perspective navigation via integration of self-motion cues ([Sherrill et al., 2013](#)). The PPC is therefore commonly considered part of a larger network of brain regions that transform information between allocentric and egocentric reference frames in the service of goal-directed navigation ([Byrne et al., 2007](#); [Wilber et al., 2014](#)). This is a functionally broad notion of the PPC's contribution to navigation, which may become comprehensible when considering that 'posterior parietal cortex' is a rather

high-level anatomical classification that describes a large portion of the human brain.⁷ Consequently, the PPC has also been attributed, for instance, a role in episodic memory retrieval as well as in subserving goal-directed and reflexive attention mechanisms (Hutchinson et al., 2009). It is therefore maybe not surprising that a detailed functional understanding of the PPC's role in spatial cognition is currently still lacking.

Contributions to a wide range of cognitive functions have also been ascribed to the retrosplenial cortex (RSC) and the parahippocampal cortex (PHC), again including both episodic memory and spatial navigation (Aminoff et al., 2013; Ranganath and Ritchey, 2012; Vann et al., 2009). In humans, it has been shown that activation in the RSC increases during memory retrieval and recollection of contextual information, but also during tasks that require participants to translate between egocentric and allocentric reference frames (Ekstrom et al., 2017; Ranganath and Ritchey, 2012). Damage to the RSC has also been reported to result in topographical disorientation where patients are unable to use landmarks in order to orient oneself, supporting the notion that the RSC is crucial in the transformation between egocentric and allocentric coordinate systems (Aguirre and D'Esposito, 1999; Hashimoto et al., 2010; Maguire, 2001). In their influential model of the processes underlying spatial memory, Byrne et al. (2007) consider the RSC to be part of a transformation circuit that maps between egocentric and allocentric representations of space. According to this model, the RSC mediates the transformation between the egocentrically represented information of the different sensory systems in the parietal cortex, and the allocentric spatial representations processed in the medial temporal lobe (also see Julian et al., 2018).

The PHC is commonly attributed to support episodic memory and visuospatial processing. Patients with lesions to the PHC show severe impairments in a wide range of cognitive processes, including spatial orientation, landmark recognition, navigation, spatial memory, and episodic memory (reviewed in detail in Aminoff et al., 2013). Aminoff et al. (2013) suggest that all these cognitive functions are built on contextual associations – defined as links between items that describe, represent, and bring meaning to an environment – and that the PHC's general function is the processing of such contextual associations. According to their framework, different areas in the PHC are optimized for processing of particular functional domains, with the posterior PHC being specialized to process particularly spatially organized contextual associations. The latter notion fits well with a large number of reports that implicate the posterior PHC in processing of particularly places and naturalistic scenes (Epstein, 2008; Epstein and Baker, 2019). This phenomenon has prompted Epstein and Kanwisher to coin the term 'parahippocampal place area' (PPA) for this brain region (Epstein and Kanwisher, 1998).

⁷Anatomically, the PPC forms the posterior part of the parietal lobe. It can be further divided along the intraparietal sulcus, into a dorsal and a ventral portion. The dorsal portion comprises the Brodmann Areas (BA) 5 and 7 – the superior parietal lobule and the precuneus; the ventral portion – sometimes also referred to as the inferior parietal lobule – consists of the angular gyrus (approx. BA 39), the supramarginal gyrus (approx. BA 40), and the functionally defined temporoparietal junction (Hutchinson et al., 2009; Jacobs et al., 2012).

The PPA, together with the with the ‘medial place area’ (MPA) and the ‘occipital place area’ (OPA), form a set of cortical regions that respond selectively to scenes and navigationally relevant visual features in fMRI, compared to other types of visual stimuli.⁸ Due to this distinct feature, these regions are commonly referred to as ‘scene-selective regions’.⁹ All three areas are purely functionally defined regions: the MPA, previously often referred to as the retrosplenial complex and sometimes confused with the (anatomically defined) retrosplenial cortex (Silson et al., 2016), lies posterior to the RSC within the posterior and ventral bank of the parieto-occipital sulcus, sometimes also extending into the RSC proper (Julian et al., 2012; Silson et al., 2016); the OPA is a region around the transverse occipital sulcus, and therefore also often referred to as TOS despite the fact that it is not an anatomically defined region, and for some participants does not even lie in the TOS proper (Dilks et al., 2013; Nasr et al., 2011); the PPA is located posterior to, and sometimes covering parts of, the PHC, spanning sections of the parahippocampal gyrus, fusiform gyrus, collateral sulcus, and lingual sulcus (Julian et al., 2012; Weiner et al., 2018). The scene-selective regions have only recently developed into a well-investigated topic in the field of navigation research and, apart from their reliable activation in scene processing tasks in general, not much is known about how these three brain areas functionally differ from, and complement each other. Though first attempts in this direction have been made (Epstein et al., 2017; Julian et al., 2018), no mechanistic framework of the scene-selective regions exists yet. Considering that most research on these regions so far has been conducted using visual or mental imagery, it is also not surprising that our understanding on how MPA, OPA, and PPA contribute to actual navigation is still quite limited.

1.3 Aim of this thesis

The previous sections summarize our current understanding of brain processes in the service of navigation, both on the cellular and the cognitive level. They furthermore show that much of what we know about the neuronal mechanisms associated with spatial information processing – the ‘inner GPS’ – derives merely from experiments in rodents. Our knowledge of navigation behavior, related cognitive processes, and the interaction between brain regions involved, on the other hand, is predominantly based on neuropsychological and neuroimaging findings in humans. Yet, how firing properties and interaction between different cell types translate into navigation behavior, and how changes in brain activity observed with neuroimaging methods during navigation can be causally attributed to cellular processes remain open questions (Zhao, 2018). Answering them, however, is important not only to extend our understanding of navigation, but

⁸Most studies on scene-selective regions consider a ‘scene’ to consist of a real-world environment that comprises background elements and discrete objects, and that can be captured in a single view (see Henderson and Hollingworth, 1999).

⁹Note that several variations to this term are found in the literature, for instance ‘scene-selective cortex’ or ‘scene-responsive regions’, which still all refer to the same set of human cortical regions: MPA, OPA, and PPA.

also in a broader context to help understand how, for instance, mental ailments such as Alzheimer's disease that severely impair patient's memory and navigation capabilities relate to neuronal processes (Coughlan et al., 2018; Lester et al., 2017). Helping to bridge this gap in our knowledge of how processes on the cellular and the cognitive level relate to each other is the goal of this thesis.

The first study, presented in Chpt. 2, uses functional magnetic resonance imaging (MRI) to investigate how activation in the human brain during a navigation task in a virtual environment relates to the task's general navigation demands, and particularly the task's spatial memory demands. The study design is inspired by the ongoing debate on how to reconcile the hippocampal system's mnemonic functions with its role in navigation (see Chpt. 1.2.2). The hippocampal formation is therefore targeted in a region-of-interest analysis that assesses how participants' task performance and use of spatial memory relate to their hippocampal activation. Furthermore, contributing to our understanding of interactions between brain areas in service of navigation beyond the hippocampal system (see Chpt. 1.2.3), the study investigates how varying navigational and mnemonic demands are reflected in brain activity across the entire brain. Participants navigate through a virtual environment in first-person perspective, presented to participants on MRI-compatible goggles, using a MRI-compatible joystick. Importantly, while most human navigation studies restrict navigation in virtual environments to a limited set of directions and/or predefined movement speed, participants freely choose both movement direction and speed in this experiment.¹⁰ Finally, the study acknowledges that translating between navigation behavior and neuronal activity on the cellular level is not only complicated by the different techniques applied – non-invasive imaging techniques versus invasive single-unit recordings – but additionally impeded by substantially different experimental paradigms used across species. Activity of spatially tuned neurons of the rodent hippocampal system is typically recorded during random foraging in geometrically simple and landmark-sparse open-field environments. Human navigation studies, on the other hand, frequently require participants to solve challenging navigation tasks in visually rich, large-scale, and, compared to the classic rodent foraging paradigm, more realistic environments, such as traveling a university campus or navigating taxis through virtual cities. Attempting to make results more comparable across species, this study therefore translates the classic rodent foraging paradigm into a virtual environment setup and combines it with navigation and memory tasks of varying difficulty.

The second study, presented in Chpt. 3, uses a similar framework to investigate participants' internal spatial representation of a quadratic open-field environment. Place-encoding neurons such as place or grid cells are typically recorded in open-field environments with geometrically simple base areas of circular or rectangular shape. Several studies have already shown that the geometry of these environments impacts the spatial firing patterns of place-encoding neurons recorded in them (see Chpt. 1.1.4). Considering that these neurons are commonly thought to form the neural basis for a cognitive map

¹⁰within the range of real-world movements

of our environment (O’Keefe and Nadel, 1978), this raises the question as to whether similar effects also apply to the cognitive representation of an environment. Hartley et al. (2004) addressed this question by testing participants’ spatial memory of three different locations in an open-field environment under varying environmental boundary configurations, and modeling participants’ responses as a function of the environment’s changing geometry. They found that participants’ location memory is best explained by a location’s proximity to the environment’s boundaries. The study presented here aims to complement these findings by systematically assessing accuracy and precision of participants’ location memory across a virtual open-field environment that is designed to closely resemble the rectangular open-field setups typically used to investigate firing properties of spatially tuned neurons in rodents. Taking participants’ location memory as a proxy for their internal representation of the test environment’s space, the study helps to compare how effects of boundary geometry that influence firing properties of spatially tuned neurons in rodents shape the cognitive representation of space in humans.

1.4 References

- Aguirre, G. K. and D’Esposito, M. (1999). Topographical disorientation: a synthesis and taxonomy. *Brain*, 122(9):1613–1628.
- Ainge, J. A., Tamosiunaite, M., Woergoetter, E., and Dudchenko, P. A. (2007). Hippocampal cal place cells encode intended destination on a maze with multiple choice points. *Journal of Neuroscience*, 27(36):9769–9779.
- Aminoff, E. M., Kveraga, K., and Bar, M. (2013). The role of the parahippocampal cortex in cognition. *Trends in Cognitive Sciences*, 17(8):379 – 390.
- Andersen, R. A., Snyder, L. H., Bradley, D. C., and Xing, J. (1997). Multimodal representation of space in the posterior parietal cortex and its use in planning movements. *Annual Review of Neuroscience*, 20(1):303–330.
- Annese, J., Schenker-Ahmed, N. M., Bartsch, H., Maechler, P., Sheh, C., Thomas, N., Kayano, J., Ghatan, A., Bresler, N., Frosch, M. P., and et al. (2014). Postmortem examination of patient h.m.’s brain based on histological sectioning and digital 3d reconstruction. *Nature Communications*, 5(1).
- Barry, C., Lever, C., Hayman, R., Hartley, T., Burton, S., O’Keefe, J., Jeffery, K., and Burgess, N. (2006). The boundary vector cell model of place cell firing and spatial memory. *Reviews in the Neurosciences*, 17(1-2).
- Barry, D. N. and Maguire, E. A. (2019). Remote memory and the hippocampus: A constructive critique. *Trends in Cognitive Sciences*, 23(2):128 – 142.
- Bicanski, A. and Burgess, N. (2018). A neural-level model of spatial memory and imagery. *eLife*, 7.
- Bjerknes, T. L., Moser, E. I., and Moser, M.-B. (2014). Representation of geometric borders in the developing rat. *Neuron*, 82(1):71 – 78.

- Boccaro, C. N., Sargolini, F., Thoresen, V. H., Solstad, T., Witter, M. P., Moser, E. I., and Moser, M.-B. (2010). Grid cells in pre- and parasubiculum. *Nature Neuroscience*, 13(8):987–994.
- Boccia, M., Nemmi, F., and Guariglia, C. (2014). Neuropsychology of environmental navigation in humans: Review and meta-analysis of fmri studies in healthy participants. *Neuropsychology Review*, 24(2):236–251.
- Buzsáki, G. (2004). Large-scale recording of neuronal ensembles. *Nature Neuroscience*, 7(5):446–451.
- Buzsáki, G. and Moser, E. I. (2013). Memory, navigation and theta rhythm in the hippocampal-entorhinal system. *Nature Neuroscience*, 16(2):130–138.
- Byrne, P., Becker, S., and Burgess, N. (2007). Remembering the past and imagining the future: A neural model of spatial memory and imagery. *Psychological Review*, 114(2):340–375.
- Cacucci, F. (2004). Theta-modulated place-by-direction cells in the hippocampal formation in the rat. *Journal of Neuroscience*, 24(38):8265–8277.
- Cheng, K., Huttenlocher, J., and Newcombe, N. S. (2013). 25 years of research on the use of geometry in spatial reorientation: a current theoretical perspective. *Psychonomic Bulletin & Review*, 20(6):1033–1054.
- Clark, I. A., Hotchin, V., Monk, A., Pizzamiglio, G., Liefgreen, A., and Maguire, E. A. (2019). Identifying the cognitive processes underpinning hippocampal-dependent tasks. *Journal of Experimental Psychology: General*.
- Corkin, S. (2002). What's new with the amnesic patient h.m.? *Nature Reviews Neuroscience*, 3(2):153–160.
- Couey, J. J., Witoelar, A., Zhang, S.-J., Zheng, K., Ye, J., Dunn, B., Czajkowski, R., Moser, M.-B., Moser, E. I., Roudi, Y., and et al. (2013). Recurrent inhibitory circuitry as a mechanism for grid formation. *Nature Neuroscience*, 16(3):318–324.
- Coughlan, G., Laczó, J., Hort, J., Minihane, A.-M., and Hornberger, M. (2018). Spatial navigation deficits — overlooked cognitive marker for preclinical alzheimer disease? *Nature Reviews Neurology*, 14(8):496–506.
- Dalton, M. A. and Maguire, E. A. (2017). The pre/parasubiculum: a hippocampal hub for scene-based cognition? *Current Opinion in Behavioral Sciences*, 17:34 – 40. Memory in time and space.
- Deshmukh, S. S. and Knierim, J. J. (2011). Representation of non-spatial and spatial information in the lateral entorhinal cortex. *Frontiers in Behavioral Neuroscience*, 5.
- Dilks, D. D., Julian, J. B., Paunov, A. M., and Kanwisher, N. (2013). The occipital place area is causally and selectively involved in scene perception. *Journal of Neuroscience*, 33(4):1331–1336.

- Doeller, C. F., Barry, C., and Burgess, N. (2010). Evidence for grid cells in a human memory network. *Nature*, 463(7281):657–661.
- Dragoi, G. and Tonegawa, S. (2011). Preplay of future place cell sequences by hippocampal cellular assemblies. *Nature*, 469(7330):397–401.
- Eichenbaum, H. (2017). The role of the hippocampus in navigation is memory. *J Neurophysiol*, 117(4):1785–1796.
- Eichenbaum, H. and Cohen, N. J. (2004). *From Conditioning to Conscious Recollection: Memory systems of the brain*. Number 35. Oxford University Press.
- Eichenbaum, H. and Cohen, N. J. (2014). Can we reconcile the declarative memory and spatial navigation views on hippocampal function? *Neuron*, 83(4):764–770.
- Ekstrom, A. D., Huffman, D. J., and Starrett, M. (2017). Interacting networks of brain regions underlie human spatial navigation: a review and novel synthesis of the literature. *J Neurophysiol*, 118(6):3328–3344.
- Ekstrom, A. D., Kahana, M. J., Caplan, J. B., Fields, T. A., Isham, E. A., Newman, E. L., and Fried, I. (2003). Cellular networks underlying human spatial navigation. *Nature*, 425(6954):184–188.
- Ekstrom, A. D. and Ranganath, C. (2017). Space, time, and episodic memory: The hippocampus is all over the cognitive map. *Hippocampus*, 28(9):680–687.
- Epstein, R. and Kanwisher, N. (1998). A cortical representation of the local visual environment. *Nature*, 392(6676):598–601.
- Epstein, R. A. (2008). Parahippocampal and retrosplenial contributions to human spatial navigation. *Trends in Cognitive Sciences*, 12(10):388–396.
- Epstein, R. A. and Baker, C. I. (2019). Scene perception in the human brain. *Annual Review of Vision Science*, 5(1):373–397.
- Epstein, R. A., Patai, E. Z., Julian, J. B., and Spiers, H. J. (2017). The cognitive map in humans: spatial navigation and beyond. *Nature Neuroscience*, 20(11):1504–1513.
- Fiete, I. R., Burak, Y., and Brookings, T. (2008). What grid cells convey about rat location. *Journal of Neuroscience*, 28(27):6858–6871.
- Franz, M. O. and Mallot, H. A. (2000). Biomimetic robot navigation. *Robotics and Autonomous Systems*, 30(1):133 – 153.
- Fuhs, M. C. (2006). A spin glass model of path integration in rat medial entorhinal cortex. *Journal of Neuroscience*, 26(16):4266–4276.
- Fyhn, M. (2004). Spatial representation in the entorhinal cortex. *Science*, 305(5688):1258–1264.
- Fyhn, M., Hafting, T., Treves, A., Moser, M.-B., and Moser, E. I. (2007). Hippocampal remapping and grid realignment in entorhinal cortex. *Nature*, 446(7132):190–194.

- Grieves, R. M. and Jeffery, K. J. (2017). The representation of space in the brain. *Behavioural Processes*, 135:113–131.
- Hafting, T., Fyhn, M., Molden, S., Moser, M.-B., and Moser, E. I. (2005). Microstructure of a spatial map in the entorhinal cortex. *Nature*, 436(7052):801–806.
- Hartley, T., Burgess, N., Lever, C., Cacucci, F., and O’Keefe, J. (2000). Modeling place fields in terms of the cortical inputs to the hippocampus. *Hippocampus*, 10(4):369–379.
- Hartley, T., Trinkler, I., and Burgess, N. (2004). Geometric determinants of human spatial memory. *Cognition*, 94(1):39–75.
- Hashimoto, R., Tanaka, Y., and Nakano, I. (2010). Heading disorientation: A new test and a possible underlying mechanism. *European Neurology*, 63(2):87–93.
- Hassabis, D. and Maguire, E. A. (2007). Deconstructing episodic memory with construction. *Trends in Cognitive Sciences*, 11(7):299–306.
- Hassabis, D. and Maguire, E. A. (2009). The construction system of the brain. *Philosophical Transactions of the Royal Society B: Biological Sciences*, 364(1521):1263–1271.
- Henderson, J. M. and Hollingworth, A. (1999). High-level scene perception. *Annual Review of Psychology*, 50(1):243–271.
- Hinman, J. R., Brandon, M. P., Climer, J. R., Chapman, G. W., and Hasselmo, M. E. (2016). Multiple running speed signals in medial entorhinal cortex. *Neuron*, 91(3):666 – 679.
- Howard, L. R., Javadi, A. H., Yu, Y., Mill, R. D., Morrison, L. C., Knight, R., Loftus, M. M., Staskute, L., and Spiers, H. J. (2014). The hippocampus and entorhinal cortex encode the path and euclidean distances to goals during navigation. *Current Biology*, 24(12):1331 – 1340.
- Hunsaker, M. R. and Kesner, R. P. (2018). Unfolding the cognitive map: The role of hippocampal and extra-hippocampal substrates based on a systems analysis of spatial processing. *Neurobiology of Learning and Memory*, 147:90 – 119.
- Hutchinson, J. B., Uncapher, M. R., and Wagner, A. D. (2009). Posterior parietal cortex and episodic retrieval: convergent and divergent effects of attention and memory. *Learn Mem*, 16(6):343–56.
- Jacobs, H. I., Van Boxtel, M. P., Jolles, J., Verhey, F. R., and Uylings, H. B. (2012). Parietal cortex matters in alzheimer’s disease: An overview of structural, functional and metabolic findings. *Neuroscience & Biobehavioral Reviews*, 36(1):297–309.
- Jacobs, J. and Kahana, M. J. (2010). Direct brain recordings fuel advances in cognitive electrophysiology. *Trends in Cognitive Sciences*, 14(4):162–171.
- Jacobs, J., Weidemann, C. T., Miller, J. F., Solway, A., Burke, J. F., Wei, X.-X., Suthana, N., Sperling, M. R., Sharan, A. D., Fried, I., and et al. (2013). Direct recordings of grid-like neuronal activity in human spatial navigation. *Nature Neuroscience*, 16(9):1188–1190.

- Jankowski, M. M. and O'Mara, S. M. (2015). Dynamics of place, boundary and object encoding in rat anterior claustrum. *Frontiers in Behavioral Neuroscience*, 9.
- Julian, J., Fedorenko, E., Webster, J., and Kanwisher, N. (2012). An algorithmic method for functionally defining regions of interest in the ventral visual pathway. *NeuroImage*, 60(4):2357–2364.
- Julian, J. B., Keinath, A. T., Marchette, S. A., and Epstein, R. A. (2018). The neurocognitive basis of spatial reorientation. *Current Biology*, 28(17):R1059 – R1073.
- Keinath, A. T., Wang, M. E., Wann, E. G., Yuan, R. K., Dudman, J. T., and Muzzio, I. A. (2014). Precise spatial coding is preserved along the longitudinal hippocampal axis. *Hippocampus*, 24(12):1533–1548.
- Kim, S., Dede, A. J. O., Hopkins, R. O., and Squire, L. R. (2015). Memory, scene construction, and the human hippocampus. *Proceedings of the National Academy of Sciences*, 112(15):4767–4772.
- Kraus, B. J., Robinson, R. J., White, J. A., Eichenbaum, H., and Hasselmo, M. E. (2013). Hippocampal “time cells”: Time versus path integration. *Neuron*, 78(6):1090 – 1101.
- Kropff, E., Carmichael, J. E., Moser, M.-B., and Moser, E. I. (2015). Speed cells in the medial entorhinal cortex. *Nature*, 523(7561):419–424.
- Krupic, J., Bauza, M., Burton, S., Barry, C., and O'Keefe, J. (2015). Grid cell symmetry is shaped by environmental geometry. *Nature*, 518(7538):232–235.
- Krupic, J., Bauza, M., Burton, S., Lever, C., and O'Keefe, J. (2014). How environment geometry affects grid cell symmetry and what we can learn from it. *Philosophical Transactions of the Royal Society B: Biological Sciences*, 369(1635):20130188.
- Krupic, J., Bauza, M., Burton, S., and O'Keefe, J. (2018). Local transformations of the hippocampal cognitive map. *Science*, 359(6380):1143–1146.
- Kubie, J. L. and Fenton, A. A. (2012). Linear look-ahead in conjunctive cells: An entorhinal mechanism for vector-based navigation. *Frontiers in Neural Circuits*, 6.
- Lester, A. W., Moffat, S. D., Wiener, J. M., Barnes, C. A., and Wolbers, T. (2017). The aging navigational system. *Neuron*, 95(5):1019 – 1035.
- Leutgeb, S. (2005). Independent codes for spatial and episodic memory in hippocampal neuronal ensembles. *Science*, 309(5734):619–623.
- Lever, C., Burton, S., Jeewajee, A., O'Keefe, J., and Burgess, N. (2009). Boundary vector cells in the subiculum of the hippocampal formation. *Journal of Neuroscience*, 29(31):9771–9777.
- Lever, C., Cacucci, F., Burgess, N., and O'Keefe, J. (1999). Squaring the circle: place cell firing patterns in environments which differ only geometrically are not unpredictable. In *Soc Neurosci Abstr*, volume 24.

- Lisman, J., Buzsáki, G., Eichenbaum, H., Nadel, L., Ranganath, C., and Redish, A. D. (2017). Viewpoints: how the hippocampus contributes to memory, navigation and cognition. *Nature Neuroscience*, 20(11):1434–1447.
- MacDonald, C. J., Carrow, S., Place, R., and Eichenbaum, H. (2013). Distinct hippocampal time cell sequences represent odor memories in immobilized rats. *Journal of Neuroscience*, 33(36):14607–14616.
- MacDonald, C. J., Lepage, K. Q., Eden, U. T., and Eichenbaum, H. (2011). Hippocampal “time cells” bridge the gap in memory for discontinuous events. *Neuron*, 71(4):737–749.
- Maguire, E. (2001). The retrosplenial contribution to human navigation: A review of lesion and neuroimaging findings. *Scandinavian Journal of Psychology*, 42(3):225–238.
- Maguire, E. A. and Mullally, S. L. (2013). The hippocampus: A manifesto for change. *Journal of Experimental Psychology: General*, 142(4):1180–1189.
- Mao, D., Kandler, S., McNaughton, B. L., and Bonin, V. (2017). Sparse orthogonal population representation of spatial context in the retrosplenial cortex. *Nature Communications*, 8(1).
- Markus, E., Qin, Y., Leonard, B., Skaggs, W., McNaughton, B., and Barnes, C. (1995). Interactions between location and task affect the spatial and directional firing of hippocampal neurons. *Journal of Neuroscience*, 15(11):7079–7094.
- Mathis, A., Herz, A. V., and Stemmler, M. (2012). Optimal population codes for space: grid cells outperform place cells. *Neural computation*, 24(9):2280–2317.
- McNaughton, B., Barnes, C., and O’Keefe, J. (1983). The contributions of position, direction, and velocity to single unit activity in the hippocampus of freely-moving rats. *Experimental Brain Research*, 52(1).
- McNaughton, B. L., Battaglia, F. P., Jensen, O., Moser, E. I., and Moser, M.-B. (2006). Path integration and the neural basis of the “cognitive map”. *Nature Reviews Neuroscience*, 7(8):663–678.
- Milford, M. J., Wiles, J., and Wyeth, G. F. (2010). Solving navigational uncertainty using grid cells on robots. *PLoS Computational Biology*, 6(11):e1000995.
- Milivojevic, B. and Doeller, C. F. (2013). Mnemonic networks in the hippocampal formation: From spatial maps to temporal and conceptual codes. *Journal of Experimental Psychology: General*, 142(4):1231–1241.
- Miller, J. F., Neufang, M., Solway, A., Brandt, A., Trippel, M., Mader, I., Hefft, S., Merkow, M., Polyn, S. M., Jacobs, J., and et al. (2013). Neural activity in human hippocampal formation reveals the spatial context of retrieved memories. *Science*, 342(6162):1111–1114.
- Moser, E. I., Moser, M.-B., and McNaughton, B. L. (2017). Spatial representation in the hippocampal formation: a history. *Nature Neuroscience*, 20(11):1448–1464.

- Muller, R., Bostock, E., Taube, J., and Kubie, J. (1994). On the directional firing properties of hippocampal place cells. *J. Neurosci.; Journal of Neuroscience*, 14(12):7235–7251.
- Muller, R. U. and Kubie, J. L. (1987). The effects of changes in the environment on the spatial firing of hippocampal complex-spike cells. *Journal of Neuroscience*, 7(7):1951–1968.
- Muller, R. U., Kubie, J. L., and Ranck, J. B. (1987). Spatial firing patterns of hippocampal complex-spike cells in a fixed environment. *Journal of Neuroscience*, 7(7):1935–1950.
- Nadasdy, Z., Nguyen, T. P., Török, Á., Shen, J. Y., Briggs, D. E., Modur, P. N., and Buchanan, R. J. (2017). Context-dependent spatially periodic activity in the human entorhinal cortex. *Proceedings of the National Academy of Sciences*, 114(17):E3516–E3525.
- Nasr, S., Liu, N., Devaney, K. J., Yue, X., Rajimehr, R., Ungerleider, L. G., and Tootell, R. B. H. (2011). Scene-selective cortical regions in human and nonhuman primates. *Journal of Neuroscience*, 31(39):13771–13785.
- O’Keefe, J. (1976). Place units in the hippocampus of the freely moving rat. *Experimental Neurology*, 51(1):78 – 109.
- O’Keefe, J. and Burgess, N. (1996). Geometric determinants of the place fields of hippocampal neurons. *Nature*, 381(6581):425–428.
- O’Keefe, J. and Dostrovsky, J. (1971). The hippocampus as a spatial map. preliminary evidence from unit activity in the freely-moving rat. *Brain Res*, 34(1):171–5.
- O’Keefe, J. and Nadel, L. (1978). The hippocampus as a cognitive map.
- O’Mara, S. M. and Aggleton, J. P. (2019). Space and memory (far) beyond the hippocampus: Many subcortical structures also support cognitive mapping and mnemonic processing. *Frontiers in Neural Circuits*, 13.
- Pastalkova, E., Itskov, V., Amarasingham, A., and Buzsaki, G. (2008). Internally generated cell assembly sequences in the rat hippocampus. *Science*, 321(5894):1322–1327.
- Poppenk, J., Evensmoen, H. R., Moscovitch, M., and Nadel, L. (2013). Long-axis specialization of the human hippocampus. *Trends in Cognitive Sciences*, 17(5):230 – 240.
- Poulter, S., Hartley, T., and Lever, C. (2018). The neurobiology of mammalian navigation. *Current Biology*, 28(17):R1023 – R1042.
- Qiu, Y., Wu, Y., Liu, R., Wang, J., Huang, H., and Huang, R. (2019). Representation of human spatial navigation responding to input spatial information and output navigational strategies: An ale meta-analysis. *Neuroscience & Biobehavioral Reviews*, 103:60 – 72.
- Quirk, G., Muller, R., and Kubie, J. (1990). The firing of hippocampal place cells in the dark depends on the rat’s recent experience. *Journal of Neuroscience*, 10(6):2008–2017.
- Ranganath, C. and Ritchey, M. (2012). Two cortical systems for memory-guided behaviour. *Nature Reviews Neuroscience*, 13(10):713–726.

- Redish, A. D. (1999). *Beyond the cognitive map: From place cells to episodic memory*. The MIT Press, Cambridge, MA, US.
- Robin, J. (2018). Spatial scaffold effects in event memory and imagination. *Wiley Interdisciplinary Reviews: Cognitive Science*, 9(4):e1462.
- Rowland, D. C., Roudi, Y., Moser, M.-B., and Moser, E. I. (2016). Ten years of grid cells. *Annual Review of Neuroscience*, 39(1):19–40.
- Sargolini, F., Fyhn, M., Hafting, T., McNaughton, B. L., Witter, M. P., Moser, M.-B., and Moser, E. I. (2006). Conjunctive representation of position, direction, and velocity in entorhinal cortex. *Science*, 312(5774):758–762.
- Savelli, F., Yoganasimha, D., and Knierim, J. J. (2008). Influence of boundary removal on the spatial representations of the medial entorhinal cortex. *Hippocampus*, 18(12):1270–1282.
- Schiller, D., Eichenbaum, H., Buffalo, E. A., Davachi, L., Foster, D. J., Leutgeb, S., and Ranganath, C. (2015). Memory and space: Towards an understanding of the cognitive map. *Journal of Neuroscience*, 35(41):13904–13911.
- Scoville, W. B. and Milner, B. (1957). Loss of recent memory after bilateral hippocampal lesions. *Journal of Neurology, Neurosurgery & Psychiatry*, 20(1):11–21.
- Sherrill, K. R., Erdem, U. M., Ross, R. S., Brown, T. I., Hasselmo, M. E., and Stern, C. E. (2013). Hippocampus and retrosplenial cortex combine path integration signals for successful navigation. *Journal of Neuroscience*, 33(49):19304–19313.
- Silson, E. H., Steel, A. D., and Baker, C. I. (2016). Scene-selectivity and retinotopy in medial parietal cortex. *Frontiers in Human Neuroscience*, 10.
- Solstad, T., Boccara, C. N., Kropff, E., Moser, M.-B., and Moser, E. I. (2008). Representation of geometric borders in the entorhinal cortex. *Science*, 322(5909):1865–1868.
- Spiers, H. J. and Maguire, E. A. (2007). A navigational guidance system in the human brain. *Hippocampus*, 17(8):618–626.
- Squire, L. R. and Zola-Morgan, J. (1991). The cognitive neuroscience of human memory since h.m. *Annual Review of Neuroscience*, 34(1):259–288.
- Stemmler, M., Mathis, A., and Herz, A. V. M. (2015). Connecting multiple spatial scales to decode the population activity of grid cells. *Science Advances*, 1(11):e1500816–e1500816.
- Stensola, H., Stensola, T., Solstad, T., Frøland, K., Moser, M.-B., and Moser, E. I. (2012). The entorhinal grid map is discretized. *Nature*, 492(7427):72–78.
- Stewart, S., Jeewajee, A., Wills, T. J., Burgess, N., and Lever, C. (2014). Boundary coding in the rat subiculum. *Philosophical Transactions of the Royal Society B: Biological Sciences*, 369(1635):20120514.

- Strange, B. A., Witter, M. P., Lein, E. S., and Moser, E. I. (2014). Functional organization of the hippocampal longitudinal axis. *Nature Reviews Neuroscience*, 15(10):655–669.
- Taube, J. S. (2007). The head direction signal: Origins and sensory-motor integration. *Annual Review of Neuroscience*, 30(1):181–207.
- Taube, J. S., Muller, R. U., and Ranck, J. B. (1990a). Head-direction cells recorded from the postsubiculum in freely moving rats. i. description and quantitative analysis. *Journal of Neuroscience*, 10(2):420–435.
- Taube, J. S., Muller, R. U., and Ranck, J. B. (1990b). Head-direction cells recorded from the postsubiculum in freely moving rats. ii. effects of environmental manipulations. *Journal of Neuroscience*, 10(2):436–447.
- Thompson, L. and Best, P. (1990). Long-term stability of the place-field activity of single units recorded from the dorsal hippocampus of freely behaving rats. *Brain Research*, 509(2):299 – 308.
- Tulving, E. (1972). Episodic and semantic memory. *Organization of Memory*, pages 381–402.
- Vann, S. D., Aggleton, J. P., and Maguire, E. A. (2009). What does the retrosplenial cortex do? *Nature Reviews Neuroscience*, 10(11):792–802.
- Wei, X.-X., Prentice, J., and Balasubramanian, V. (2015). A principle of economy predicts the functional architecture of grid cells. *eLife*, 4.
- Weible, A., Rowland, D., Monaghan, C., Wolfgang, N., and Kentros, C. (2012). Neural correlates of long-term object memory in the mouse anterior cingulate cortex. *J. Neurosci.; Journal of Neuroscience*, 32(16):5598–5608.
- Weiner, K. S., Barnett, M. A., Witthoft, N., Golarai, G., Stigliani, A., Kay, K. N., Gomez, J., Natu, V. S., Amunts, K., Zilles, K., and Grill-Spector, K. (2018). Defining the most probable location of the parahippocampal place area using cortex-based alignment and cross-validation. *NeuroImage*, 170:373 – 384. Segmenting the Brain.
- Widloski, J. and Fiete, I. R. (2014). A model of grid cell development through spatial exploration and spike time-dependent plasticity. *Neuron*, 83(2):481 – 495.
- Wilber, A. A., Clark, B. J., Forster, T. C., Tatsuno, M., and McNaughton, B. L. (2014). Interaction of egocentric and world-centered reference frames in the rat posterior parietal cortex. *Journal of Neuroscience*, 34(16):5431–5446.
- Williams, H. L., Conway, M. A., and Cohen, G. (2008). Autobiographical memory. *Memory in the real world*, 3:21–90.
- Wilson, M. and McNaughton, B. (1993). Dynamics of the hippocampal ensemble code for space. *Science*, 261(5124):1055–1058.
- Wood, E. R., Dudchenko, P. A., Robitsek, R., and Eichenbaum, H. (2000). Hippocampal neurons encode information about different types of memory episodes occurring in the same location. *Neuron*, 27(3):623 – 633.

- Xing, J. and Andersen, R. A. (2000). Models of the posterior parietal cortex which perform multimodal integration and represent space in several coordinate frames. *Journal of Cognitive Neuroscience*, 12(4):601–614.
- Yartsev, M. M., Witter, M. P., and Ulanovsky, N. (2011). Grid cells without theta oscillations in the entorhinal cortex of bats. *Nature*, 479(7371):103–107.
- Yoder, R. M., Clark, B. J., Brown, J. E., Lamia, M. V., Valerio, S., Shinder, M. E., and Taube, J. S. (2011a). Both visual and idiothetic cues contribute to head direction cell stability during navigation along complex routes. *J Neurophysiol*, 105(6):2989–3001.
- Yoder, R. M., Clark, B. J., and Taube, J. S. (2011b). Origins of landmark encoding in the brain. *Trends in Neurosciences*, 34(11):561–571.
- Zeidman, P. and Maguire, E. A. (2016). Anterior hippocampus: the anatomy of perception, imagination and episodic memory. *Nature Reviews Neuroscience*, 17(3):173.
- Zhao, M. (2018). Human spatial representation: what we cannot learn from the studies of rodent navigation. *J Neurophysiol*, 120(5):2453–2465.

The Impact of Varying Navigational and Spatial Memory Demands on Human Brain Activity during Spatial Exploration

Authors' contributions

“The Impact of Varying Navigational and Spatial Memory Demands on Human Brain Activity during Spatial Exploration” (in prep.)

C. Roppelt, S. Glasauer, V. L. Flanagin

CR, SG, and VLF designed the study;

CR and VLF conducted the pilot studies;

CR and SG programmed the task and virtual environment;

CR and VLF conducted the data collection;

CR and VLF designed and programmed the MRI data analysis;

CR designed and programmed the behavioral data analysis;

CR and VLF interpreted the data;

CR wrote the manuscript and designed the figures;

VLF critically revised the manuscript;

VLF supervised the project.

The Impact of Varying Navigational and Spatial Memory Demands on Human Brain Activity during Spatial Exploration

Christopher Roppelt^{1,2}, Stefan Glasauer¹, and Virginia L. Flanagan¹

¹*German Center for Vertigo and Balance Disorders, Munich, Germany*

²*Graduate School for Systemic Neurosciences, Munich, Germany*

Abstract

Several brain regions are frequently found to be activated during neuroimaging studies of human navigation, yet their exact contribution to navigation is often unclear. Particularly the role of the human hippocampus, essential also for several mnemonic functions, is debated. Here, participants (N=27) explore an open-field virtual environment (VE) while their brain activity is recorded using functional magnetic resonance imaging (fMRI). We apply a paradigm that allows us to separate out both passive and active components of spatial exploration, and to vary the spatial memory demand during active exploration. We additionally examine how specifically hippocampal activation relates to participants' performance and spatial memory usage in this task. We find regions of the scene-selective cortex to be already recruited during passive navigation, and to further increase activity with increasing navigational demand. None of the task conditions reveal hippocampal activity on the group level, but activity in participants' anterior medial hippocampus (amHipp) positively correlates with their spatial memory usage. Our results suggest a role for the scene-selective cortex beyond scene perception, in which these regions engage in navigation-related information processing regardless of task demands, and additionally contribute specifically to active navigation. Our results furthermore support the recent notion whereby the amHipp provides a coherent spatial representation of one's environment, and we conclude that this representation is built on spatial memory.

1 Introduction

Our ability to navigate through our environment is an important skill that we crucially rely on in our everyday lives. Navigation involves a complex interplay between processing of various sensory cues, spatial computations, and memory processes (Wolbers and Hegarty, 2010). The hippocampus, together with the medial temporal lobe (MTL), a major input region to the hippocampus, has long been considered one of the pivotal brain regions for spatial processing, yet, the exact contribution of these regions to spatial cognition remains unclear.

Two predominant views have developed about the role of these regions in spatial cognition. In one view, the hippocampus is thought to be the seat of an internal orientation-independent representation of space. This view is based primarily on electrophysiological research in rodents and computational modeling (for reviews see e.g. Hartley et al., 2014; Moser et al., 2008). Place cells, pyramidal neurons originally found in area CA1 in the rat hippocampus, fire at specific spatial locations when the animal moves through its environment (O'Keefe and Dostrovsky, 1971). A decrease in spatial specificity of place cell firing is typically associated with a decrease in spatial performance (e.g. Terrazas et al., 2005). Other cell types such as grid cells, border cells, head-direction cells, and a multitude of other cells that fire in a spatially dependent fashion have been found in the hippocampus and MTL, are thought to work together to provide animals with information about themselves in space (Hafting et al., 2005; Lever et al., 2009; Solstad et al., 2008; Taube et al., 1990). Importantly, in rats, these cells can be recorded in paradigms during which no explicit memory task is given.

The other theory postulates that the hippocampus is crucial for memory, and is therefore particularly relevant for the memory encoding components of spatial processing. This hypothesis is based on research from both humans and rodents. A seminal case study by Scoville and Milner reported severe and persistent episodic memory deficits in a patient after bilateral hippocampal lesion (Scoville and Milner, 1957). The importance of the hippocampus particularly for spatial memory was demonstrated in rats with hippocampal lesions that were, in contrast to healthy controls, not able to remember the location of a platform hidden in a pool filled with opaque liquid when that platform was removed (Morris et al., 1982). This finding has also been replicated in human patients several times (e.g. Astur et al., 2002; Banta Lavenex et al., 2014; Goodrich-Hunsaker et al., 2010), and many studies emphasising the role of the hippocampus in navigation exclusively for memory processes followed (for a recent review see Eichenbaum, 2017a).

A unifying concept has not yet emerged, and functional and anatomical differences in the rodent and human hippocampus (Buzsáki and Moser, 2013; Insausti, 1993; Jacobs, 2014; Strange et al., 2014; van Dijk et al., 2016; Watrous et al., 2013) as well as the methodological and conceptual discrepancies have made the development of a common framework challenging. In humans, electrophysiological evidence providing insights into spatial perception processes on a cellular level is scarce. Interestingly, however, though place-, grid-, and border cell-like activity in the human MTL using extracellular recordings from epilepsy patients has been reported, these experiments all used paradigms with an explicit spatial memory task (Ekstrom et al., 2003; Jacobs et al., 2010, 2013; Lee et al., 2018).

Furthermore, lesion studies provide conflicting evidence towards the idea that the human hippocampus performs the spatial computations underlying spatial cognition. Amnesic patients with lesions including one or both hippocampal gyri are as successful as healthy controls at a number of spatial processing tasks. They performed equal to healthy controls in several tasks that required processing of landmark information (Bohbot et al., 1998). They were able to describe short-cuts and detours in a familiar large-scale environment (Teng and Squire, 1999), could successfully navigate around a large-scale environment with only mild impairment on spatial details (Maguire et al., 2006), solved path integration tasks equal to healthy controls (Kim et al., 2013; Shrager et al., 2008), and were able to transform map coordinates into geographical coordinates for successful navigation (Urgolites et al., 2016).

Lastly, neuroimaging studies often fail to find significant activation in the human hippocampus during spatial navigation tasks (for a meta-analysis see Boccia et al., 2014). Instead, neural activity in the hippocampus is often found only during the encoding phase of spatial memory (Baumann et al., 2010; Iaria et al., 2007), or when correlated with participants task performance (Baumann et al., 2010; Hartley et al., 2003; Janzen et al., 2008; Mellet et al., 2010; Rauchs et al., 2008; Wolbers et al., 2007). This suggests that hippocampal activity reflects individual strategies (Bohbot et al., 2007; Hartley et al., 2003; Iaria et al., 2003; Ishikawa and Montello, 2006; Marchette et al., 2011) and memory processes rather than general spatial processing (Eichenbaum, 2017b).

In the present study, we wished to contribute to closing the gap between human and animal research by adopting a foraging paradigm that has been used to identify the spatially tuned cells in the rodent medial temporal lobe (Muller and Kubie, 1987), thereby increasing the similarity in setup and design between rodent and human experiments. We developed a visually sparse, open-field virtual environment (VE) and allowed participants to determine their own speed and direction of travel, while measuring brain activity using functional magnetic resonance imaging (fMRI). The level of active exploration and spatial processing demand was systematically varied across three different test conditions. With this paradigm we explored the brain regions that contribute to navigational and spatial memory processes during exploration of an open virtual environment. We also examined how hippocampal activation relates to both performance and spatial memory usage in this task. We hypothesized that, while exploring the VE already recruits the brain regions commonly found in navigation tasks (Boccia et al., 2014; Epstein et al., 2017), hippocampal activity would only be found when spatial memory demands are high (Eichenbaum, 2017b).

2 Methods

2.1 Participants

Thirty-three healthy, adult volunteers were recruited from the nearby university campus and the university hospital's employees. All participants were fluent in German, gave their written informed consent to participate in this study, and were reimbursed for their participation based on the time spent for the experiment. Six of these participants were then excluded from the study prior to analysis.

Three participants were excluded due to technical issues on the MRI machine, one participant resigned from the experiment, one participant was excluded due to an incidental pathological finding, and one participant was excluded due to low-quality MRI data. Twenty-seven participants (16 female) are included in the final analysis, ranging in age from 18 to 29 (mean: 24.6, SD: 2.8) years. All participants were right-handed except for one, however all movements during the experiment were executed with the right hand.

2.2 Virtual environment and setup

The virtual environment (VE) was custom made with Vizard (version 3, WorldViz, Santa Barbara, California, USA), a Python-based virtual reality development interface. The VE was kept constant throughout the experiment. It consisted of a texture-free blue sky, a ground plane, textured with fine-grained white noise and a cylindrical enclosure of 50 virtual meters (vm) in diameter and 15 vm high, that was white with black section of 100 degrees, and hereafter referred to as “landmark” (Muller and Kubie, 1987). Both the landmark and the height of the enclosure were the only landmark cues in the experiment; all other environmental features provided only optic flow information. The enclosed space is referred to as “arena” and can be seen in an areal view in Figure 1A. In addition to the environmental components, 50 collectable objects, referred to as “items”, were distributed with equal probability within the arena. These items could be blue spheres, red boxes, or green tori, each approximately 0.8 vm in diameter, but were all the same shape at one time. Items were positioned at participants’ virtual eye level for collection convenience. Importantly, items were only visible within a radius of 5 vm around a participant’s position or “scope” and within a participant’s field of view. This area is referred to as the “viewed area” and is visualized in Fig. 1C. Only items within the viewed area could be collected.

To navigate through the VE and to collect items, participants used a MRI-compatible joystick (HHSC-JOY-1 by Current Designs, Philadelphia, Pennsylvania, USA) that allowed them to change their viewing angle (simulating head rotation) and to move forward or backward along their current viewing direction (simulating body movement) by deflecting the joystick along its X - or Y -axis, respectively. Larger joystick deflection resulted in faster speed of the corresponding head rotation or body movement, but was limited to a maximum that was within the range of real-world movements. Items were collected by pressing either of two available joystick buttons. All participants controlled the joystick with their right, and the buttons with their left hand. In a training session prior to imaging (see Procedure), participants were trained in an upright position in front of a standard computer screen. During the MRI experiment, participants were supine and the VE was presented on MRI-compatible goggles (VisualSystem by Nordic Neuro Lab, Bergen, Norway) with a field of view of 52° which were fixed on the head coil and adjusted to fit participants’ eye distance and visual acuity. While participants were navigating in the VE, their position in the virtual space (as X , Y , and Z values in the VE), their virtual heading angle, and the number of items collected at each time point were recorded into a tab-delimited text file with a sampling rate of approximately 50 milliseconds.

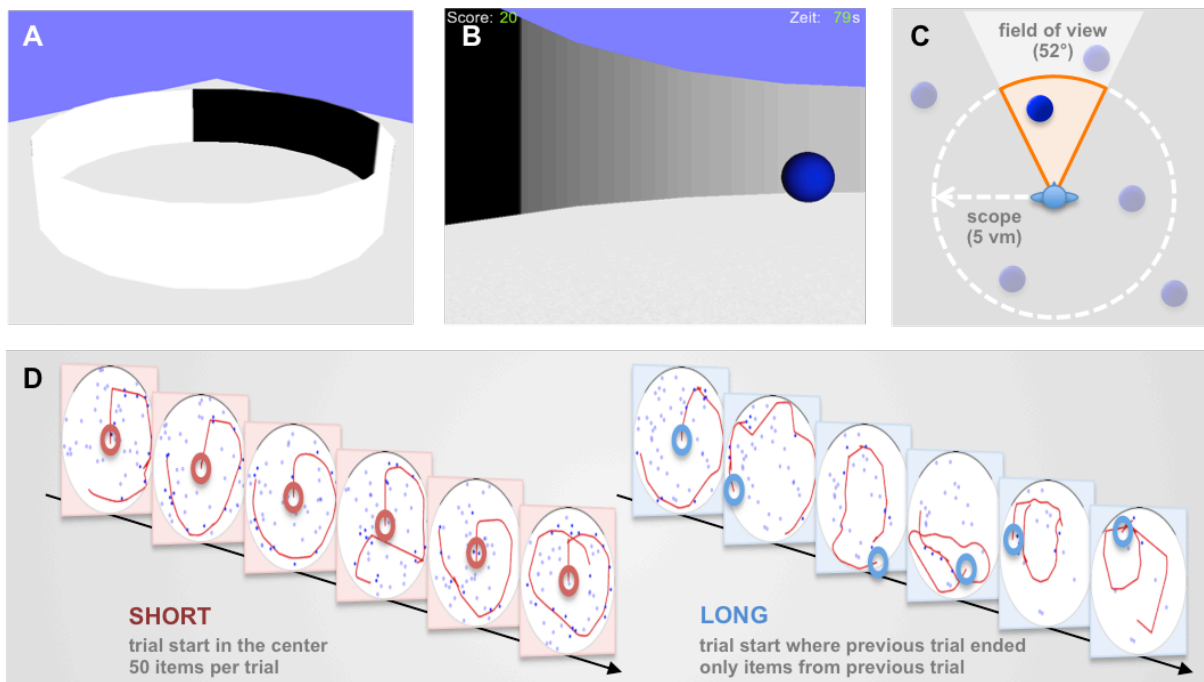


Figure 1: The virtual environment and active exploration conditions. (A) A bird's eye-view of the circular arena. Visual landmark information is limited to the black cue card, all other features providing only boundary, height, or optic flow information. (B) An example view of the arena as the participant saw it in the experiment. Virtual items were positioned at participants' virtual eye level. Counters at the top of the screen inform participants about the time elapsed and the number of items collected throughout the task. (C) Virtual items were only visible and collectable within the intersection of participants' scope and their virtual field of view, highlighted by the orange area. This area is considered the "viewed area" in our analysis. (D) Example tracks across all of the six trials in both of the active exploration conditions. In SHORT, each trial represented a single search task of 30 seconds duration, with 50 items. Participants always started in the centre of the (red shaded circle). In LONG, participants started the first trial in the centre of the arena. Subsequent trials continued from the last position in the previous trial, and only with items remaining from the previous trial (blue shaded circle). Each figure represents one trial. The participant's entire track (red line) from one trial is shown together with the items available (collected and missed items as small closed and open blue circles, respectively), and the trial start position located in the large red and blue circles (in SHORT and LONG condition trials).

2.3 Paradigm

Participants were tested on three different navigational test conditions termed "LONG", "SHORT", and "PASSIVE". Each navigational test condition was three minutes in total, broken up into six trials of 30 seconds duration each. The goal of each test condition was always to collect as many items as possible within the time allotted.

There were a number of differences between the three test conditions with the aim of testing different components of exploratory behaviour (Fig. 2). In the LONG condition, the 50 collectable items were randomly distributed only at the beginning of the first trial. The remaining items were in the same location as before. Already collected items were not restored. Hence, in order to efficiently collect

	LONG	SHORT	PASSIVE
task duration	180 s	6x 30 s	6x 30 s
exploration type	active exploration	active exploration	passive exploration
memory demand	high memory demand	low memory demand	no memory demand

Figure 2: A schematic overview of the test conditions and manipulations they achieve. Task duration and exploration type differed across the three test conditions LONG, SHORT, and PASSIVE, thereby varying the demand for memory of item locations in each condition. This way we were able to test for brain regions involved in high and low memory demand as well as during active and passive exploration.

as many items as possible, participants had to keep track of the already collected items' locations throughout all six trials and across the control conditions. Holding spatial information in memory over multiple seconds while performing an alternative task leads to decreased performance in patients with hippocampal lesions (Shrager et al., 2008) so we would expect the hippocampal activity in the LONG condition. Participants started the first trial in the center of the arena, facing the middle of the cue card. In each subsequent trial, participants continued from the same location and orientation as they ended the previous trial.

In the SHORT condition, the 50 collectable items were randomly distributed at the beginning of each 30-second trial. Participants started each trial at the center of the arena and had to collect as many of the 50 items as possible each time with whatever strategy worked best for them. In the PASSIVE condition, participants were passively moved through the arena. They could influence neither the speed, nor the direction or the viewing angle of their path. Their only task was to press one of the two joystick buttons to collect the items that appeared along their path. To keep the optic flow comparable between the active and passive conditions, the tracks used in the PASSIVE condition trials were chosen randomly from each participant's own active trials, either from the training or the actual experiment. All of the six PASSIVE trials in one complete condition were chosen from one of the other test conditions (LONG or SHORT); the other test condition was then used for the second repetition. In the PASSIVE test condition, participants do not require any form of spatial processing or memory.

In addition to the test conditions, a control condition was presented for 15 seconds in between subsequent trials of the same condition. The control condition was an even-odd discrimination task, known to be a good baseline condition for hippocampal studies (Stark and Squire, 2001). Digits between 1–9 were randomly presented and participants were asked to categorise the digit as even or odd as quickly as possible. Participants received short feedback on their choice in form of either a green smiley (correct answer) or a red “wrong!” (wrong answer) displayed on screen to motivate them to solve the task properly.

2.4 Procedure

One experimental run consisted of a single presentation of each of the three test conditions. Participants completed two runs during the MRI scanning such that each condition was tested twice per participant. The order of test conditions was balanced across participants such that all three test conditions were presented as a run's first, second, or third condition with approximately equal frequency across participants. To compensate for potential performance bias in the two active conditions, the order of the LONG and SHORT test conditions were always switched between each participant's first and second experimental run. A 30-second instruction screen preceded each test condition that labeled the upcoming condition and reminded participants to collect as many items as possible. Five seconds prior to each trial contained an information screen with the test condition, the upcoming trial number, the number of items still available in that trial and a picture of the items to be collected. After each trial, participants were given a five-second feedback that showed the number of items collected in that trial and a measure of performance to motivate them in each trial. We chose to provide them with the ratio of collected to available items in that trial and compared it to their mean ratio across previous trials in that condition. Therefore, each condition took a total of five minutes and 45 seconds including: 30 s instruction screen + 6 x (5 s info screen + 30 s search + 5 s feedback) + 5x 15 s odd-even task = 345 s.

The experiment consisted of two training days, followed by one MRI scanning session on a third day. On the first training day participants were presented with a written introduction to the experiment on the screen. Each of the two training days started with one full experimental run, followed by repetitions of the LONG and SHORT conditions in alternating order (i.e., LONG, SHORT, LONG, SHORT, and so on) until a participant had collected at least 85% of available items in LONG twice. Only when a participant achieved this on both training days were they qualified to participate in the MRI session.

Participants were all very familiar with the VE and the joystick controls, and were experienced in solving the task at the time of testing. This extensive training served two purposes. First, we wished to minimize learning effects and systematic performance improvements between the two experimental runs and to minimize effects of gaming experience. Second, training served to ensure that all participants could solve the task comparably well, thus reducing performance heterogeneity in our sample.

After the MRI scanning, participants filled out a questionnaire about the experiment including a question whether or not they recognised the tracks in the PASSIVE conditions as being from their own active trials to control for memory recall from the active to the passive condition.

2.5 MRI data acquisition

MRI data was acquired using a 3T Signa HDx (General Electric Healthcare, Milwaukee, Wisconsin, USA) operated with a standard 8-channels head coil and A/P phase encoding direction. Functional images were acquired using a single-shot echo planar imaging (EPI) sequence of 391 volumes per run, with 40 milliseconds echo time (TE), 2616 milliseconds repetition time (TR), 75° flip angle (FA), and axial slice order. Slices were ordered sequentially in top/down view order, with a slice thickness of

3.5 millimeters, and 2.29×2.29 millimeters in-plane resolution. Slice angulation was set to cover participants' whole brain and generally aligned to the anterior-posterior axes when possible; for some participants whole-brain coverage could only be achieved with slightly adapted angulation. Cerebellum and brain stem were included in the acquisition when possible. Five 'dummy scans' for T1 stabilization were recorded prior to each run; they were not reconstructed on the MRI machine. Acquisition of one functional run took 1024 seconds. An anatomical image of each participant's whole brain was recorded using a fast spoiled gradient recalled 3D sequence (FSPGR 3D), with an out of phase echo time (TE), 15° flip angle (FA), and 500 milliseconds inversion time (TI) after both functional runs. Slices were acquired with an in-plane resolution of 0.86×0.86 millimeters and a slice thickness of 0.7 millimeters, with interleaved slice order and bottom/up view order.

2.6 Behavioural data analyses

All of the analyses were performed in Matlab (version 2014b; The MathWorks, Natick, USA) with self-written scripts. Data were imported from the text-files and interpolated for equal temporal sampling prior to analysis. From the positional and item collection data we quantified participants' performance using the score, velocity, score to velocity ratio, as well as their spatial memory performance using the viewed-area measures "once viewed area" (OVA) and "total viewed area" (TVA). These measures are described in detail below. These values were calculated on an individual trial level and then averaged or summarised across all trials when necessary.

We extracted the score, or the number of items a participant collected in one trial, as a measure of performance since the goal of all test conditions was to collect as many items as possible in one 30 second trial. For the LONG condition we also calculated the total score across the 6 trials of one test condition, since the items were not replaced after each trial. The score is limited to 50 items and can have a minimum value of zero.

Velocity was computed as the distance travelled within one trial, divided by 30 seconds, the duration of a single trial. Assuming participants were still able to collect items at faster speeds, the faster participants should perform better. Neither score, nor speed were useful measures for comparing participants' behaviour across the two active exploration conditions. We therefore additionally calculated the score/velocity ratio, where velocity was defined as a participant's trajectory length in vm, divided by the trial duration (i.e., 30 seconds), and score the total number of items collected in that trial.

For the LONG condition, participants that view more of the entire arena across all six trials should perform better on the task. Therefore, we additionally considered measures involving the "viewed area", the area inside the virtual arena that lies both within a participant's scope and its field of view for each time point in each trial of the LONG condition (see Fig. 1C). The viewed area was assessed numerically by overlaying the arena with a 500×500 grid of 0.1×0.1 vm each, and counting the number of times a participant's viewed area covered that bin. For the same bin to be counted as viewed again, at least five seconds must have passed, otherwise it was still considered the first view. Bins that did not fully fall within the arena's area were discarded for the analysis. The resulting histogram

across all trials of one LONG condition was referred to as “total viewed area”. Additionally, the “once viewed area” was calculated from this histogram: the OVA was defined as the area (i.e., number of bins) that was covered only once throughout the duration of a condition. The theoretical maximum for both values was $1,972 \text{ vm}^2$ and due to the numerical estimation differs slightly from the arena’s geometrically exact total area of $1,963 \text{ vm}^2$ (difference 0.4%).

To assess spatial memory within individuals, the “viewed area” measures are not useful on their own because they are highly dependent on participants’ individual velocity. Instead we calculated for each participant, and for each LONG condition separately, the ratio of OVA to TVA. This measure is unitless and independent of velocity. It describes how much of the total area that each participant viewed on the LONG condition, they only saw once. High values therefore represent a better spatial memory performance. To achieve this in LONG, participants must keep track of previously visited locations in the arena, over all six of the trials. Values are between 0 and 1; 0 meaning that the parts of the arena that the participant saw, it saw more than once, and 1 meaning that the participant never saw any part of the arena more than once.

Using the behavioural variables described above, we tested whether or not the two experimental runs differed from one another, in order to check that the two runs were comparable in terms of behaviour. For this we used paired (dependent) two-tailed *t*-tests or, for non-parametric data based upon the Shapiro-Wilk test for normality, the Wilcoxon signed-rank test was used. We examined whether the score-to-velocity ratio differed between the six SHORT trials using a two-way repeated measures ANOVA with factors run (two levels) and trial (six levels). Finally, we used the average score and average OVA/TVA for each participant across runs to correlate behavioral activity with brain activity between participants.

2.7 MRI data analysis

All stages of preprocessing and analysis of MRI data were conducted in SPM8 (version 6313; www.fil.ion.ucl.ac.uk/spm), using Matlab (version 2013a; The MathWorks, Natick, USA), except where otherwise noted.

Prior to any analysis the functional images were visually checked for artifacts using the function to detect abnormal slices from Volumes toolbox for SPM developed by Volkmar Glauche (version r630; sourceforge.net/projects/spmtools/). Here we identified small joystick-related movement artifacts in the data and therefore used the SOCK automated independent component analysis (ICA) algorithm (Bhaganagarapu et al., 2013) to clean the data before continuing with the preprocessing. Preprocessing and estimation of the independent components for SOCK was done as described in Bhaganagarapu et al. (2013) in FSL (version 5.0.7; fsl.fmrib.ox.ac.uk/). The resulting adjusted fMRI data were kept in native participant space for further analysis.

All MRI data were manually repositioned so that the origin of the images was approximately located at the anterior commissure. Realignment parameters were estimated for the functional images, and the structural image was then coregistered to the mean functional image that resulted from realignment. Next, the coregistered structural image was segmented with unified segmentation for SPM8 based

on the ICBM European brains space template using very light regularization parameters. All images were then normalized to MNI space and voxel values recalculated to $1.7 \times 1.7 \times 1.7$ millimeters for the functional images and $1 \times 1 \times 1$ millimeters for the structural image. Images were finally spatially smoothed using a Gaussian kernel (FWHM of $6 \times 6 \times 6$ millimeters). SPM default values were used for all above steps, except where mentioned otherwise.

For each participant, the LONG, SHORT, and PASSIVE conditions of each of the two runs were modeled separately as blocks of 30 seconds each convolved with the canonical hemodynamic response function (HRF) and together with the six estimated rotation and translation movement parameters served as independent variables for a mass univariate linear regression. The control condition was not explicitly modeled, but the mean signal across each run was. Temporal correlations were modeled using an AR(1) autocorrelation model. Contrasts were created for each of the test conditions (LONG, SHORT and PASSIVE) as well as difference contrasts between the three test conditions.

All contrasts from the single-subject analysis were then evaluated individually with *t*-tests on the group level. We additionally assessed the correlation between participants' behaviour in the LONG exploration task and their BOLD response in the LONG > SHORT contrast to look for regions with variability in the BOLD signal that correlates with spatial memory behaviour. Behaviour was represented by their score and their ratio of once to total viewed area (OVA/TVA), both as separate covariates in the same model. These values were defined as either the sum of scores or the sum of OVA/TVA ratio, respectively, across the two repetitions of LONG.

Because we were interested in both whole-brain activity as well as smaller clusters in subcortical regions like the hippocampus, we chose to statistically evaluate the activity with cluster-based methods using the threshold-free cluster enhancement (TFCE) method (Smith and Nichols, 2009). We used the TFCE toolbox for SPM developed by Christian Gaser (version r95; `dbm.neuro.uni-jena.de/tfce/`) that adds this functionality to SPM. Statistical parametric maps were corrected for multiple comparisons and all results reported here exceed the corresponding voxel-level height threshold of $p < 0.05$ (familywise error rate; FWE), except where otherwise noted.

In addition, we sought to determine those brain regions common to both active exploration conditions when compared against the passive task. We therefore calculated a conjunction of LONG > PASSIVE and SHORT > PASSIVE, in which only those voxels were included that were present in both contrasts.

We were specifically interested in the activity of the hippocampus in this task. Therefore, in addition to the whole-brain analysis, we analysed all contrasts using the bilateral hippocampal formation as a region of interest (ROI). Analyses were carried out using the TFCE toolbox for SPM, and results were corrected for multiple comparisons at the $p < 0.05$ (FWE) level, similar to the whole-brain analyses described above. To create the mask for the ROI analyses, we used the left and right hippocampus templates of hippocampal subfields CA1, CA2, CA3, the dentate gyrus, and subiculum (Amunts et al., 2005) from the Anatomy toolbox for SPM (version 2.2b) (Eickhoff et al., 2006b, 2007, 2005). We multiplied them with the grey matter mask obtained from the mean image of all participants' structural images after preprocessing. The resulting mask contained all grey matter voxels that fell into any of

either the bilateral hippocampus proper or the bilateral subiculum, and was used to restrict the ROI analyses of the hippocampal formation to this set of voxels.

3 Results

3.1 Behaviour

Behaviour in the passive task was not analysed in depth. However, we checked that all participants collected the items when they appeared on the screen, suggesting that they correctly followed instructions and were engaged in the task. Further, in a post-experiment interview, no participant reported to have recognised the presented tracks in PASSIVE as their own previous tracks.

Participants did not show a significant difference in behaviour between the two runs of LONG that could be indicative of learning or fatigue effects, neither with regard to their score (paired t test: $t(26) = -1.01$, $p = 0.32$) nor to their once-to-total viewed area ratio (paired t test: $t(26) = 1.06$, $p = 0.30$). We therefore later used the respective averages across the two runs reported above as covariates in the group level analysis of LONG > SHORT.

Participants showed similar performance between each other and compared to training in the LONG testing session. They collected 83.6% (mean: 41.8, SD: 2.5) of the 50 items available in LONG, averaged across runs and participants. Participants collected between 34 and 47 (mean: 41.4, SD: 3.2) in the first, and between 32 and 49 (mean: 42.2, SD: 3.3) items in the second run.

Interestingly, we saw a wider variety in how much of the arena participants viewed in the LONG condition. Example trajectories from four subjects can be seen in Fig. 3. Participants' ratio of once-to-total viewed area assesses how well a participant remembered previously visited locations in the VE, under the assumption that participants aim to explore and collect items in the VE efficiently. Participants achieved once-to-total viewed area ratios between 0.25 and 0.62 (mean: 0.41, SD: 0.10) in the first, and between 0.18 and 0.60 (mean: 0.39, SD: 0.11) in the second run, which equals an average of 40% of total (mean: 0.40, SD: 0.09) across both runs of LONG. We found no correlation between score and the ratio of once-to-total viewed area in any of the two runs (Pearson's r : $r = 0.02$; $p = 0.89$), suggesting that OVA/TVA was an important additional measure to examine.

To examine possible differences in behaviour between the LONG and the SHORT condition, we used the velocity and the score-to-velocity ratio in the first trial, as none of the other measures were comparable between tasks and runs (see Supplement, Figs. 6, 7, 8, 9). We first tested participants score-to-velocity ratio across SHORT employing a two-way repeated measures ANOVA with factors run and trial to see whether the first trial in SHORT was comparable to all other trials. This revealed no significant main effect for run ($F(1, 312) = 0.30$, $p = 0.58$), nor for trial ($F(5, 312) = 0.25$, $p = 0.94$), nor did this show any interaction effect between run and trial ($F(5, 312) = 0.77$, $p = 0.57$), suggesting that participants showed rather consistent behaviour across both trials and runs during the short exploration task. We then tested the difference in participants score-to-velocity ratio between the LONG and SHORT condition in the first trial. This revealed statistically marginal differences between the two

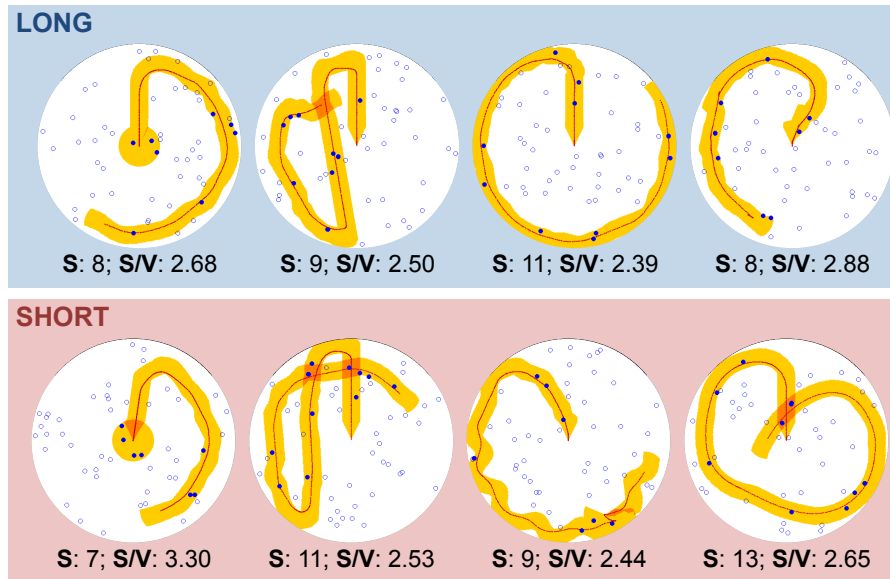


Figure 3: Individual variability in exploratory behaviour. First trial of the LONG and SHORT test conditions for 4 example subjects. As in Fig. 2, each circle represents an areal view of the arena for the respective condition's first trial. The participant's track is depicted with a thin red line, and collected and missed items are shown as closed and open blue circles, respectively. The viewed area is depicted as a semi-transparent thick yellow line. When participants view an area more than once, the line becomes orange. The score and the score/speed ratio are shown below (S and S/V, respectively). Note that each trial took 30 seconds; therefore longer path length indicates higher velocity. Participants showed a range of different exploration strategies. Individual participants either applied a similar or different strategies for the LONG or SHORT test condition.

conditions (paired t tests: $t(26) = -1.68$, $p = 0.11$ [1st run]; $t(26) = -1.84$; $p = 0.08$ [2nd run]), thus indicating marginal differences in participants' behaviour between the two active navigation tasks.

A qualitative examination of the participants' paths and behaviour also revealed that participants used highly varying exploration strategies to solve both the LONG and the SHORT test conditions, but that they tended to be internally consistent.

3.2 Passive exploration

We were first interested in the base network of brain regions that were involved in passive exploration, even if the participants did not have control over where they traveled in the arena (Fig. 4A; Tab. 1). To perform well in this task, it was therefore not necessary for participants to efficiently navigate through the VE nor for them to remember visited locations along the traveled path, but rather to focus their attention on items that would appear at unpredictable times and locations on the screen.

Activation observed in the BOLD response during the PASSIVE condition is found in several regions considered key nodes in the dorsal and ventral attention networks (Corbetta et al., 2008; Corbetta and Shulman, 2002) and that are often found in navigational experiments. We found activity in the left and right anterior temporoparietal junction (TPJ), in the right frontal eye fields (FEF) at the region between the posterior end of the superior frontal gyrus and the superior pre-central sulcus, in

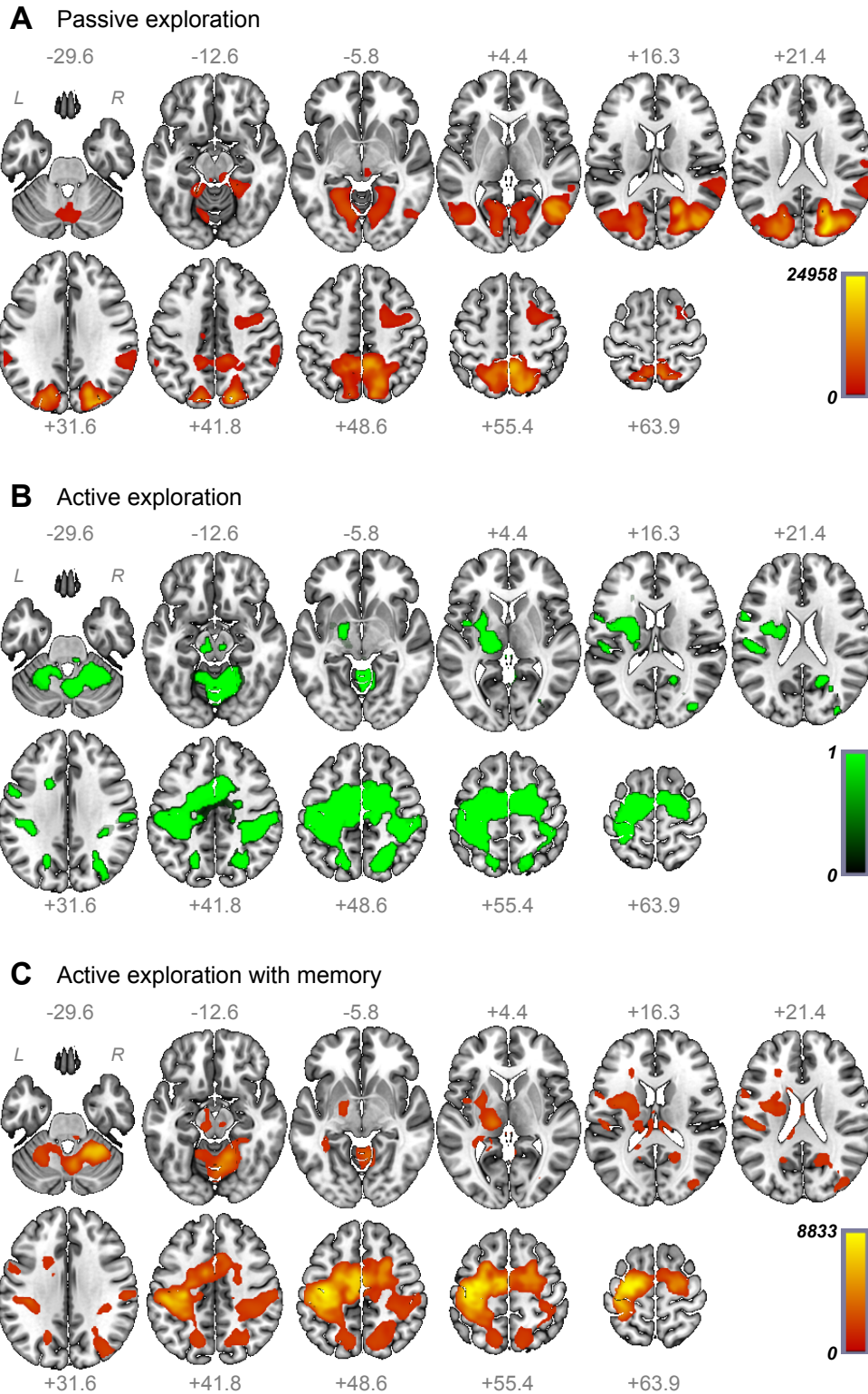


Figure 4: Brain activity during active and passive exploration. Axial slices of brain activity revealed in the PASSIVE condition (A), the conjunction of LONG > PASSIVE & SHORT > PASSIVE (B), and the LONG > PASSIVE contrast (C). All slices are reported with respect to their corresponding Z coordinate in millimetres in MNI space, and activity is overlaid on the MNI152 T1 template provided with MRICroGL (www.mccauslandcenter.sc.edu/mricrogl/) that is based on the ICBM 2009b Nonlinear Asymmetric 0.5mm T1 template image from (Fonov et al., 2009).

the right posterior middle temporal gyrus (pMTG), and in the dorso-medial bank of the intraparietal sulcus (IPS) in both hemispheres. Further activation was found in areas 7A and 7P of the superior parietal lobule (SPL) and in parts of the precuneus that have been found during attention pursuit (Gillebert et al., 2013; Ohlendorf et al., 2007), stimulus-driven attention reorientation (Shulman et al., 2009), and that corresponded to attention-grabbing events while participants were passively moved through a complex VE (Nardo et al., 2011).

Notably, the uncorrected ($p < 0.001$) non-TFCE T contrast (not shown) also reveals activation of the right anterior insula, right inferior frontal gyrus, and the FEF bilaterally. These regions are attributed to the ventral attention network, and their activation pattern shows the well-known right lateralisation of attention-related processes (Corbetta et al., 2008; Corbetta and Shulman, 2002). This further supports the notion that the BOLD response observed in PASSIVE strongly reflects the passive exploration task's attentional demands.

We also found activity in the left cingulate sulcus at the transition between the anterior and posterior cingulate cortex, a region suggested to contain the cingulate eye fields (CEF; Gaymard et al., 1998; Pierrot-Deseilligny et al., 2004) and to be particularly egomotion-sensitive (Wall and Smith, 2008), in the superior colliculi (Mysore and Knudsen, 2011), and the oculomotor vermis VI, VII/VIII (Diedrichsen et al., 2009). All these regions are part of the human gaze control networks and are also closely associated with the visuospatial attention control regions mentioned above (Vernet et al., 2014). In addition to the activation attributed to eye movement and attention control networks, we observed strong bilateral activation in the lingual gyrus and the visual cortices (V1, V2, V3, V4) of the occipital lobe, in the human motion complex in the middle temporal cortex area MT/V5 (Watson et al., 1993; Zeki et al., 1991), and in the dorsalmost part of parieto-occipital fissure that has been suggested to contain the egomotion-sensitive human visual cortex V6 (Cardin and Smith, 2010; Pitzalis et al., 2006, 2010). Given the continuous optic flow experienced in the passive task, these regions are expected to be found also during PASSIVE exploration.

Interestingly, the passive exploration task also revealed significant BOLD responses in regions typically associated with spatial navigation tasks. First, large parts in the dorsal region of the precuneous cortex show significant activation bilaterally. We also found bilateral activation in the anterior lingual gyrus and extending into the posteriormost part of the parahippocampal gyrus, a region termed parahippocampal place area (PPA) due to its involvement in scene processing and recognition (Epstein and Kanwisher, 1998; Epstein, 2008). Parts of the retrosplenial complex (RSC; Epstein, 2008) of both hemispheres were also active, a functionally defined region comprising the posterior Brodmann areas BA 29 and BA 30 (i.e., the retrosplenial cortex; Maguire, 2001; Morris et al., 2000) and regions further posterior, reaching towards the merging point of calcarine sulcus and parieto-occipital fissure (Epstein, 2008). It should be noted that we only found activation in the region posterior to the retrosplenial cortex and not spanning the retrosplenial cortex proper (Silson et al., 2016; Vann et al., 2009). This also is the area that commonly shows the peak scene-selective activity associated with the RSC, and therefore has recently been termed the medial place area (MPA) in order to clearly distinguish it from the retrosplenial cortex proper (Silson et al., 2016). Finally, we found significant BOLD response in and around the anterior half of the transverse occipital sulcus, again in both hemispheres. This

X	Y	Z	peak region	k	covered regions
<i>Contrast PASSIVE</i>					
+22.3	-84.8	+24.8	R occipital cortex	28294	L+R brainstem, L+R cerebellum, L+R parahippocampal gyrus, L+R lingual gyrus, L+R fusiform gyrus, L+R lateral occipital cortex, L+R medial occipital cortex, R supramarginal gyrus, R angular gyrus, R secondary somatosensory cortex, L+R superior parietal lobule, L+R precuneous cortex, L+R cuneal cortex
+39.3	-4.9	+45.2	R premotor cortex	1652	R premotor cortex, R superior frontal gyrus
-61.0	-38.9	+35.0	L supramarginal gyrus	282	L supramarginal gyrus
-11.7	-18.5	+38.4	L cingulate gyrus	95	L cingulate gyrus
<i>Contrast LONG > PASSIVE</i>					
-30.4	-13.4	+58.8	L motor cortex	39896	L+R brainstem, L+R cerebellum, L+R lingual gyrus, L+R fusiform gyrus, R parahippocampal gyrus, L+R thalamus, L putamen, L pallidum, L insular cortex, L+R lateral occipital cortex, L+R precuneous cortex, L central opercular cortex, L secondary somatosensory cortex, L+R supramarginal gyrus, L+R postcentral gyrus, L+R superior parietal lobule, L+R cingulate gyrus, L+R paracingulate gyrus, L+R primary somatosensory cortex, L+R superior frontal gyrus, L+R premotor cortex, L primary motor cortex

Table 1: Brain activity during passive exploration and active exploration with memory. Table shows all significant (voxel-wise FWE corrected $p < 0.05$) cluster peak voxels for the indicated contrast, with corresponding location by coordinates in MNI space in millimetres (X, Y, Z) and anatomical region (peak region), cluster’s size in voxels (k), and remaining anatomical regions covered by the corresponding cluster (covered regions). Corresponding brain hemispheres are reported for each region listed (L: left, R: right). Note that, for each cluster, only the cluster’s peak voxel location is reported.

region has been reported to be selectively involved in scene processing, similar to the PPA, and therefore has been termed the occipital place area (OPA; [Dilks et al., 2013](#); [Grill-Spector, 2003](#); [Nasr et al., 2011](#)). These three regions, PPA, RSC, and OPA, are commonly referred to as scene-selective regions due to their prominent and selective engagement in visual scene processing ([Dilks et al., 2013](#)). It should be noted though that this term is somewhat misleading, as these regions are equally involved in processing of objects that make potential landmarks as well ([Epstein et al., 2017](#)).

3.3 Active exploration

Next, we were interested in brain regions generally involved in active exploration of our VE compared to passive exploration. In contrast to the passive exploration task, both the long and short exploration tasks required participants to actively navigate through the VE. To identify brain regions commonly active in both active navigation conditions compared to the passive condition, we employed a con-

junction of the two group level contrasts LONG > PASSIVE and SHORT > PASSIVE, in which only voxels that reached statistical significance in both contrasts are included (Fig. 4B; Tab. 2).

In the active exploration conditions, in contrast to the passive task, participants had to control the joystick in order to navigate the environment. All participants were required to use their right hand with the joystick and press the button to collect items with any finger of their left hand. Accordingly, we observed left-lateralized activity in the primary motor cortex, BA4a and BA4p (Geyer et al., 1996); in the left supplementary motor area (SMA; Neubert et al., 2015); in the left and, to a lesser extent, the right dorsal premotor cortex; in the left ventral premotor cortex regions 6r of the central opercular cortex region and 6v of the opercular part in the inferior frontal gyrus (Neubert et al., 2014)¹; in the supplementary motor area (SMA) in both hemispheres (Neubert et al., 2015); and in the left and right posterior part of the caudal cingulate zone (CCZ) and the posterior rostral cingulate zone (RCZp), both of which are considered parts of the cingulate motor area (CMA; Neubert et al., 2015). We further found subcortical activation in those parts of the left putamen that have been found to show strong anatomical connections with the premotor and motor cortices (Tziortzi et al., 2014); in the internal and external left globus pallidus; and in left thalamic subregions reported to have strong anatomical connections with posterior parietal, premotor, primary motor, and sensory cortices (Behrens et al., 2003a,b; Johansen-Berg et al., 2005).

Controlling the joystick in the active exploration tasks also requires grasping and deflecting the joystick – in contrast to the passive exploration where participants did not deflect or grasp the joystick at all – which, in addition to motor control processing, also involves a somatosensory component. Accordingly, we found activation in the primary somatosensory cortices of the left (Brodmann areas BA1, 2, 3a, 3b) and right (BA2, 3a, 3b) hemispheres, and in the caudal part of the left secondary somatosensory cortex, labelled OP 1 (Eickhoff et al., 2006a,c), associated with somatosensory perception and tactile activation maps (Burton et al., 2008a,b; Eickhoff et al., 2010). We further observed activation in the left and right cerebellar hemispheres in regions V and VI (Diedrichsen et al., 2009), and in crus regions I and II (Diedrichsen et al., 2009), that have been associated with sensorimotor processing and motor execution in a recent meta-analysis of cerebellar function (Stoodley and Schmahmann, 2009).

Apart from the aforementioned motor and perception regions, the conjunction analysis further revealed activation mostly in regions that already showed a significant BOLD response in PASSIVE. This includes the right FEF (Vernet et al., 2014); the superior parietal lobule regions 7P in the right hemisphere, and 7PC in the left hemisphere (Scheperjans et al., 2008a,b); the right OPA; and the right RSC. We also observed activations along the bilateral ventral branches of the IPS (vIPS; sometimes also referred to as the IPS-PO) that lie deepest inside the parietal lobe and that partly overlap with regions already observed in PASSIVE.

¹Neubert et al. (2014) only labeled regions in the right brain hemisphere. The regions reported here to be 6r and 6v are located in the left hemisphere and therefore should be considered to fall into the putative left homologues of the regions reported in (Neubert et al., 2014).

X	Y	Z	centre region	k	covered regions
<i>Conjunction (LONG > PASSIVE) AND (SHORT > PASSIVE)</i>					
-4.2	-24.1	+49.5	L posterior cingulate gyrus	21483	R lateral occipital cortex, L opercular cortex, L+R supramarginal gyrus, L+R cingulate gyrus, L+R paracingulate gyrus, L+R juxtapositional lobule cortex, L+R superior frontal gyrus, L precentral gyrus, L+R postcentral gyrus
+4.7	-54.7	-19.5	R cerebellum	8325	L+R cerebellum, L+R brainstem
-24.7	-8.4	+9.0	R putamen	2952	L putamen, L pallidum, L thalamus, L insular cortex
-54.8	+4.7	+26.6	L precentral gyrus	317	L precentral gyrus
+19.0	-56.7	+20.4	R precuneous cortex	183	R precuneous cortex
-16.1	+12.0	+29.1	L white matter	160	L white matter
+6.1	-21.5	-16.7	R brainstem	104	R brainstem
-22.9	+27.9	+11.8	L white matter	32	L white matter
-3.2	-88.2	-20.2	L inferior occipital lobe	2	L inferior occipital lobe
-22.8	-33.8	+6.1	L white matter	2	L white matter

Table 2: Active exploration. Table shows the location of each cluster’s centre of gravity in MNI space in millimetres (X, Y, Z) and the corresponding anatomical region (centre region), the cluster’s size in voxels (k), and remaining anatomical regions covered by that cluster (covered regions). Each anatomical region is reported with the corresponding hemisphere (L: left, R: right).

3.4 Active exploration with memory

We were highly interested in revealing those brain regions that are involved in navigation with memory, so we looked closer into the LONG condition and compared it first against the PASSIVE navigation task – which shows regions involved in active navigation with memory – and then against the SHORT active navigation condition – which was designed to reveal brain regions specifically related to memory processes during active navigation.

LONG > PASSIVE shows, in addition to all regions already revealed by the conjunction analysis mentioned above, activation of two more regions. First, additional activation was found in the left and right parahippocampal and adjacent temporal fusiform cortices; and second, complementing the right RSC region activation already revealed in the conjunction analysis, there is also RSC activity found in the left hemisphere (Fig. 4C; Tab. 1). No activation was found in the hippocampus, and the ROI analysis for the hippocampus does not show any statistically significant BOLD response in LONG > PASSIVE either.

LONG > SHORT, the contrast designed to precisely assess the impact of memory demand in our spatial exploration task, revealed no statistically significant activity, neither in the whole brain analysis, nor in the hippocampus ROI analysis.

3.5 Individual differences

Finally, we were interested in the relationship between participants’ brain activity and their behaviour during the active navigation tasks. The different strategies applied by participants to solve the long

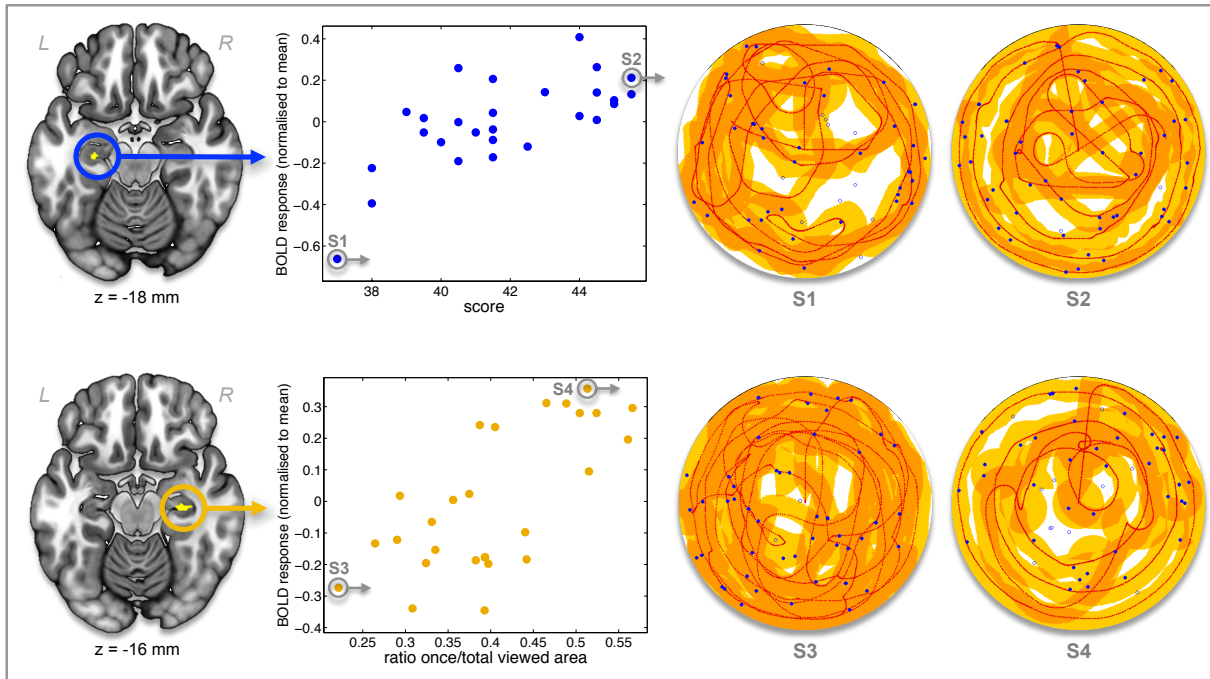


Figure 5: Individual differences correlate with hippocampal brain activity. The hippocampal BOLD signal during long against short exploration corresponds with participants' average score (**upper row**) and average ratio between once and total viewed area (**lower row**) in the long exploration condition. Voxels that show statistically significant ($p_{FWE} < 0.05$) correlation with participants' behaviour are shown in the left panels. Middle panels show corresponding correlations and highlight two sample participants – one at each end of participants' behavioural spectrum. Detailed behaviour of highlighted sample participants is displayed as a top-down view on the virtual arena in the two right-most panels, showing participants' track (red), collected (blue dots) and missed (blue circles) items, and Once (yellow) and repeatedly (orange) viewed areas.

exploration task show that behaviour in this condition in fact differed across participants and suggest a correlation also on a neuronal level that should be reflected in the BOLD signal. It has also often been reported that participants' brain activity in a navigation task correlates with their performance (Baumann et al., 2010; Hartley et al., 2003; Janzen et al., 2008; Mellet et al., 2010; Rauchs et al., 2008; Wolbers et al., 2007), and we hypothesise that a particular task's memory demand is the driving factor that underlies this correlation in these studies.

In the present study, we examined the between-subjects correlation of participants' neural activity with their behaviour as quantified by score and the ratio of once-to-total viewed area. For score, the whole brain analysis showed no statistically significant activation, but the hippocampal ROI analysis revealed statistically significant BOLD response in a cluster of 8 voxels in the left anterior medial hippocampus, with the peak voxel located at $x = -27.0$ mm, $y = -18.5$ mm, $z = -17.7$ mm in MNI space. Similarly, the whole brain analysis with participants' ratio of once-to-total viewed area as a covariate showed no statistically significant effects, but the hippocampal ROI analysis revealed a statistically significant effect in a cluster of 12 voxels in the right anterior medial hippocampus, with the peak voxel located at $x = 29.1$ mm, $y = -18.5$ mm, $z = -16.0$ mm in MNI space (Fig. 5).

Relaxing the significance level from $p_{\text{FWE}} < 0.05$ to $p_{\text{FWE}} < 0.15$ shows that the positive correlation of participants' BOLD response with increasing once-to-total viewed area ratio extends from the intermedial to anterior hippocampus, and, notably, in both hemispheres (not shown). For score, in contrast, no such subthreshold activation is found, indicating a clearly unilateral effect located in the right hippocampus.

4 Discussion

The goal of this study was to disentangle the contribution of different brain regions to the varying navigational and spatial memory demands during naturalistic navigation, and particularly to examine the role of the hippocampus in spatial exploration. Inspired by a classic foraging paradigm used to investigate path integration and spatially tuned cells in the rat medial temporal lobe, we designed a visually sparse open field VE, within which participants freely navigated to forage for hidden items. We recorded participants' brain activity and behaviour during passive exploration, short active exploration, and long active exploration in this VE, thereby varying the task's navigational and spatial memory demands. We found that passive exploration recruited central dorsal and ventral attention network hubs, along with scene-selective regions OPA, PPA, and RSC. Active exploration of the VE further increased activity of dorsal attention regions vIPS and SPL, and the scene-selective regions. We did not find a significant group effect for increased spatial memory demand between long and short exploration, and in particular no additional hippocampal activity during the LONG condition. However between-subjects task success and spatial memory usage was positively correlated with left and right anterior hippocampal BOLD response, respectively.

4.1 Passive exploration

The passive exploration condition in our paradigm was designed to be free of navigational and spatial memory demands in that participants neither had to navigate nor to keep track of previously visited arena locations. Instead, participants were moved through the VE along their own previous tracks that had been recorded during the trials in the two active navigation conditions, LONG and SHORT. Participants consequently could not influence the route taken (i.e., navigate) and therefore also did not need to memorise and recall the locations visited along the path. Instead, in order to collect as many items as possible, they had to pay close attention to items that would appear at unpredictable times and locations on the screen. The PASSIVE condition thus constitutes a 3D visuospatial attention task rather than a navigation task.

This notion is well reflected in the BOLD response recorded during PASSIVE (Fig. 4A), which shows prominent activity in regions attributed to the dorsal and ventral attention networks (Corbetta et al., 2008; Corbetta and Shulman, 2002). The observed right lateralization of activation in these regions, particularly with regard to the FEF, TPJ, and right insula, is a phenomenon commonly reported in studies on attention control and stimulus-driven attention reorientation (Corbetta and Shulman, 2002; de Schotten et al., 2011; Shulman et al., 2009). Relatedly, a significant BOLD response is also

found in several regions commonly reported to be involved in both attention control and eye movement control (Vernet et al., 2014), namely in the posterior cingulate cortex in a region suggested to contain the CEF (Gaymard et al., 1998; Pierrot-Deseilligny et al., 2004), in the superior colliculi, and the cerebellar oculomotor vermis.

In addition to the ventral and dorsal attention networks, the BOLD response in PASSIVE also revealed the ventral and dorsal visual processing pathways (Macko et al., 1982; Mishkin et al., 1983; Ungerleider and Mishkin, 1982), including the visual cortices, human motion complex, lingual and fusiform gyrus, and parts of the posterior parietal cortex. These regions are, to varying degrees, under control of the attention networks or themselves involved in controlling attention (Gilbert and Li, 2013; Meehan et al., 2017), and considered to extract object feature and location information from the stream of visual sensory input (Goodale and Milner, 1992; Kravitz et al., 2011; Mishkin et al., 1983; Ungerleider and Mishkin, 1982). It has been proposed that the dorsal stream gives rise to three more distinct pathways in the posterior parietal cortex with one of which, termed the parieto-medial temporal pathway, targeting the medial temporal lobe, both directly and via the retrosplenial cortex and posterior cingulate cortex, thereby providing information particularly relevant for navigation (Kravitz et al., 2011).

Interestingly, we also found activity in the OPA, PPA, and RSC – regions that are frequently reported to be involved specifically in spatial scene² perception and landmark processing (e.g. Dilks et al., 2013; Epstein, 2008; Epstein et al., 2017; Epstein and Vass, 2014; Hodgetts et al., 2016). Their specific individual contributions, however, are still heavily under investigation and a clear picture has not yet emerged (Lescroart et al., 2015). Our study suggests that these regions contribute to the attentional components of navigation that are also part of passive movement but not to the active components of navigation.

The OPA has been reported to be causally and selectively involved in scene perception (Dilks et al., 2013) and particularly during first-person perspective motion through scenes (Kamps et al., 2016b); to encode specifically local rather than the global elements of a scene, compared to PPA and RSC (Kamps et al., 2016a); to be sensitive to egocentric distance information (Persichetti and Dilks, 2016); to be specifically involved in spatial memory retrieval of boundary- compared to landmark-tethered objects (Julian et al., 2016); and also to automatically encode navigational affordances in scenes even when they are not task-relevant (Bonner and Epstein, 2017). The OPA has been suggested to contribute the perceptual features of scenes, particularly those of environmental boundaries, to scene perception and navigation (Julian et al., 2016; Marchette et al., 2015; Troiani et al., 2014).

The PPA has not only been associated with various different aspects of scene processing, but, more specifically, has been suggested to be particularly involved in landmark recognition and coding of landmark identity (Epstein and Vass, 2014; Marchette et al., 2015). It has, for example, been shown to respond specifically to objects suitable as landmarks, either due to their particular features (Troiani et al., 2014) or due to their presence at navigationally relevant locations in the environment (Janzen and van Turennout, 2004).

²Most papers on this topic consider a scene to consist of an overall spatial layout, and the objects in it, that can be captured in a single view (for details, see MacEvoy and Epstein, 2011).

The RSC has also been attributed to landmark recognition (e.g. [Auger et al., 2012](#); [Epstein and Vass, 2014](#)), however in a broader context in which the RSC is suggested to help translating locations between world-centered (allocentric) and self-centered (egocentric) frames of reference, thereby enabling orientation in one's environment ([Burgess et al., 2001](#); [Byrne et al., 2007](#); [Epstein and Vass, 2014](#); [Kravitz et al., 2011](#); [Marchette et al., 2015](#); [Vann et al., 2009](#)).

A division of labour amongst these three regions has thus been proposed (e.g. [Epstein et al., 2017](#)), whereby the OPA is considered the perceptual source of an environment's visual features and boundary information ([Julian et al., 2016](#)), with the PPA being involved in landmark recognition and identity coding ([Epstein, 2008](#); [Epstein and Vass, 2014](#); [Marchette et al., 2015](#)), and the RSC retrieving spatial and conceptual information about the coded places ([Epstein and Vass, 2014](#); [Marchette et al., 2015](#)). We therefore speculate that, with respect to the BOLD response observed in PASSIVE, activity in these regions can be explained by the OPA updating the boundary information which constantly changes as a participant is moved through the VE; the PPA being activated by the constantly changing scene and particularly when one of the black cue card's two borders are within a participant's field of view; and the RSC providing the participant with a sense of orientation in our visually sparse VE.

Taken together, we suggest that, despite the passive exploration task merely being a form of real-world visuospatial attention task that requires participants to only attend to items "popping up" at unpredictable times on the screen, processes in OPA, PPA, and RSC are so automated that they occur even in the absence of active navigation.

4.2 Active exploration

The conjunction of brain activity for both active exploration conditions shows activations in premotor, primary motor, and somatosensory cortex, as well as in the CMA, SMA, putamen, globus pallidus, thalamus, and cerebellum, thus strongly reflecting the additional motor demand and sensorimotor processing associated with controlling the joystick.

The conjunction also revealed large activations in the posterior parietal cortex (PPC) that can be further divided to fall into two distinct PPC regions: the dorsal SPL, and the vIPS. Both regions are considered parietal hubs in the frontoparietal attention network and have been reported to be involved in a number of different tasks, including visuospatial attention control ([Corbetta et al., 2008](#); [Corbetta and Shulman, 2002](#); [Hutchinson et al., 2009](#); [Molenberghs et al., 2007](#)), execution of grasping and reaching hand and arm movements ([Konen et al., 2013](#)), storage and manipulation of items held in working memory ([Humphreys and Lambon Ralph, 2015](#)), and perceptual search tasks ([Sestieri et al., 2010, 2017](#)). These functions are all required for active navigation, and therefore all potentially contribute to the significant BOLD response observed in those regions. Our experiment design does not allow for further disentangling of these components, and we suggest, in line with [Humphreys and Lambon Ralph \(2015\)](#), that the observed SPL and vIPS activations reflect the general non-automatic, goal-directed, and executively demanding nature of active navigation.

With respect to scene-selective regions, the conjunction of active exploration conditions versus the passive condition reveals significant BOLD response in the right OPA and the right RSC. Both regions

showed significant activation already in the passive exploration task, which we suggest reflects their general involvement in scene and landmark processing. The finding that they also show a significant BOLD response during active compared to passive exploration indicates that both regions also play a role in active navigation beyond their general scene-selective contributions. It has to be noted that the OPA borders several retinotopically defined regions (Silson et al., 2016) and has been linked with visual stream pathways involved in visuospatial perception and visuomotor processing (Goodale and Milner, 1992; Kravitz et al., 2011), and recently was also found to show a retinotopic bias towards the lower visual field (Silson et al., 2015). We did not measure participants' eye movements during the experiment and, though our passive exploration task closely resembles participants' active exploration, we cannot rule out the possibility that the observed OPA activity is caused by systematically different eye movement behaviour between the two conditions.

That being said, recent studies also provide evidence that supports a direct role of the OPA specifically in active navigation, as opposed to general scene-selectivity (Dilks et al., 2011; Julian et al., 2016; Persichetti and Dilks, 2016). Julian and colleagues found that applying transcranial magnetic stimulation (TMS) to participants' right OPA impairs their spatial memory for boundary-tethered, but not landmark-tethered, objects, indicating that the OPA is the perceptual source for an environment's boundary information and therefore causally involved in spatial navigation that relies on this sort of information (Julian et al., 2016). In our experiment, the cue card was the only available landmark and it was not always present in the visual field, whereas a boundary is always in sight and therefore constantly provides boundary-based perceptual information. We therefore hypothesise that participants in the active exploration task base their navigation mostly on the constantly available boundary-based information and less on information derived from the only occasionally available landmark and that this is reflected in the OPA activity.

Further support for a causal role of the OPA, and the RSC, in navigation comes from two recent studies which found that OPA and RSC, but not PPA, show sensitivity to (a) a scene's sense (i.e., when a scene is tested against its vertically mirrored equivalent) (Dilks et al., 2011); and (b) to egocentric distance information (Persichetti and Dilks, 2016). The authors conclude that only OPA and RSC are directly involved in navigation, whereas PPA is predominantly involved in recognition processes (Persichetti and Dilks, 2016). In line with this notion, we observe OPA and RSC activation in both active exploration tasks, while PPA shows a significant BOLD response only in LONG > PASSIVE, where we expect participants to rely significantly more on spatial memory, compared to SHORT > PASSIVE.

While Persichetti and Dilks (2016) do not elaborate on the mechanisms underlying RSC's specific contribution to navigation, we suggest that demands on functions attributed to RSC, such as egocentric-to-allothetic information translation (Auger et al., 2012; Burgess et al., 2001; Byrne et al., 2007; Epstein and Vass, 2014; Kravitz et al., 2011; Marchette et al., 2015; Vann et al., 2009), judgement of viewing angle changes (Sulpizio et al., 2013), translation and rotation tracking (Chrastil et al., 2016), and updating and orienting spatial location information (Burles et al., 2017), are the reason why this region is more active during active exploration in our paradigm.

4.3 Active exploration with memory

The LONG and SHORT conditions in our paradigm were designed to investigate the role of varying spatial memory demand during active exploration on the BOLD signal. Participants were given 30 seconds for the exploration of the VE in SHORT, a timespan reportedly short enough for MTL-lesioned patients to solve simple navigation tasks based on their working memory capacity (Shrager et al., 2008). In contrast, participants collect items for 180 seconds in LONG, and considering the 25-seconds-breaks between subsequent trials, the whole search stretches to a total duration of 330 seconds from the beginning of the first to the end of the last trial. The long exploration task thus clearly exceeds the duration reported by Shrager et al. (2008). Due to the longer task duration, participants also visit relatively more of the VE's area in LONG compared to SHORT, and should remember where they had already collected items to effectively solve the LONG task. Hence, the long exploration task poses relatively higher demands on participants' spatial memory, both in terms of the amount of information to remember and the duration this information should be accessible.

We quantified consistency of participants' behaviour across the two active exploration conditions and found that their score-to-velocity ratio shows a marginal statistical difference between the two conditions. This indicates a rather consistent navigation behaviour across both active exploration tasks. We therefore conclude that, as intended with the design of our experiment, differences in the BOLD response between the two conditions merely reflect changes in participants' spatial memory usage.

In LONG > PASSIVE, in addition to the activation revealed by the conjunction of both active exploration tasks, we found significant BOLD response in the posterior parahippocampal cortex bilaterally, and in the RSC of the left hemisphere (thereby complementing the right RSC activation already found in the conjunction). The finding that these two regions are only observed in LONG > PASSIVE, but not SHORT > PASSIVE, might indicate that specifically these regions contribute to the increased spatial memory processing relevant in the long exploration task. LONG > SHORT, the contrast that directly tests for brain regions recruited with increased spatial memory demand, would be suitable to confirm this hypothesis. However, LONG > SHORT does not reveal statistically significant activation anywhere in the brain. We therefore cannot conclusively answer which brain regions are sensitive to increased spatial memory demands in our exploration task.

4.4 Individual differences

In past studies, hippocampal BOLD activity was often found only when correlated with some variable reflecting performance in the navigation task under investigation: In a wayfinding task, navigation accuracy was found to correlate with right posterior hippocampal activation, while between-subjects navigation accuracy correlated with left, and subthreshold right, activation of the anterior hippocampus (Hartley et al., 2003). In a triangle completion task, between-subjects accurate pointing performance and response consistency values were reported to correlate with the right anterior hippocampus (Wolbers et al., 2007). Posterior bilateral hippocampus activation associated with landmark memory consolidation was found to covary with participants' navigational skills (Janzen et al.,

2008); between-subjects navigation performance was reported to correlate with left posterior hippocampal BOLD response in two memory-based navigation tasks (Rauchs et al., 2008); and in a spatial memory task, where participants had to memorize and then return to a target location, right anterior hippocampal activity in the encoding phase, and left posterior hippocampal activity in the retrieval phase, correlated with within-subjects average metric accuracy (Baumann et al., 2010). No comprehensive picture regarding the hippocampus' role in performance of navigation tasks emerges from these studies – not with respect to its exact contribution, nor to the exact site (i.e., anterior, middle, or posterior hippocampus) or the hemisphere(s) (i.e., left, right, or bilateral hippocampus activation) involved.

Based on these inconclusive findings, we hypothesised that the driving factor behind the commonly observed correlation of participants' behaviour with hippocampal BOLD response really is the spatial memory demand associated with the navigation task tested. In our study, score, the measure that captures success, was not correlated with participants' once-to-total viewed area ratio, the measure assessing spatial memory usage during exploration. Task success is therefore not indicative of a participant's usage of spatial memory in our paradigm. Rather, these two variates reflect independent effects.

An increase in score correlates with increased activation of the left anterior hippocampus. As score cannot be explained by spatial memory usage in our exploration task, this raises the question what else the observed correlation could reflect. The human anterior hippocampus, and the homologous ventral hippocampus in rats and mice, show strong reciprocal connectivity with the amygdala, and has been associated with goal- and reward-directed functions (for reviews see Fanselow and Dong, 2010; Strange et al., 2014). In a functional MRI study on human route planning, Viard et al. (2011) found strong correlation between bilateral anterior hippocampal BOLD response and goal proximity, which they interpret to reflect reward expectancy (Viard et al., 2011). Since in our experiment an increasing score may well correlate with increasing reward, we speculate, in line with these previous findings, that the observed correlation between score and anterior hippocampal activation may reflect reward-related processes in this area.

The once-to-total viewed area ratio covaries most strongly with the BOLD response in the left and, at a slightly less strict statistical significance level, also with the right anterior medial hippocampus (amHipp). This region has been shown to form a functionally distinct unit with particularly high functional heterogeneity within the hippocampal formation (Blessing et al., 2016; Robinson et al., 2015). Zeidman and Maguire (2016) summarised several recent functional MRI studies, anatomical data, and findings from lesion patients, that all covered the hippocampus and particularly its anterior region. Based on that, they proposed that the amHipp supports several cognitive functions, including episodic memory, imagination, and scene perception, by providing coherent spatial representations to these processes. They suggest that, in the hippocampus, specifically the amHipp supports modeling of scenes through continuously constructing and refining a representation of the currently experienced scene. They further predict that, when a spatially coherent representation of a scene is required, the amHipp becomes engaged. Their model refers to scenes as “coherent object-containing spaces within which we can potentially operate” (Zeidman and Maguire (2016), p. 175), explicitly in-

cluding navigation into the set of tasks that essentially rely on processing of scenes. In line with this notion, we suggest that achieving a high once-to-total viewed area ratio in the long exploration task requires a participant to have formed a highly coherent, i.e. metrically accurate, spatial representation of the VE, thus explaining the positive correlation of participants' once-to-total viewed area ratio with the amHipp BOLD response in LONG > SHORT.

Our results cannot reconcile the ambiguous results from recent performance-based correlations with the hippocampal BOLD response outlined above. However, analysing the observed correlations reported in previous studies in detail reveals a very heterogenous mix of behaviour associated with participants' performance: it is either not related to spatial memory at all (Baumann et al., 2010; Wolbers et al., 2007); or derived from indirect measures of general navigation skills like the Santa Barbara Sense of Direction questionnaire (Hegarty et al., 2002) as in Janzen et al. (2008); or captures performance only at one (Rauchs et al., 2008), or just a few (Hartley et al., 2003) discrete points in time during the respective navigation task. The ratio of once-to-total viewed area assessed in our experiment, by contrast, targets specifically participants' use of spatial memory while separating it from purely task-related success reflected by participants' score. In addition, the once-to-total viewed area ratio does not only incorporate performance captured at certain times during the task, but throughout the whole task instead, thus reflecting participants' performance balanced across the whole task duration. Compared to measures of behaviour applied in previous studies, the ratio of once-to-total viewed area used in our task is a quite suitable measure to characterise participants' use of spatial memory in a naturalistic navigation task.

4.5 Conclusion

In conclusion, in this study we developed a paradigm that allowed us to separate out both passive and active components of spatial exploration, as well as to vary the spatial memory demand during active exploration. We showed that passive navigation is already sufficient to recruit scene-selective regions of the navigation network including OPA, PPA, and RSC. This confirms recent findings, whereby OPA encodes navigational affordances even when they are not task-relevant (Bonner and Epstein, 2017), and suggest that not just OPA, but all three scene-selective regions, may automatically engage in navigation-related processing regardless of actual task demands. We also showed that these regions, along with dorsal visuospatial attention hubs, increase activity with increasing navigational demand, providing further evidence for a role of these regions beyond scene perception, in which they contribute information processing relevant specifically for active navigation. Finally, although we increased spatial memory demand, hippocampal activation was not present throughout this task condition. Instead, participants' spatial memory usage positively correlated with anterior medial hippocampus activation, thereby supporting the notion that this region provides a coherent spatial representation of one's environment, and suggesting that during realistic navigation in a landmark-sparse environment, spatial memory is the driving factor behind such a metrically coherent spatial representation of one's environment.

Acknowledgements

The authors thank Franz L. Hell for help with automated fMRI artifact detection. Support and funding for this study were provided by the German Federal Ministry of Education and Research (grants: BMBF IFB 01 EO 0901; BMBF BCCN 01 GQ 0440) and the German Research Foundation (grant: DFG GSC 82-3). The authors declare no competing financial interests.

References

- Amunts, K., Kedo, O., Kindler, M., Pieperhoff, P., Mohlberg, H., Shah, N., Habel, U., Schneider, F., and Zilles, K. (2005). Cytoarchitectonic mapping of the human amygdala, hippocampal region and entorhinal cortex: intersubject variability and probability maps. *Anatomy and Embryology*, 210(5-6):343–352.
- Astur, R. S., Taylor, L. B., Mamelak, A. N., Philpott, L., and Sutherland, R. J. (2002). Humans with hippocampus damage display severe spatial memory impairments in a virtual morris water task. *Behav Brain Res*, 132(1):77–84.
- Auger, S. D., Mullally, S. L., and Maguire, E. A. (2012). Retrosplenial cortex codes for permanent landmarks. *PLoS ONE*, 7(8):e43620.
- Banta Lavenex, P. A., Colombo, E., Ribordy Lambert, F., and Lavenex, P. (2014). The human hippocampus beyond the cognitive map: evidence from a densely amnesic patient. *Frontiers in Human Neuroscience*, 8.
- Baumann, O., Chan, E., and Mattingley, J. B. (2010). Dissociable neural circuits for encoding and retrieval of object locations during active navigation in humans. *NeuroImage*, 49(3):2816–2825.
- Behrens, T., Woolrich, M., Jenkinson, M., Johansen-Berg, H., Nunes, R., Clare, S., Matthews, P., Brady, J., and Smith, S. (2003a). Characterization and propagation of uncertainty in diffusion-weighted mr imaging. *Magnetic Resonance in Medicine*, 50(5):1077–1088.
- Behrens, T. E. J., Johansen-Berg, H., Woolrich, M. W., Smith, S. M., Wheeler-Kingshott, C. A. M., Boulby, P. A., Barker, G. J., Sillery, E. L., Sheehan, K., Ciccarelli, O., Thompson, A. J., Brady, J. M., and Matthews, P. M. (2003b). Non-invasive mapping of connections between human thalamus and cortex using diffusion imaging. *Nat Neurosci*, 6(7):750–757.
- Bhaganagarapu, K., Jackson, G. D., and Abbott, D. F. (2013). An automated method for identifying artifact in independent component analysis of resting-state fmri. *Frontiers in Human Neuroscience*, 7.
- Blessing, E. M., Beissner, F., Schumann, A., Br nner, F., and B r, K.-J. (2016). A data-driven approach to mapping cortical and subcortical intrinsic functional connectivity along the longitudinal hippocampal axis. *Human Brain Mapping*, 37(2):462–476.

- Boccia, M., Nemmi, F., and Guariglia, C. (2014). Neuropsychology of environmental navigation in humans: Review and meta-analysis of fmri studies in healthy participants. *Neuropsychology Review*, 24(2):236–251.
- Bohbot, V. D., Kalina, M., Stepankova, K., Spackova, N., Petrides, M., and Nadel, L. (1998). Spatial memory deficits in patients with lesions to the right hippocampus and to the right parahippocampal cortex. *Neuropsychologia*, 36(11):1217–38.
- Bohbot, V. D., Lerch, J., Thorndyraft, B., Iaria, G., and Zijdenbos, A. P. (2007). Gray matter differences correlate with spontaneous strategies in a human virtual navigation task. *Journal of Neuroscience*, 27(38):10078–10083.
- Bonner, M. F. and Epstein, R. A. (2017). Coding of navigational affordances in the human visual system. *Proceedings of the National Academy of Sciences*, 114(18):4793–4798.
- Burgess, N., Becker, S., King, J. A., and O’Keefe, J. (2001). Memory for events and their spatial context: models and experiments. *Philosophical Transactions of the Royal Society B: Biological Sciences*, 356(1413):1493–1503.
- Burles, F., Slone, E., and Iaria, G. (2017). Dorso-medial and ventro-lateral functional specialization of the human retrosplenial complex in spatial updating and orienting. *Brain Structure and Function*, 222(3):1481–1493.
- Burton, H., Sinclair, R. J., and McLaren, D. G. (2008a). Cortical network for vibrotactile attention: A fmri study. *Human Brain Mapping*, 29(2):207–221.
- Burton, H., Sinclair, R. J., Wingert, J. R., and Dierker, D. L. (2008b). Multiple parietal operculum subdivisions in humans: Tactile activation maps. *Somatosensory & Motor Research*, 25(3):149–162.
- Buzsáki, G. and Moser, E. I. (2013). Memory, navigation and theta rhythm in the hippocampal-entorhinal system. *Nature neuroscience*, 16(2):130–138.
- Byrne, P., Becker, S., and Burgess, N. (2007). Remembering the past and imagining the future: a neural model of spatial memory and imagery. *Psychological Review*, 114(2):340.
- Cardin, V. and Smith, A. T. (2010). Sensitivity of human visual and vestibular cortical regions to egomotion-compatible visual stimulation. *Cerebral Cortex*, 20(8):1964–1973.
- Chrastil, E. R., Sherrill, K. R., Hasselmo, M. E., and Stern, C. E. (2016). Which way and how far? tracking of translation and rotation information for human path integration. *Human Brain Mapping*, 37(10):3636–3655.
- Corbetta, M., Patel, G., and Shulman, G. L. (2008). The reorienting system of the human brain: From environment to theory of mind. *Neuron*, 58(3):306–324.
- Corbetta, M. and Shulman, G. L. (2002). Control of goal-directed and stimulus-driven attention in the brain. *Nature Reviews Neuroscience*, 3(3):215–229.

- de Schotten, M. T., Dell'Acqua, E., Forkel, S. J., Simmons, A., Vergani, E., Murphy, D. G. M., and Catani, M. (2011). A lateralized brain network for visuospatial attention. *Nature Neuroscience*, 14(10):1245–1246.
- Diedrichsen, J., Balsters, J. H., Flavell, J., Cussans, E., and Ramnani, N. (2009). A probabilistic mr atlas of the human cerebellum. *NeuroImage*, 46(1):39–46.
- Dilks, D. D., Julian, J. B., Kubilius, J., Spelke, E. S., and Kanwisher, N. (2011). Mirror-image sensitivity and invariance in object and scene processing pathways. *Journal of Neuroscience*, 31(31):11305–11312.
- Dilks, D. D., Julian, J. B., Paunov, A. M., and Kanwisher, N. (2013). The occipital place area is causally and selectively involved in scene perception. *Journal of Neuroscience*, 33(4):1331–1336.
- Eichenbaum, H. (2017a). Memory: Organization and control. *Annual Review of Psychology*, 68(1):19–45.
- Eichenbaum, H. (2017b). The role of the hippocampus in navigation is memory. *J Neurophysiol*, 117(4):1785–1796.
- Eickhoff, S. B., Amunts, K., Mohlberg, H., and Zilles, K. (2006a). The human parietal operculum. ii. stereotaxic maps and correlation with functional imaging results. *Cerebral Cortex*, 16(2):268–279.
- Eickhoff, S. B., Heim, S., Zilles, K., and Amunts, K. (2006b). Testing anatomically specified hypotheses in functional imaging using cytoarchitectonic maps. *NeuroImage*, 32(2):570–582.
- Eickhoff, S. B., Jbabdi, S., Caspers, S., Laird, A. R., Fox, P. T., Zilles, K., and Behrens, T. E. J. (2010). Anatomical and functional connectivity of cytoarchitectonic areas within the human parietal operculum. *Journal of Neuroscience*, 30(18):6409–6421.
- Eickhoff, S. B., Paus, T., Caspers, S., Grosbras, M.-H., Evans, A. C., Zilles, K., and Amunts, K. (2007). Assignment of functional activations to probabilistic cytoarchitectonic areas revisited. *NeuroImage*, 36(3):511–521.
- Eickhoff, S. B., Schleicher, A., Zilles, K., and Amunts, K. (2006c). The human parietal operculum. i. cytoarchitectonic mapping of subdivisions. *Cerebral Cortex*, 16(2):254–267.
- Eickhoff, S. B., Stephan, K. E., Mohlberg, H., Grefkes, C., Fink, G. R., Amunts, K., and Zilles, K. (2005). A new spm toolbox for combining probabilistic cytoarchitectonic maps and functional imaging data. *NeuroImage*, 25(4):1325–1335.
- Ekstrom, A. D., Kahana, M. J., Caplan, J. B., Fields, T. A., Isham, E. A., Newman, E. L., and Fried, I. (2003). Cellular networks underlying human spatial navigation. *Nature*, 425(6954):184–188.
- Epstein, R. and Kanwisher, N. (1998). A cortical representation of the local visual environment. *Nature*, 392(6676):598–601.

- Epstein, R. A. (2008). Parahippocampal and retrosplenial contributions to human spatial navigation. *Trends in Cognitive Sciences*, 12(10):388–396.
- Epstein, R. A., Patai, E. Z., Julian, J. B., and Spiers, H. J. (2017). The cognitive map in humans: spatial navigation and beyond. *Nature Neuroscience*, 20(11):1504–1513.
- Epstein, R. A. and Vass, L. K. (2014). Neural systems for landmark-based wayfinding in humans. *Philosophical Transactions of the Royal Society of London B: Biological Sciences*, 369(1635).
- Fanselow, M. S. and Dong, H.-W. (2010). Are the dorsal and ventral hippocampus functionally distinct structures? *Neuron*, 65(1):7–19.
- Fonov, V. S., Evans, A. C., McKinstry, R. C., Almlí, C., and Collins, D. (2009). Unbiased nonlinear average age-appropriate brain templates from birth to adulthood. *NeuroImage*, 47(Supplement 1):S102. Organization for Human Brain Mapping 2009 Annual Meeting.
- Gaymard, B., Rivaud, S., Cassarini, J. E., Dubard, T., Rancurel, G., Agid, Y., and Pierrot-Deseilligny, C. (1998). Effects of anterior cingulate cortex lesions on ocular saccades in humans. *Experimental Brain Research*, 120(2):173–183.
- Geyer, S., Ledberg, A., Schleicher, A., Kinomura, S., Schormann, T., Bürgel, U., Klingberg, T., Larsson, J., Zilles, K., and Roland, P. E. (1996). Two different areas within the primary motor cortex of man. *Nature*, 382(6594):805–807.
- Gilbert, C. D. and Li, W. (2013). Top-down influences on visual processing. *Nature Reviews Neuroscience*, 14(5):350–363.
- Gillebert, C. R., Mantini, D., Peeters, R., Dupont, P., and Vandenberghe, R. (2013). Cytoarchitectonic mapping of attentional selection and reorienting in parietal cortex. *Neuroimage*, 67:257–272.
- Goodale, M. A. and Milner, A. D. (1992). Separate visual pathways for perception and action. *Trends Neurosci*, 15(1):20–5.
- Goodrich-Hunsaker, N. J., Livingstone, S. A., Skelton, R. W., and Hopkins, R. O. (2010). Spatial deficits in a virtual water maze in amnesic participants with hippocampal damage. *Hippocampus*, pages NA–NA.
- Grill-Spector, K. (2003). The neural basis of object perception. *Curr Opin Neurobiol*, 13(2):159–66.
- Hafting, T., Fyhn, M., Molden, S., Moser, M.-B., and Moser, E. I. (2005). Microstructure of a spatial map in the entorhinal cortex. *Nature*, 436(7052):801–806.
- Hartley, T., Lever, C., Burgess, N., and O’Keefe, J. (2014). Space in the brain: how the hippocampal formation supports spatial cognition. *Philosophical Transactions of the Royal Society of London B: Biological Sciences*, 369(1635).
- Hartley, T., Maguire, E. A., Spiers, H. J., and Burgess, N. (2003). The well-worn route and the path less traveled: distinct neural bases of route following and wayfinding in humans. *Neuron*, 37(5):877–88.

- Hegarty, M., Richardson, A. E., Montello, D. R., Lovelace, K., and Subbiah, I. (2002). Development of a self-report measure of environmental spatial ability. *Intelligence*, 30(5):425 – 447.
- Hodgetts, C., Shine, J., Lawrence, A., Downing, P., and Graham, K. (2016). Evidencing a place for the hippocampus within the core scene processing network. *Human Brain Mapping*, 37(11):3779–3794.
- Humphreys, G. F. and Lambon Ralph, M. A. (2015). Fusion and fission of cognitive functions in the human parietal cortex. *Cerebral Cortex*, 25(10):3547–3560.
- Hutchinson, J. B., Uncapher, M. R., and Wagner, A. D. (2009). Posterior parietal cortex and episodic retrieval: convergent and divergent effects of attention and memory. *Learn Mem*, 16(6):343–56.
- Iaria, G., Chen, J.-K., Guariglia, C., Ptito, A., and Petrides, M. (2007). Retrosplenial and hippocampal brain regions in human navigation: complementary functional contributions to the formation and use of cognitive maps. *European Journal of Neuroscience*, 25(3):890–899.
- Iaria, G., Petrides, M., Dagher, A., Pike, B., and Bohbot, V. D. (2003). Cognitive strategies dependent on the hippocampus and caudate nucleus in human navigation: Variability and change with practice. *Journal of Neuroscience*, 23(13):5945–5952.
- Insausti, R. (1993). Comparative anatomy of the entorhinal cortex and hippocampus in mammals. *Hippocampus*, 3(S1):19–26.
- Ishikawa, T. and Montello, D. (2006). Spatial knowledge acquisition from direct experience in the environment: Individual differences in the development of metric knowledge and the integration of separately learned places. *Cognitive Psychology*, 52(2):93–129.
- Jacobs, J. (2014). Hippocampal theta oscillations are slower in humans than in rodents: implications for models of spatial navigation and memory. *Philosophical Transactions of the Royal Society of London B: Biological Sciences*, 369(1635).
- Jacobs, J., Kahana, M. J., Ekstrom, A. D., Mollison, M. V., and Fried, I. (2010). A sense of direction in human entorhinal cortex. *Proceedings of the National Academy of Sciences*, 107(14):6487–6492.
- Jacobs, J., Weidemann, C. T., Miller, J. F., Solway, A., Burke, J. F., Wei, X.-X., Suthana, N., Sperling, M. R., Sharan, A. D., Fried, I., and et al. (2013). Direct recordings of grid-like neuronal activity in human spatial navigation. *Nature Neuroscience*, 16(9):1188–1190.
- Janzen, G., Jansen, C., and Turennout, M. v. (2008). Memory consolidation of landmarks in good navigators. *Hippocampus*, 18(1):40–47.
- Janzen, G. and van Turennout, M. (2004). Selective neural representation of objects relevant for navigation. *Nature Neuroscience*, 7(6):673–677.
- Johansen-Berg, H., Behrens, T. E., Sillery, E., Ciccarelli, O., Thompson, A. J., Smith, S. M., and Matthews, P. M. (2005). Functional–anatomical validation and individual variation of diffusion tractography-based segmentation of the human thalamus. *Cerebral Cortex*, 15(1):31–39.

- Julian, J. B., Ryan, J., Hamilton, R. H., and Epstein, R. A. (2016). The occipital place area is causally involved in representing environmental boundaries during navigation. *Current Biology*, 26(8):1104–1109.
- Kamps, F. S., Julian, J. B., Kubiľius, J., Kanwisher, N., and Dilks, D. D. (2016a). The occipital place area represents the local elements of scenes. *NeuroImage*, 132(Supplement C):417 – 424.
- Kamps, F. S., Lall, V., and Dilks, D. D. (2016b). The occipital place area represents first-person perspective motion information through scenes. *Cortex*, 83(Supplement C):17 – 26.
- Kim, S., Sapiurka, M., Clark, R. E., and Squire, L. R. (2013). Contrasting effects on path integration after hippocampal damage in humans and rats. *Proceedings of the National Academy of Sciences*, 110(12):4732–4737.
- Konen, C. S., Mruczek, R. E. B., Montoya, J. L., and Kastner, S. (2013). Functional organization of human posterior parietal cortex: grasping- and reaching-related activations relative to topographically organized cortex. *J Neurophysiol*, 109(12):2897–908.
- Kravitz, D. J., Saleem, K. S., Baker, C. I., and Mishkin, M. (2011). A new neural framework for visuospatial processing. *Nature Reviews Neuroscience*, 12(4):217–230.
- Lee, S. A., Miller, J. E., Watrous, A. J., Sperling, M. R., Sharan, A., Worrell, G. A., Berry, B. M., Aronson, J. P., Davis, K. A., Gross, R. E., and et al. (2018). Electrophysiological signatures of spatial boundaries in the human subiculum. *The Journal of Neuroscience*, 38(13):3265–3272.
- Lescroart, M. D., Stansbury, D. E., and Gallant, J. L. (2015). Fourier power, subjective distance, and object categories all provide plausible models of bold responses in scene-selective visual areas. *Frontiers in Computational Neuroscience*, 9.
- Lever, C., Burton, S., Jeewajee, A., O’Keefe, J., and Burgess, N. (2009). Boundary vector cells in the subiculum of the hippocampal formation. *Journal of Neuroscience*, 29(31):9771–9777.
- MacEvoy, S. P. and Epstein, R. A. (2011). Constructing scenes from objects in human occipitotemporal cortex. *Nature Neuroscience*, 14(10):1323–1329.
- Macko, K., Jarvis, C., Kennedy, C., Miyaoka, M., Shinohara, M., Sololoff, L., and Mishkin, M. (1982). Mapping the primate visual system with [2-14c]deoxyglucose. *Science*, 218(4570):394–397.
- Maguire, E. (2001). The retrosplenial contribution to human navigation: A review of lesion and neuroimaging findings. *Scandinavian Journal of Psychology*, 42(3):225–238.
- Maguire, E. A., Nannery, R., and Spiers, H. J. (2006). Navigation around london by a taxi driver with bilateral hippocampal lesions. *Brain*, 129(11):2894–2907.
- Marchette, S. A., Bakker, A., and Shelton, A. L. (2011). Cognitive mappers to creatures of habit: Differential engagement of place and response learning mechanisms predicts human navigational behavior. *Journal of Neuroscience*, 31(43):15264–15268.

- Marchette, S. A., Vass, L. K., Ryan, J., and Epstein, R. A. (2015). Outside looking in: Landmark generalization in the human navigational system. *Journal of Neuroscience*, 35(44):14896–14908.
- Meehan, T. P., Bressler, S. L., Tang, W., Astafiev, S. V., Sylvester, C. M., Shulman, G. L., and Corbetta, M. (2017). Top-down cortical interactions in visuospatial attention. *Brain Structure and Function*, 222(7):3127–3145.
- Mellet, E., Laou, L., Petit, L., Zago, L., Mazoyer, B., and Tzourio-Mazoyer, N. (2010). Impact of the virtual reality on the neural representation of an environment. *Human Brain Mapping*, 31(7):1065–1075.
- Mishkin, M., Ungerleider, L. G., and Macko, K. A. (1983). Object vision and spatial vision: two cortical pathways. *Trends in Neurosciences*, 6(Supplement C):414 – 417.
- Molenberghs, P., Mesulam, M. M., Peeters, R., and Vandenberghe, R. R. C. (2007). Remapping attentional priorities: differential contribution of superior parietal lobule and intraparietal sulcus. *Cereb Cortex*, 17(11):2703–12.
- Morris, R., Paxinos, G., and Petrides, M. (2000). Architectonic analysis of the human retrosplenial cortex. *The Journal of Comparative Neurology*, 421(1):14–28.
- Morris, R. G. M., Garrud, P., Rawlins, J. N. P., and O’Keefe, J. (1982). Place navigation impaired in rats with hippocampal lesions. *Nature*, 297(5868):681–683.
- Moser, E. I., Kropff, E., and Moser, M.-B. (2008). Place cells, grid cells, and the brain’s spatial representation system. *Annual Review of Neuroscience*, 31(1):69–89.
- Muller, R. and Kubie, J. (1987). The effects of changes in the environment on the spatial firing of hippocampal complex-spike cells. *The Journal of Neuroscience*, 7(7):1951–1968.
- Mysore, S. P. and Knudsen, E. I. (2011). The role of a midbrain network in competitive stimulus selection. *Curr Opin Neurobiol*, 21(4):653–60.
- Nardo, D., Santangelo, V., and Macaluso, E. (2011). Stimulus-driven orienting of visuo-spatial attention in complex dynamic environments. *Neuron*, 69(5):1015–1028.
- Nasr, S., Liu, N., Devaney, K. J., Yue, X., Rajimehr, R., Ungerleider, L. G., and Tootell, R. B. H. (2011). Scene-selective cortical regions in human and nonhuman primates. *Journal of Neuroscience*, 31(39):13771–13785.
- Neubert, F.-X., Mars, R. B., Sallet, J., and Rushworth, M. F. S. (2015). Connectivity reveals relationship of brain areas for reward-guided learning and decision making in human and monkey frontal cortex. *Proceedings of the National Academy of Sciences*, 112(20):E2695–E2704.
- Neubert, F.-X., Mars, R. B., Thomas, A. G., Sallet, J., and Rushworth, M. F. S. (2014). Comparison of human ventral frontal cortex areas for cognitive control and language with areas in monkey frontal cortex. *Neuron*, 81(3):700–713.

- Ohlendorf, S., Kimmig, H., Glauche, V., and Haller, S. (2007). Gaze pursuit, “attention pursuit” and their effects on cortical activations. *European Journal of Neuroscience*, 26(7):2096–2108.
- O’Keefe, J. and Dostrovsky, J. (1971). The hippocampus as a spatial map. preliminary evidence from unit activity in the freely-moving rat. *Brain Res*, 34(1):171–5.
- Persichetti, A. S. and Dilks, D. D. (2016). Perceived egocentric distance sensitivity and invariance across scene-selective cortex. *Cortex*, 77(Supplement C):155 – 163.
- Pierrot-Deseilligny, C., Milea, D., and Müri, R. M. (2004). Eye movement control by the cerebral cortex. *Current opinion in neurology*, 17(1):17–25.
- Pitzalis, S., Galletti, C., Huang, R.-S., Patria, F., Committeri, G., Galati, G., Fattori, P., and Sereno, M. I. (2006). Wide-field retinotopy defines human cortical visual area v6. *Journal of Neuroscience*, 26(30):7962–7973.
- Pitzalis, S., Sereno, M. I., Committeri, G., Fattori, P., Galati, G., Patria, F., and Galletti, C. (2010). Human v6: The medial motion area. *Cerebral Cortex*, 20(2):411–424.
- Rauchs, G., Orban, P., Balteau, E., Schmidt, C., Degueldre, C., Luxen, A., Maquet, P., and Peigneux, P. (2008). Partially segregated neural networks for spatial and contextual memory in virtual navigation. *Hippocampus*, 18(5):503–518.
- Robinson, J. L., Barron, D. S., Kirby, L. A. J., Bottenhorn, K. L., Hill, A. C., Murphy, J. E., Katz, J. S., Salibi, N., Eickhoff, S. B., and Fox, P. T. (2015). Neurofunctional topography of the human hippocampus. *Human Brain Mapping*, 36(12):5018–5037.
- Scheperjans, F., Eickhoff, S. B., Homke, L., Mohlberg, H., Hermann, K., Amunts, K., and Zilles, K. (2008a). Probabilistic maps, morphometry, and variability of cytoarchitectonic areas in the human superior parietal cortex. *Cerebral Cortex*, 18(9):2141–2157.
- Scheperjans, F., Hermann, K., Eickhoff, S. B., Amunts, K., Schleicher, A., and Zilles, K. (2008b). Observer-independent cytoarchitectonic mapping of the human superior parietal cortex. *Cerebral Cortex*, 18(4):846–867.
- Scoville, W. B. and Milner, B. (1957). Loss of recent memory after bilateral hippocampal lesions. *Journal of Neurology, Neurosurgery & Psychiatry*, 20(1):11–21.
- Sestieri, C., Shulman, G. L., and Corbetta, M. (2010). Attention to memory and the environment: Functional specialization and dynamic competition in human posterior parietal cortex. *Journal of Neuroscience*, 30(25):8445–8456.
- Sestieri, C., Shulman, G. L., and Corbetta, M. (2017). The contribution of the human posterior parietal cortex to episodic memory. *Nat Rev Neurosci*, 18(3):183–192.

- Shrager, Y., Kirwan, C. B., and Squire, L. R. (2008). Neural basis of the cognitive map: Path integration does not require hippocampus or entorhinal cortex. *Proceedings of the National Academy of Sciences*, 105(33):12034–12038.
- Shulman, G. L., Astafiev, S. V., Franke, D., Pope, D. L. W., Snyder, A. Z., McAvoy, M. P., and Corbetta, M. (2009). Interaction of stimulus-driven reorienting and expectation in ventral and dorsal frontoparietal and basal ganglia-cortical networks. *Journal of Neuroscience*, 29(14):4392–4407.
- Silson, E. H., Chan, A. W.-Y., Reynolds, R. C., Kravitz, D. J., and Baker, C. I. (2015). A retinotopic basis for the division of high-level scene processing between lateral and ventral human occipitotemporal cortex. *Journal of Neuroscience*, 35(34):11921–11935.
- Silson, E. H., Steel, A. D., and Baker, C. I. (2016). Scene-selectivity and retinotopy in medial parietal cortex. *Frontiers in Human Neuroscience*, 10.
- Smith, S. and Nichols, T. (2009). Threshold-free cluster enhancement: Addressing problems of smoothing, threshold dependence and localisation in cluster inference. *NeuroImage*, 44(1):83–98.
- Solstad, T., Boccara, C. N., Kropff, E., Moser, M.-B., and Moser, E. I. (2008). Representation of geometric borders in the entorhinal cortex. *Science*, 322(5909):1865–1868.
- Stark, C. E. L. and Squire, L. R. (2001). When zero is not zero: The problem of ambiguous baseline conditions in fmri. *Proceedings of the National Academy of Sciences*, 98(22):12760–12766.
- Stoodley, C. and Schmahmann, J. (2009). Functional topography in the human cerebellum: A meta-analysis of neuroimaging studies. *NeuroImage*, 44(2):489–501.
- Strange, B. A., Witter, M. P., Lein, E. S., and Moser, E. I. (2014). Functional organization of the hippocampal longitudinal axis. *Nature Reviews Neuroscience*, 15(10):655–669.
- Sulpizio, V., Committeri, G., Lambrey, S., Berthoz, A., and Galati, G. (2013). Selective role of lingual/parahippocampal gyrus and retrosplenial complex in spatial memory across viewpoint changes relative to the environmental reference frame. *Behavioural Brain Research*, 242:62 – 75.
- Taube, J., Muller, R., and Ranck, J. (1990). Head-direction cells recorded from the postsubiculum in freely moving rats. i. description and quantitative analysis. *Journal of Neuroscience*, 10(2):420–435.
- Teng, E. and Squire, L. R. (1999). Memory for places learned long ago is intact after hippocampal damage. *Nature*, 400(6745):675–677.
- Terrazas, A., Krause, M., Lipa, P., Gothard, K. M., Barnes, C. A., and McNaughton, B. L. (2005). Self-motion and the hippocampal spatial metric. *Journal of Neuroscience*, 25(35):8085–8096.
- Troiani, V., Stigliani, A., Smith, M. E., and Epstein, R. A. (2014). Multiple object properties drive scene-selective regions. *Cerebral Cortex*, 24(4):883–897.

- Tziortzi, A. C., Haber, S. N., Searle, G. E., Tsoumpas, C., Long, C. J., Shotbolt, P., Douaud, G., Jbabdi, S., Behrens, T. E. J., Rabiner, E. A., and et al. (2014). Connectivity-based functional analysis of dopamine release in the striatum using diffusion-weighted mri and positron emission tomography. *Cerebral Cortex*, 24(5):1165–1177.
- Ungerleider, L. G. and Mishkin, M. (1982). Two cortical visual systems. *Analysis of Visual Behavior*, pages 549–586.
- Urgolites, Z. J., Kim, S., Hopkins, R. O., and Squire, L. R. (2016). Map reading, navigating from maps, and the medial temporal lobe. *Proceedings of the National Academy of Sciences*, 113(50):14289–14293.
- van Dijk, R. M., Huang, S.-H., Slomianka, L., and Amrein, I. (2016). Taxonomic separation of hippocampal networks: Principal cell populations and adult neurogenesis. *Frontiers in Neuroanatomy*, 10.
- Vann, S. D., Aggleton, J. P., and Maguire, E. A. (2009). What does the retrosplenial cortex do? *Nature Reviews Neuroscience*, 10(11):792–802.
- Vernet, M., Quentin, R., Chanes, L., Mitsumasu, A., and Valero-Cabré, A. (2014). Frontal eye field, where art thou? anatomy, function, and non-invasive manipulation of frontal regions involved in eye movements and associated cognitive operations. *Frontiers in Integrative Neuroscience*, 8.
- Viard, A., Doeller, C. F., Hartley, T., Bird, C. M., and Burgess, N. (2011). Anterior hippocampus and goal-directed spatial decision making. *Journal of Neuroscience*, 31(12):4613–4621.
- Wall, M. B. and Smith, A. T. (2008). The representation of egomotion in the human brain. *Current Biology*, 18(3):191–194.
- Watrous, A. J., Lee, D. J., Izadi, A., Gurkoff, G. G., Shahlaie, K., and Ekstrom, A. D. (2013). A comparative study of human and rat hippocampal low-frequency oscillations during spatial navigation. *Hippocampus*, 23(8):656–661.
- Watson, J. D. G., Myers, R., Frackowiak, R. S. J., Hajnal, J. V., Woods, R. P., Mazziotta, J. C., Shipp, S., and Zeki, S. (1993). Area v5 of the human brain: Evidence from a combined study using positron emission tomography and magnetic resonance imaging. *Cerebral Cortex*, 3(2):79–94.
- Wolbers, T. and Hegarty, M. (2010). What determines our navigational abilities? *Trends in Cognitive Sciences*, 14(3):138–146.
- Wolbers, T., Wiener, J. M., Mallot, H. A., and Buchel, C. (2007). Differential recruitment of the hippocampus, medial prefrontal cortex, and the human motion complex during path integration in humans. *Journal of Neuroscience*, 27(35):9408–9416.
- Zeidman, P. and Maguire, E. A. (2016). Anterior hippocampus: the anatomy of perception, imagination and episodic memory. *Nature Reviews Neuroscience*, 17:173–182.

Zeki, S., Watson, J., Lueck, C., Friston, K., Kennard, C., and Frackowiak, R. (1991). A direct demonstration of functional specialization in human visual cortex. *Journal of Neuroscience*, 11(3):641–649.

Supplement

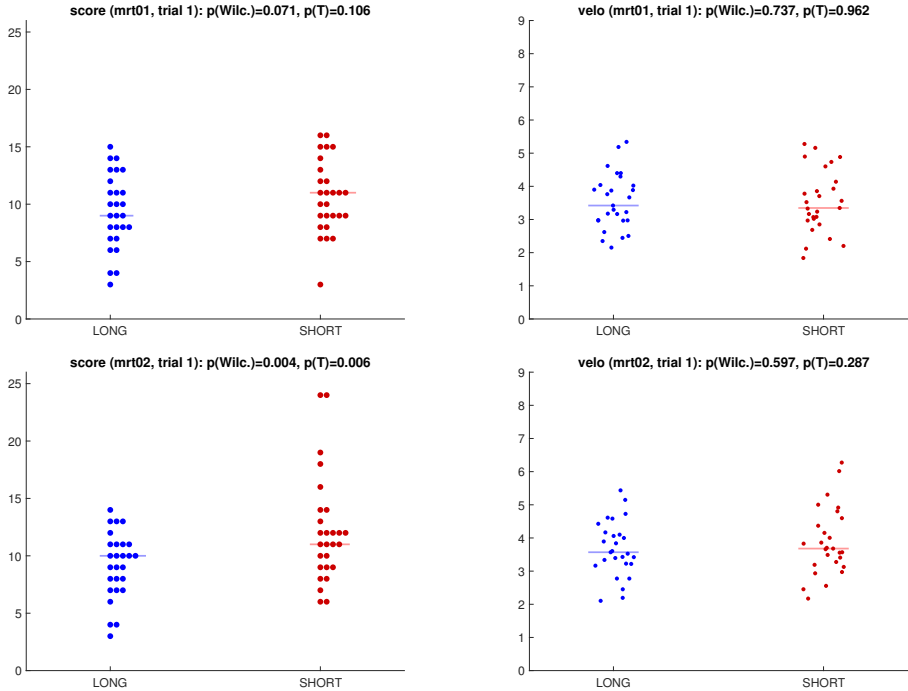


Figure 6: Comparison of participants' score and velocity between 1st trials of LONG and SHORT. Depicted are each participant's score (left column) and velocity (right column), and the corresponding median across participants (horizontal lines), for the 1st trial of LONG and SHORT (blue and red dots, respectively) of each run. The title indicates the p value obtained from a Wilcoxon signed-rank test (Wilc.) and a paired-sample t -test (T). Note that the Shapiro-Wilk test finds normally distributed data for all but the score in SHORT for run "mrt02".

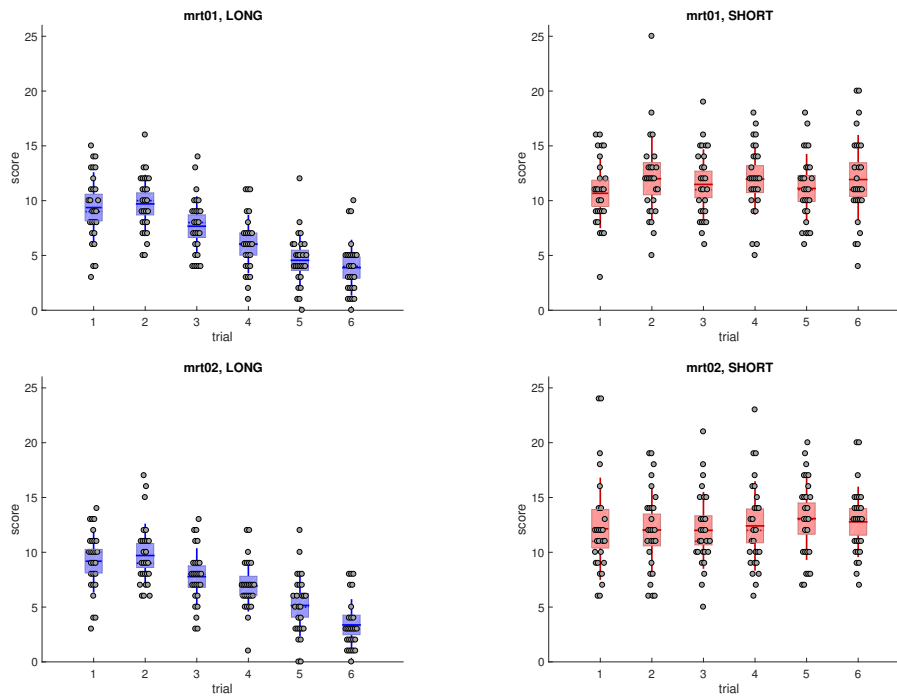


Figure 7: Participants' mean score across LONG and SHORT trials. Depicted are, for each trial, each participant's score (grey dots), standard deviation (vertical lines), standard error of the mean (patches), and mean and median across participants (horizontal and dashed lines, respectively).

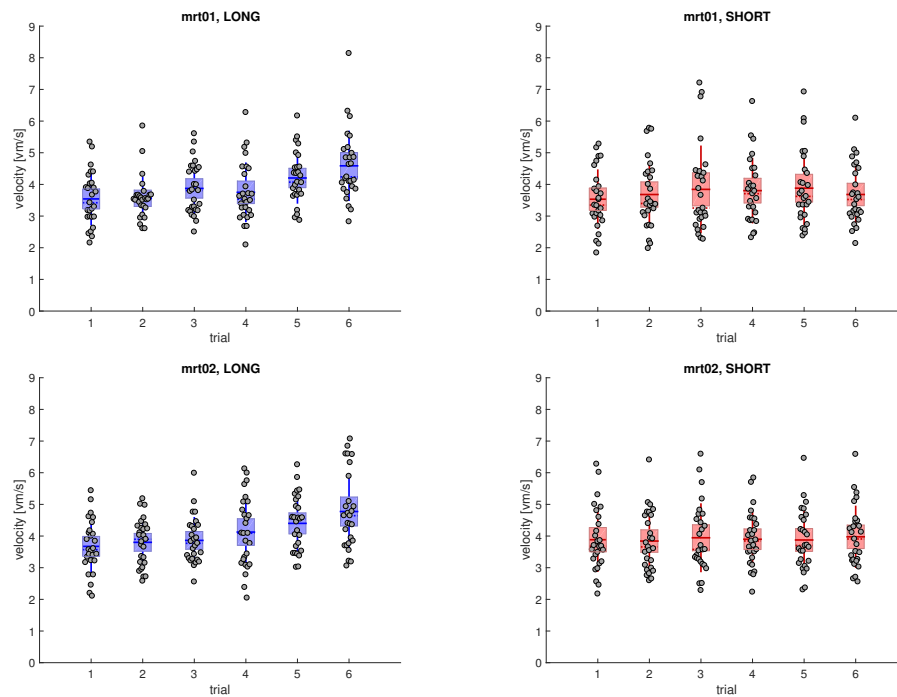


Figure 8: Participants' mean velocity across LONG and SHORT trials. Depicted are, for each trial, each participant's velocity (grey dots), standard deviation (vertical lines), standard error of the mean (patches), and mean and median across participants (horizontal and dashed lines, respectively).

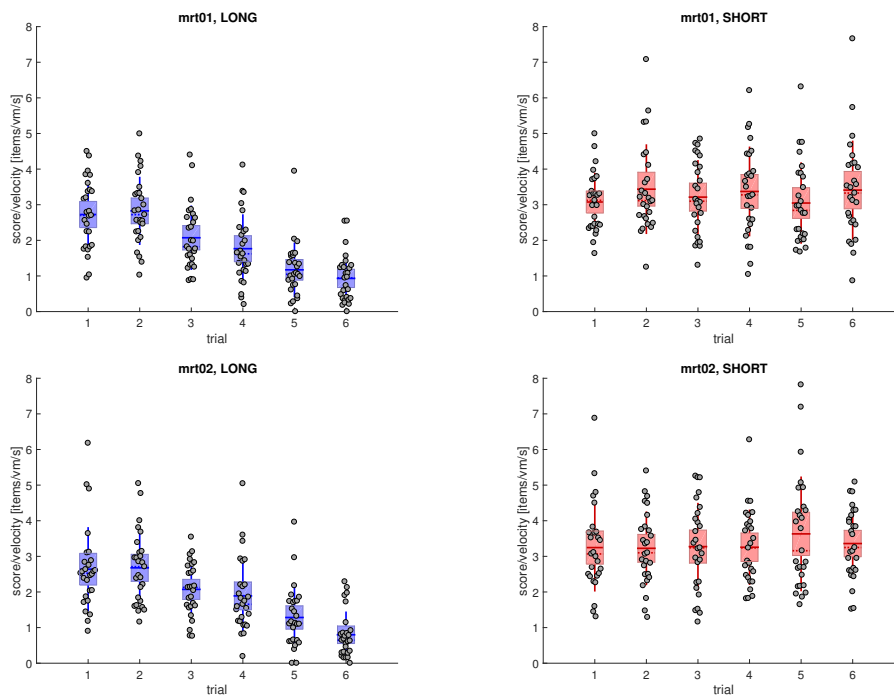


Figure 9: Participants' mean score-to-velocity ratio across LONG and SHORT trials. Depicted are, for each trial, each participant's score-to-velocity ratio (grey dots), standard deviation (vertical lines), standard error of the mean (patches), and mean and median across participants (horizontal and dashed lines, respectively).

Human Spatial Accuracy in an Open-Field Virtual Environment

Authors' contributions

“Human Spatial Accuracy in an Open-Field Virtual Environment” (in prep.)

C. Roppelt, V. L. Flanagin

CR and VLF conceived and designed the study;

CR programmed the task and virtual environment;

CR supervised the data collection;

CR designed and programmed the analyses;

VLF contributed to modeling of the data;

CR and VLF interpreted the data;

CR wrote the paper manuscript and designed the figures;

VLF critically revised the paper manuscript;

VLF supervised the project.

Human Spatial Accuracy in an Open-Field Virtual Environment

Christopher Roppelt^{1,2} and Virginia L. Flanagan¹

¹*German Center for Vertigo and Balance Disorders, Munich, Germany*

²*Graduate School for Systemic Neurosciences, Munich, Germany*

Abstract

Some neurons in the mammalian brain exhibit firing patterns that encode an animal's location in space, and that are influenced by the environment's geometric configuration. Their firing properties are thought to shape the animal's spatial representation of its environment, but the exact extent and mechanisms are unclear. To better understand this relationship, here we measure accuracy and precision of participants' location memory as a proxy for their spatial representation of a quadratic open-field virtual environment (VE) similar to those used to record spatially tuned neurons in humans, and explore the underlying geometric determinants. We find that, first, in line with a previously published model, the variance in participants' responses is well explained by locations' proximity to the environment's boundaries. Second, accounting for accuracy of participants' responses further improved the model fit. Finally, participants' responses and orientation are also affected by the virtual arena's diagonals. We conclude that both variability and accuracy in participants' location memory should be considered when modeling the underlying geometric determinants, and furthermore propose that participants' representation of space in our quadratic open-field VE is shaped both by a locations' boundary proximity and its proximity to the diagonals spanned by the environment's boundaries. These effects should be reflected in the firing properties of place encoding neurons if they provide the neural substrate for a cognitive representation of space.

1 Introduction

Several types of neurons with spatially relevant firing properties have been discovered over the past few decades, such as place cells (O'Keefe and Dostrovsky, 1971), grid cells (Hafting et al., 2005), and boundary-related cells (Lever et al., 2009; Solstad et al., 2008). These types of neurons fire whenever an animal is at particular locations in its environment. This correlation between spatially tuned neurons' firing properties and an animal's location in space builds the foundation for theories about the cognitive representation of space (e.g. O'Keefe and Nadel, 1978). However, it is still unclear to which extent spatially tuned neurons' firing properties – the shape and size of their firing fields – determine our internal representation of space.

Spatially tuned neurons in rodents are typically recorded in open-field environments. These consist of a simple rectangular or cylindrical enclosure that define an arena within which an animal can freely move; landmarks are typically sparse. These environments are therefore primarily determined by the geometry of their boundary configuration, which has been shown to substantially influence the location, size, and shape of place- and grid cells' receptive fields (Hardcastle et al., 2015; Keinath et al., 2017; Krupic et al., 2015; Lee et al., 2018; Lever et al., 2002; O'Keefe and Burgess, 1996; Savelli et al., 2017; Stensola et al., 2015).

Despite the importance of the environmental geometry for the study of place- and grid cells, few attempts have been made to systematically investigate the role of local boundary geometry on the cognitive representation of an environment, as seen in an animal's behavior. Hartley and colleagues examined how participants' representation of three locations within a virtual rectangular open-field environment changed when varying the size and aspect ratio of the arena between presentation and testing (Hartley et al., 2004). The design of their study was similar to a previous experiment in rats that found a tendency for the peak firing rate and receptive fields of hippocampal place cells to vary systematically with changes in the arena's dimensions. Specifically, in rats, receptive fields stretched or squeezed along the direction in which the arena's size was increased or decreased, respectively (O'Keefe and Burgess, 1996). These electrophysiological findings inspired models of place cell firing that explain the representation of a particular location in an environment as a function of that location's proximity to local boundaries (Barry et al., 2006; Hartley et al., 2000; O'Keefe and Burgess, 1996). When Hartley and colleagues compared the spatial distribution of participants' responses with predictions of several geometrically determined models, they found such a boundary proximity model (BPM) to provide the best fit of all models tested (Hartley et al., 2004). They concluded that participants represent the cued locations in terms of boundary proximity consistent with the theoretical framework derived from neural representations in the rat hippocampus (Hartley et al., 2004).

The study by Hartley et al. (2004) provides important insights into the geometric determinants underlying our cognitive representation of space. However, their results are based on the comparison of the representation of these locations across different boundary configurations. They focussed on regions of the environment that changed the most between different environments, and therefore did not systematically sample the entire environment, and did not focus on cognitive representations within

a stable environment. More subtle effects on participants' representation of space may exist beyond those tested and explained by the boundary proximity model.

The current study aims to complement the findings from [Hartley et al. \(2004\)](#) by measuring accuracy and precision of participants' spatial representation in detail across the entire space of a stable environment. Like [Hartley et al. \(2004\)](#), we employed a location recognition task in a virtual quadratic open-field environment; similar setups have more recently also been used to record spatially tuned neurons in humans ([Doeller et al., 2010](#); [Jacobs et al., 2013](#); [Lee et al., 2018](#)) and look at behavior in artificial agents ([Banino et al., 2018](#)). Unlike [Hartley et al. \(2004\)](#), we did not change the environment's boundary configuration throughout the duration of the experiment, but instead measured participants' representation of 36 locations that systematically covered the entire environment. To focus entirely on the geometric determinants of participants' representation of space, our virtual environment (VE) consisted only of a cobblestone-resembling ground plane and four differently colored walls. We did not provide any additional distal landmarks for orientation that could potentially be used by participants as additional navigational cues; orientation could only be determined by the configuration of the four differently colored walls. By tracking participants' paths and orientation in the VE throughout the duration of the experiment we aimed to (1) precisely measure the spatial accuracy and distribution of their responses; (2) assess how well the models of geometric determinants on human spatial memory ([Hartley et al., 2004](#)) can explain participants' responses across the entire environmental space; and (3) explore additional aspects of boundary geometry that influence participants' representation of space as measured by their behavior on a location recognition task.

2 Methods

2.1 Participants

Twenty-nine healthy, adult volunteers were recruited from the nearby university campus. All participants gave their written informed consent to participate in this study in accordance with the Declaration of Helsinki, and were reimbursed for their participation based on the time spent for the experiment. Prior to testing, all participants underwent a color discrimination test to ensure they were able to distinguish the four differently colored arena walls by their color. Although all participants were instructed not to do so, two participants used an angulation strategy that allowed them to measure distances without forming an implicit representation of space and were therefore excluded from any analysis. Two additional participants resigned from the experiment due to motion-induced sickness. Thus, twenty-five (13 female) were included in the final analysis (age 19–33 years; mean: 23.7 years).

2.2 Virtual environment and setup

We used a custom-made virtual environment (VE) created with the Python-based virtual reality toolkit Vizard (version 4; WorldViz, Santa Barbara, USA). The VE was designed to feel as naturalistic as possible for the participants without providing any navigational cues other than those derived from its

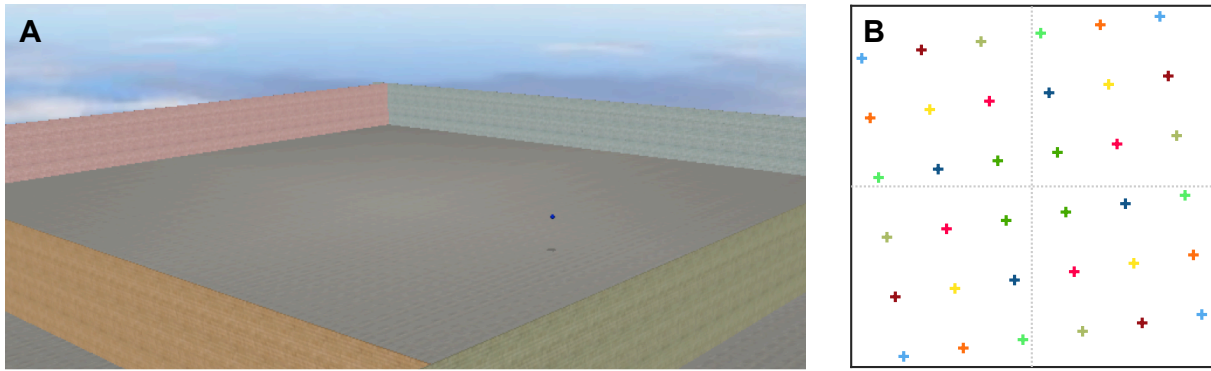


Figure 1: Virtual arena and tested item positions. (A) Four identically textured but differently colored walls enclose the 50×50 virtual square meters large room, in which a sample target, the blue sphere, and its shadow can be seen. (B) The 36 cued locations are arranged at the intersections of an equidistant 6×6 grid. Each of the nine item positions in a quadrant corresponds, in terms of distance to the enclosing walls, to a similar position in any other quadrant. Target locations are indicated by crosses and corresponding target locations share the same color; dashed gray lines highlight quadrants' borders.

boundary geometry. It consisted of a cobblestone-textured ground plane, four differently colored walls of 50 virtual meters (vm) in length (wall colors: red, blue, green, yellow), and a sky texture featuring sun and some white clouds projected at infinity (Fig. 1A). Item color was altered from trial to trial, from red trough yellow, green, turquoise, blue, and pink, to minimize confusion of subsequently tested item positions by participants. To provide a more realistic impression and allow for better determination of its location, an item's virtual shadow was projected on the ground right below the item.

Although the sky contained landmark information, the sky's texture was randomly rotated before each navigation phase (i.e. the collection and return phase, see section 2.3.2 for details) to ensure participants could not use any sky texture feature as a navigational cue for memorizing or recovering an item position. The sky texture could not only be used as potential landmark information in itself; participants could also use it to memorize the configuration of the sky with respect to certain texture features on the arena's boundaries to infer on an item's position in the arena. Therefore, for our experiment, the sky was changed in every phase of each trial.

Participants used a Thrustmaster T.Flight Stick X joystick (Guillemot Corporation, La Gacilly, France) to navigate through the environment that allowed them to freely change their viewing angle (resulting in a virtual whole-body rotation) and travel speed (resulting in virtual forward or backward movement) by deflecting the joystick along its *X*- and *Y*-axis, respectively (not deflecting the joystick in any direction resulted in no movement or head rotation). Speed of body rotation and translation was controlled by the extent of joystick deflection in the corresponding direction and was limited to a maximum that was within the range of real-world movements.

2.3 Paradigm and procedure

2.3.1 Paradigm

We tested participants' location recognition (i.e. the ability to collect and return objects) for 36 object locations ("item positions") within the boundaries of our virtual open-field arena.

Item positions were arranged at the intersections of an equidistant 6×6 grid which was anchored at the center of the VE and rotated 7 degrees counter-clockwise. We chose this item configuration for three important reasons: First, because of the symmetry of the environment we can treat the 6×6 object locations as four repetitions of a 3×3 item position configuration, and collapse the data, thereby increasing the number of trials each participant completed. This is achieved by rotating all item positions inside a particular quadrant by either 90, 180, or 270 degrees (depending on the quadrant) around the VE's center. Second, each of the 3×3 item positions has a unique distance to any of the arena's boundaries which allows us to assess participants' representation of item positions in terms of the distance to boundaries. Finally, it obfuscates the regular arrangement of item positions to participants. During piloting of the experiment we found that in a 5×5 object location configuration, some participants could deduce the item position arrangement along one side of the grid and therefore assumed a regular structure for the object locations. In a 5×5 configuration, or any odd symmetrical configuration, one item position will be located halfway between two walls. This is quickly detected by participants, even for rotated item configurations. The regularity in item positions was, however, not detected by participants for the 6×6 item position configuration (Fig. 1B).

To keep the distance between the start of a path to the object location equal for all objects and all phases of the experiment (see section 2.3.2), we defined eight starting positions for each of the object positions. The starting positions were equidistantly arranged on the full circle defined by a radius of 20 vm around the corresponding item position. For item positions close to boundaries, only those start positions that were within the arena could be chosen as start positions. Each of the eight start positions could only be chosen once in the experiment.

2.3.2 Procedure

The experiment consisted of four runs, in which each of the 6×6 item positions was tested once. Each of the 36 item positions was therefore tested four times (once per run) for each participant. The order of the tested item positions was chosen pseudo-randomly and differed for each run and across participants.

Each trial consisted of three phases: a collection phase, a return phase, and a feedback phase (Fig. 2A). At the beginning of the collection phase, a participant was pseudo-randomly positioned inside the arena at one of the eight (or less) possible start positions. Participants were positioned such that they directly looked towards the cued item position where a virtual sphere ("item") was located at participants' virtual eye height. Participants were instructed to move through the arena to collect an item, such that they could remember the item location as accurately as possible. Thereby they received

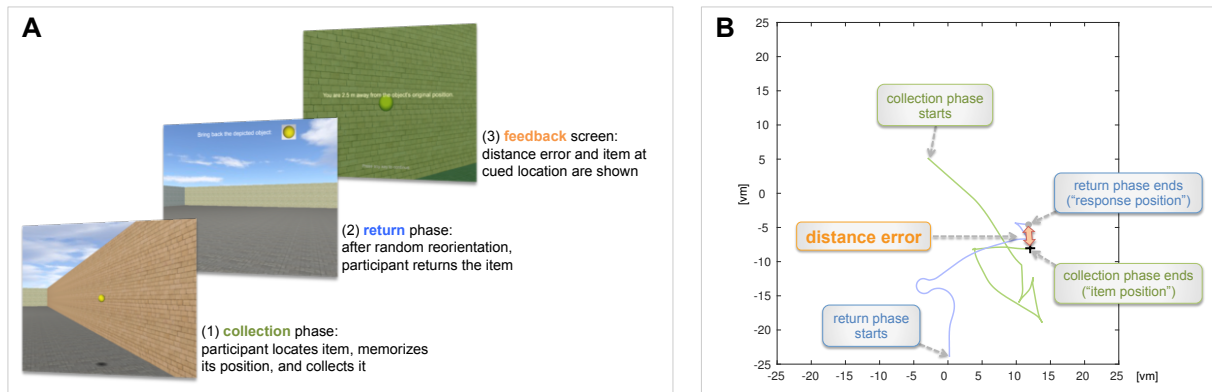


Figure 2: Task and procedure. (A) Each trial consists of three trial stages: (1) participants are positioned in the arena at a pseudo-random start position and collect an object randomly appearing at one of the 6×6 item locations; (2) they are randomly reoriented and repositioned, and have to return the previously collected object at its initial position; (3) distance feedback is given. (B) Sample trial: A participant's track during the collection (green) and return (blue) phases, and distance error, defined as the shortest Euclidean distance between an object's cued and the response position (orange).

additional tips that (1) it is helpful to view the cued item from different perspectives in order to develop a precise estimate of its position; and (2) they should only collect an item only when they felt confident about its position. Items were collected by entering a radius of 0.5 vm around the item's center. No time constraint was given. The collection phase ended when the item was collected. The VE was then locked to that position and the screen smoothly changed color (over 0.5 seconds) until the VE was no longer visible on the monitor.

The return phase started immediately after the collection phase. Participants were pseudo-randomly positioned at one of eight start positions associated with the collected item for the current trial but not the start position from the collection phase. Participant's viewing direction for the start position of the return phase was randomly chosen with no constraints. A short message appeared on the upper middle of the screen informing participants to return the previously collected item. An image of the item to be collected was also presented on the middle of the screen. To return an item, participants navigated the arena and, when they were confident to have reached the item's initial position, they pressed a joystick button to "drop" the collected item at the participant's current location. This we then called the "response position" (as opposed to the initial "item position"; see Fig. 2B). The return phase ended as soon as the joystick button was pressed, and participants could no longer move through the VE. The screen became semi-transparent (duration: 0.5 seconds).

The feedback phase began immediately thereafter. In the feedback phase, the cued item appeared at its position in the arena. The participant was smoothly and passively turned (duration: 1 second) from the current viewing angle to the angle that pointed to the middle of the item position, so that the participants could see how far away they were from the originally remembered position. Additional feedback was provided in the form of a message on the screen that stated the corresponding "distance error" defined as the shortest Euclidean distance between item position and the response position (Fig. 2B). The feedback phase ended as soon as a participant pressed any joystick button (no time constraint was given) and the screen became fully opaque.

At the beginning of each trial, prior to the collection phase, the screen displayed the number of the current trial to inform participants about their progress. Participants were aware of the total number of trials per run. The collection phase would only begin after participants pressed a joystick button, so that this period also served as an opportunity for participants to shortly rest before continuing with the experiment.

Participants were given both the number of runs and the number of trials per run during introduction into the experiment. The 6×6 item position configuration gives a conspicuously unintuitive number of trials per run. For this reason, and because even with the even number of item positions per run participants may still learn the structure of the item locations, we added four random item position trials. The actual item positions were randomly chosen but not one of the 6×6 item positions. Random item position trials were not included in the analysis.

After finishing the experiment, participants were verbally questioned about the organization of the item positions within the arena. If a participant suspected a regularity in item positions, he or she was asked to describe the regularity in detail. Only a few participants suspected non-random item positions, but none of them correctly described the item position configuration.

2.4 Data analyses

During navigation in the VE, the participants' virtual position (x , y , and z values) and viewing angle were recorded with a sampling rate of approximately 50 milliseconds, together with the exact recording time of each sample. The item position and response position were also stored for each trial in a separate text file.

Data were analyzed in Matlab (version R2016a, The MathWorks, Natick, USA). Before the data were analyzed, they were preprocessed for “rotational errors” in participants' responses (for a review see [Cheng et al., 2013](#)). In a quadratic arena, a rotational error is observed when a participant returns an item at a location in the arena that is geometrically equivalent to the cued item position but refers to an incorrect boundary combination. For example, if an item is cued close to the corner between the red and the blue wall, and the participant returns it to a location that has approximately similar distances to a corner, but the walls are now yellow and green. This would result in a large distance error which is not the result of a highly inaccurate memory of the cued location but rather confusion or forgetting the configuration (in this case color) of the closest walls ([Cheng et al., 2013](#)). Our pilot studies suggested that rotational errors occur in our experiment in approx. 4.5% of trials. We therefore implemented the following automatic correction mechanism. For trials with distance errors of 20 cm or higher, the corresponding response position was rotated by 0, 90, 270, or 360 degrees around the center of the arena. The position that yielded the smallest distance error was assumed to be the participant's intended response position and replaced the recorded response position; the corresponding viewing angle was adjusted accordingly.

After adjustment of putative rotational errors, the data was scanned for outlier trials. For each item position, all corresponding responses positions of a participant that fell outside the 99% confidence

interval around the participant's mean response position at that item position are considered outliers and excluded from any further analysis.

After preprocessing and outlier detection were complete, we wished to collapse participants' responses from four quadrants into one. To determine the validity of this approach, we conducted a two-way repeated measures analysis of variance testing for the effects of item position and arena quadrant on distance error across all trials for each participant. Only participants, for which neither a statistically significant interaction effect of item position and arena quadrant, nor a statistically significant main effect for arena quadrant on distance error was found (significance level .05, corrected for multiple comparison by the number of participants [$N = 25$]: $\alpha = 0.002$), were included in subsequent analyses. Participants' responses were collated by rotating all response positions in the upper right, lower right, and lower left arena quadrants by 90, 180, and 270 degrees (counterclockwise), respectively, into the upper left arena quadrant. This reduced the 6×6 to a 3×3 item position configuration while at the same time quadrupling the number of response positions available at each of the 3×3 item positions.

We first examined how the spread of participants responses (that is, the precision of participants' location memory) is influenced by the geometry of the environment by comparing the response distributions of each item position to two models (see section 2.5 below). However, these models do not account for deviations between the mean response position and the original item position (that is, the accuracy of participants' location memory). To statistically evaluate this assumption, we tested each of the 3×3 item positions against their corresponding mean response positions across all participants using multivariate one-sample Hotelling's T^2 tests.

We wished to additionally explore and characterize participants' responses beyond the model fit. The models reproduce response position densities that have a maximum variance parallel to the walls of the arena (the arena's cardinal directions), however, our pilot data suggested that the main direction of the spread of response positions was not along the arena's cardinal directions. To characterize the spread and direction of the spatial distribution of participants' responses at each item position, we calculated the eigenvectors of the response positions at each item position. We then computed the eigenvector deviation from the arena's cardinal directions. For a given item position, cardinal directions are defined by the four vectors arising from the corresponding mean response position and pointing perpendicularly towards the arena's walls. Eigenvector deviation was defined as the angle in degrees between any eigenvector and the closest cardinal direction vector. Values range from 0 (eigenvectors aligned parallel to arena boundaries) through 45 degrees (eigenvectors are aligned parallel to diagonals spanned by the arena's boundaries).

We then tested for a linear correlation between deviation of eigenvectors and proximity of corresponding item positions to arena diagonals (Pearson's correlation coefficient). Proximity to the arena's diagonals at an item position is defined as the Euclidean distance between item position and the point closest to it on any of the two diagonals spanned between opposite arena corners. Eigenvector deviation was calculated for each of the 3×3 item positions separately for each participant and the Pearson's correlation coefficient r was calculated across all participants.

It is possible that participants try and match the view of the visual scene when they returned an item to their memory of that visual scene when the item was collected, and that the viewing angles were not randomly distributed but aligned to the only landmarks available; the corners of the arena. To examine this we calculated histograms of participants' viewing angles when they collected an item (i.e., when they reached the item position) and when they returned that item (i.e., when they dropped it at the response position) separately for each participant and trial, and sorted by the 3×3 item positions. Polar histograms were calculated for a bin width of 10 degrees. We then calculated the angle between the item position and the corner of the arena between the two closest walls, and between the mean response position and that corner for each item position separately. These angles represent the participants' viewing direction if they had been facing the corner between the two walls closest to them when collecting and returning an item. These angles are indicated together with participants' viewing angles in the polar histograms.

2.5 Models

We fitted three different models to participants' response positions. The first two were taken from [Hartley et al. \(2004\)](#) and named accordingly: the Absolute Distance Model (ADM), and the Boundary Proximity Model (BPM) ([Hartley et al., 2004](#)). In our study, these two models describe the spread of the response positions for each individual location, but because the environment does not change, the mean of the response distribution is centered at the item position. The final model was the BPM model but adapted to represent the participants' mean responses and not the original item position. The change in this model is akin to stating that an individual's internal representation of the item position is not necessarily the actual item position.

Models are calculated and applied similar to [Hartley et al. \(2004\)](#). Using a bin size of 1×1 vm, we first calculated response density maps (RDM) for each of the 3×3 item positions and smoothed them applying a 2D Gauss kernel (size 3×3 bins; $\sigma = 1.5$ bins). Then, for each model, we calculated the corresponding similarity matrices (with bin size equal to RDMs) at each item position. For a given model and item position, the similarity matrix contains the Euclidean distance between the model's representation at a particular bin and the model's representation at a constant reference position. For the ADM and the BPM, this reference position is the respective item position; for the BPM at participants' mean response, this is the corresponding mean across participants' response positions. For a given model, we then calculated at each item position the probability distribution of responses falling into the 50×50 bins that best explains participants' response positions at an item position given the model. The models' corresponding log likelihood values at each of the 3×3 item positions are reported in [Tab. 2](#) and used to compare the quality of the tested models.

Note that both the BPM and the BPM at participants' mean responses incorporate a constant c that [Hartley et al. \(2004\)](#) set to $c = 128$ for their reported simulations. How they derived this value is not explained, but we speculate that it was chosen because it represents half the length of a boundary in their small quadratic arena setup ([Hartley et al., 2004](#)). We set c accordingly, equalling 25 vm in all our simulations.

3 Results

3.1 Raw data

The first step in our analysis was to automatically correct for potential rotational errors by examining whether for response locations with large errors (greater than 20 cm) the distance error could be reduced by rotating the arena by a multiple of 90 degrees. On average 1.48 response positions out of 144 (range: 0–7; standard deviation: 1.69) per participant were adjusted in this way. Thirty-seven response positions in total were adjusted across all 25 participants (1% of total). Participant M19 marks a particularly extreme case, for which seven response positions were adjusted, and for all of which it seems plausible that the participant remembered the cued item position but confused the quadrant (see Supplement Fig. 8).

Next, our automated outlier detection identified between zero and five responses to be outliers for each participant (mean \pm standard deviation: 1.48 ± 1.69). In total 40 responses from 25 participants (1.1% of total) were labeled as outliers and excluded from any further analysis (Supplement Fig. 9). For three participants, a total of four of the adjusted response positions were then discarded in the outlier detection process. Figure 3 shows all response positions along with the total number of response positions included in the analysis after adjustment and outlier detection at each item position, after collating the data from 6 \times 6 to 3 \times 3 item positions.

For each participant, we tested the effects of item position and item position's quadrant on the observed distance errors with a two-way repeated measures ANOVA. There was no significant main effect of item position quadrant (four levels, one for each of the four quadrants) on the distance error of any participant; a significant effect of item position (nine levels, one for each of the 3 \times 3 item positions) on participants' distance errors; and no significant interaction effect (results for all participants are listed in Supplement Tab. 3). We therefore concluded that we could collate our data accordingly, and the rest of the analyses were then done on the 3 \times 3 reduced item position matrix.

For the rest of the analysis, "item positions" is therefore used to refer to the nine item positions from the 3 \times 3 configuration (as opposed to the 6 \times 6 item position configuration). They are labelled 1 through 9 according to their position from the upper left to the lower right corners of the arena's upper left quadrant, as depicted in Fig. 3. With this configuration, we tested whether the mean response position significantly differed from the item position and found this to be true for all item positions except the one closest to the arena's center. Exact cued item positions and corresponding mean response positions for each item position are listed in Tab. 1.

3.2 Models

The aim of the study was to understand participants' response as a function of the arena's geometry. To do this we modeled the participants' responses starting with the simplest assumption, in which each of the arena's four walls is equally important for the participant to represent an item location somewhere in the arena. In this model, termed "Absolute Distance Model" (ADM) by [Hartley et al.](#)

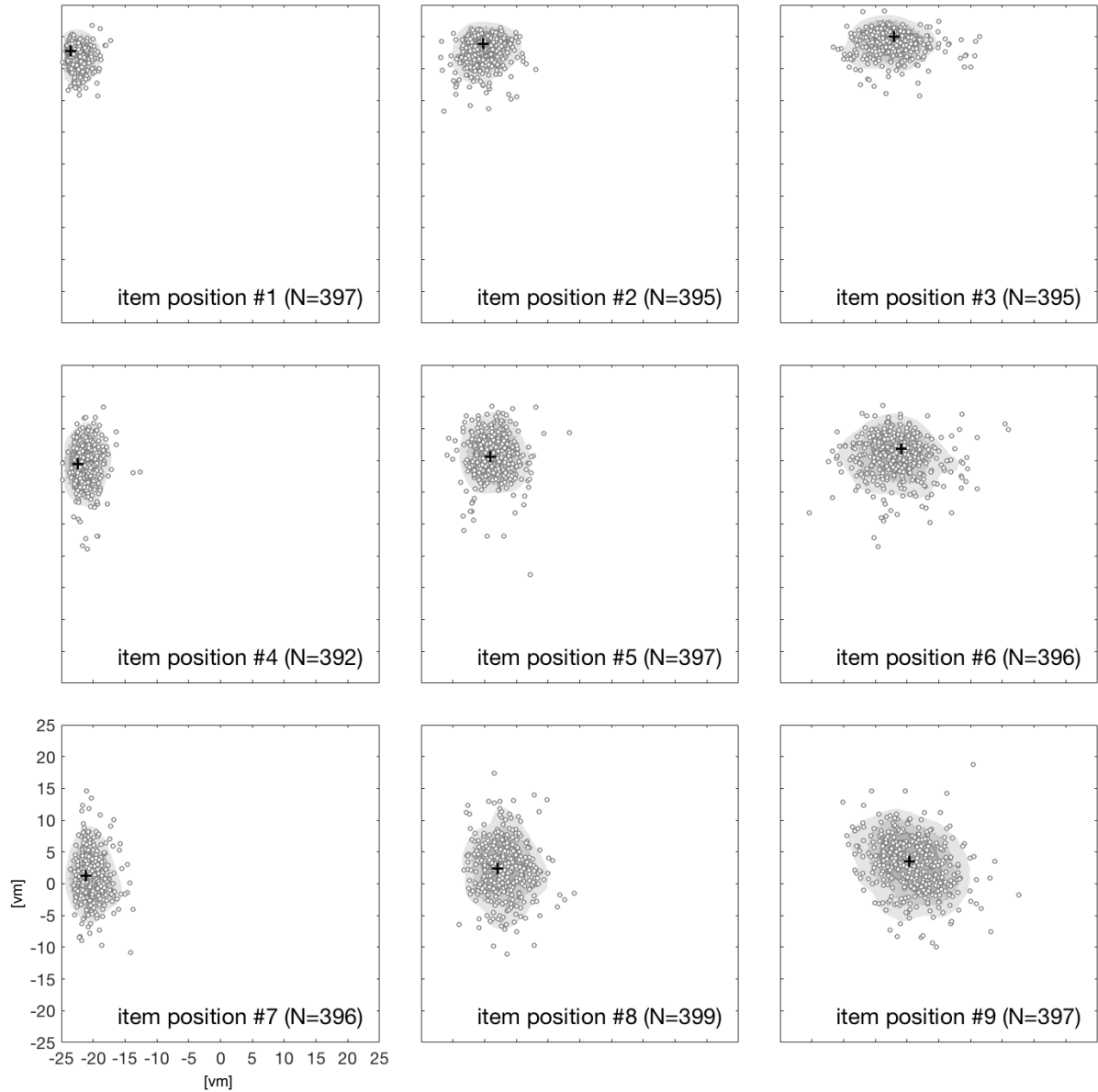


Figure 3: Raw data after collating data into one arena quadrant. All drop positions (unfilled circles) included in the analysis after removing outliers are shown for each of the 3×3 item positions (black plus). The shaded areas in the background represent the smoothed response density maps (RDM) at the respective item position and indicate the 10, 25, and 50% levels of the maximum number of responses per bin (from lighter to darker shading). The label and number of data points (N) included in the analysis at each item position is shown in the lower right corner of each panel.

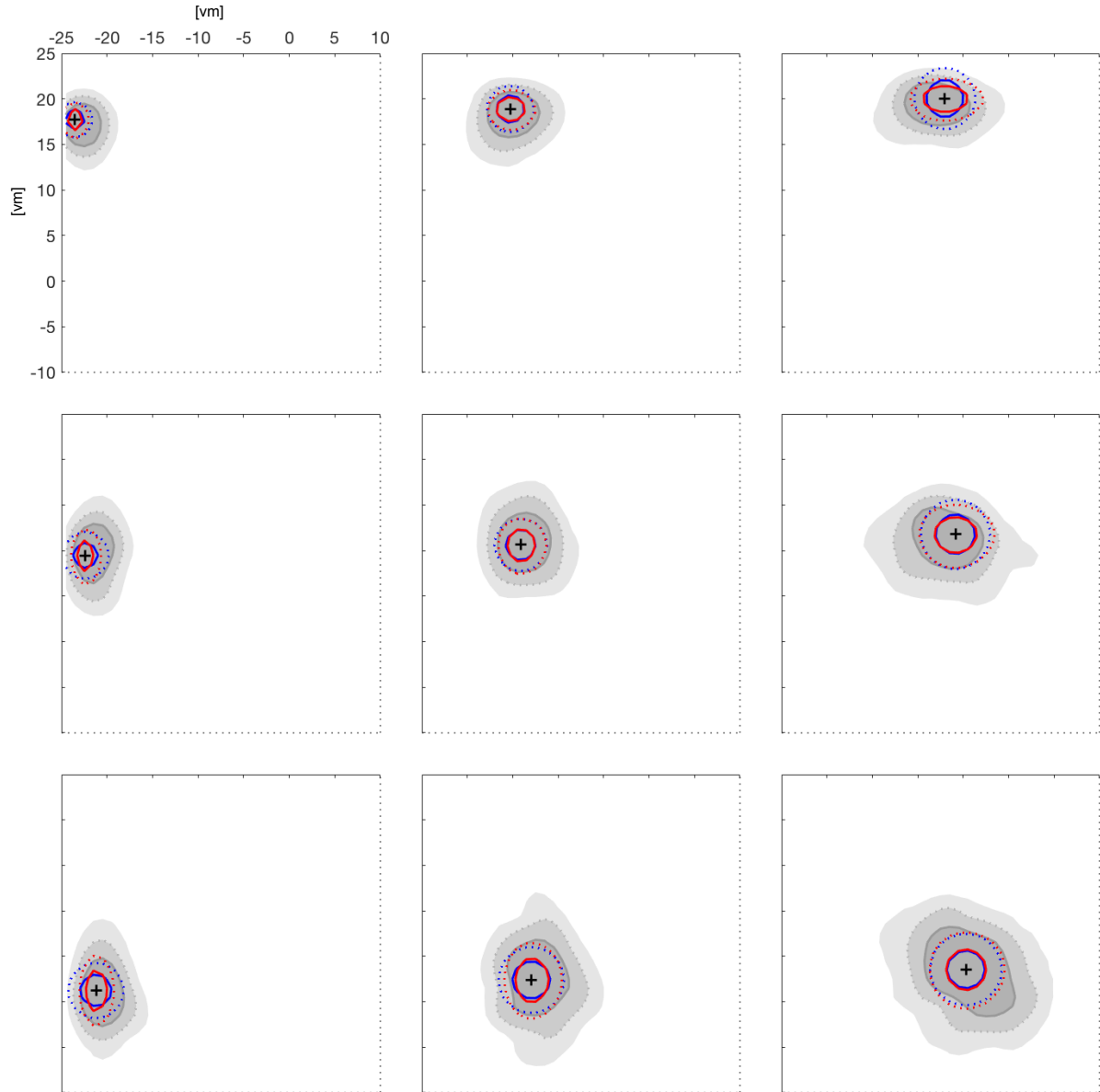


Figure 4: Fit of the ADM and BPM to the data. Panels show the optimal fit of the ADM (blue) and BPM (red) to the distribution of drop positions at each of the 3×3 item positions (black plus). Drop positions are represented by their respective RDMs as shaded areas in the background, as described in Fig. 3. Models are indicated by colored dashed and solid lines that indicate regions within which the corresponding model's response density is greater than 25% and 50% of the maximum, respectively. Note that panels show a zoomed-in top-down view of the arena and not the whole area.

position	cued (X,Y)	mean (X,Y)	d [vm]	Hotelling's T^2 test
1	-23.53, +17.73	-22.45, +16.90	1.36	$T^2 = 405.89$; $F(2, 395) = 202.43$; $p < .001$
2	-15.28, +18.89	-15.02, +17.63	1.28	$T^2 = 142.14$; $F(2, 393) = 70.89$; $p < .001$
3	-7.03, +20.05	-7.51, +18.92	1.23	$T^2 = 150.49$; $F(2, 393) = 75.05$; $p < .001$
4	-22.37, +9.48	-21.20, +9.39	1.17	$T^2 = 252.79$; $F(2, 390) = 126.07$; $p < .001$
5	-14.12, +10.64	-13.62, +10.62	0.50	$T^2 = 15.70$; $F(2, 395) = 7.83$; $p < .001$
6	-5.87, +11.80	-6.58, +10.58	1.41	$T^2 = 66.46$; $F(2, 394) = 33.14$; $p < .001$
7	-21.21, +1.23	-20.24, +1.09	0.98	$T^2 = 135.22$; $F(2, 394) = 67.44$; $p < .001$
8	-12.96, +2.39	-12.01, +2.41	0.95	$T^2 = 43.54$; $F(2, 397) = 21.71$; $p < .001$
9	-4.71, +3.55	-4.15, +3.08	0.73	$T^2 = 9.10$; $F(2, 395) = 4.54$; n.s.

Table 1: Relation of cued item positions and participants' responses. For each of the 3×3 item positions the table shows the cued location and the mean across all corresponding drop locations and participants. The deviation of the mean response from the cued item position is expressed by the shortest Euclidean distance d (in [vm]) between these two locations. The results from Hotelling's T^2 test show whether or not a statistically significant difference between the distribution of drop positions and its expected mean with the item position exists.

(2004), participants estimate the distance from the item position to each of the four walls to determine where to return the item.

The ADM has been found by Hartley et al. (2004) to be outperformed by the "Boundary Proximity Model" (BPM). This model was inspired by electrophysiologically observed firing rates of place cells in rats (Hartley et al., 2000; O'Keefe and Burgess, 1996). It gives each of the arena's walls a different weight in the representation of a location, where the weight decreases with increasing distance towards that wall. In other words, the closer a wall to an item position, the more important it becomes for participants' representation of that position.

When we quantified the models' fit of the data by their respective log likelihood values, we found that, similar to Hartley et al. (2004), the BPM fits participants' responses better than the ADM (Fig. 4). The BPM captures the elongated response density maps (RDMs) that the ADM does not. Importantly, while Hartley et al. 2004 only reported a quantitative comparison across varying arena geometry but not within the same arena, we found this to be true – to varying degrees – for all nine item positions, that is, across the whole space within the same arena (Tab. 2).

3.3 Mean response positions

The framework described by Hartley et al. (2004), within which the ADM and BPM were proposed and tested, is suited to model the distribution of response positions, but it is not designed to account for an offset of the distribution's mean from the actual item position. However, the mean response position did differ from the corresponding cued item position for all item positions except for position 9, the one closest to the arena's center (statistical results: Tab. 1).

To evaluate if accounting for the mean response position has an effect on how well the BPM is able to fit participants' response locations, we again calculated the best fitting BPM, however this time centered around the mean response position rather than the actual item position (Fig. 5). This yielded

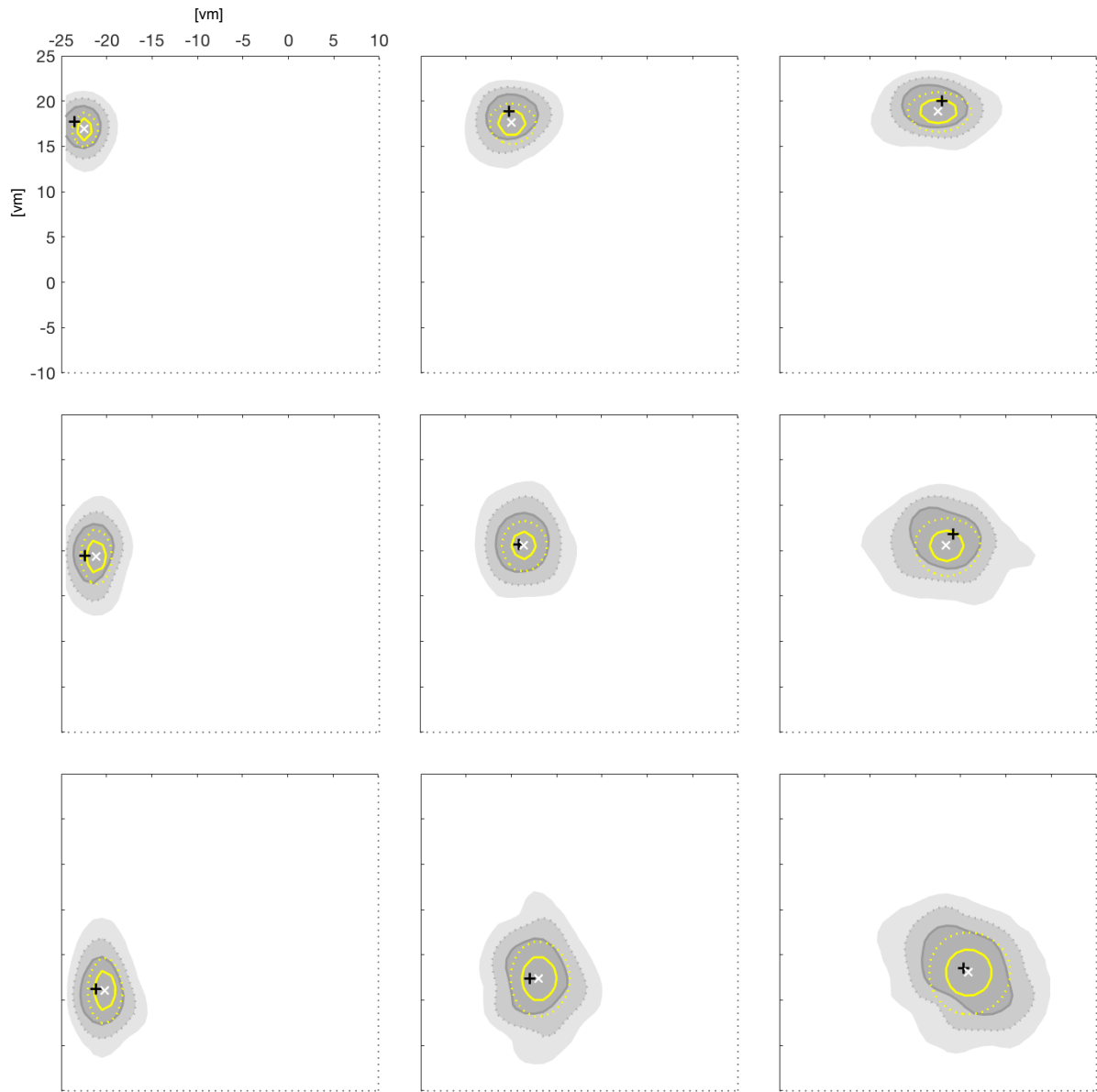


Figure 5: Fit of the adapted BPM to the data. Panels show the optimal fit of the adapted BPM (yellow) to the RDM (shaded areas) at each of the 3×3 item positions (black plus); description see Fig. 4. In addition, mean drop positions (at which the adapted BPM is calculated) are indicated by white crosses.

Model	Fit $\log(p(\text{data} \text{model}))$ by item position								
	1	2	3	4	5	6	7	8	9
ADM	-1473	-1802	-1951	-1768	-1966	-2197	-1902	-2166	-2299
BPM	-1465	-1774	-1902	-1739	-1958	-2180	-1844	-2140	-2289
BPM at mean response	-1410	-1778	-1876	-1709	-1962	-2167	-1835	-2142	-2292

Table 2: Quantitative comparison of tested models. The table lists the negative log likelihood values of the three models at each of the 3×3 item positions. It indicates how well the model explains the data at a particular item position (smaller values indicate a better fit).

a smaller log likelihood for the adapted BPM at five of the nine item positions, indicating a better fit of the data by the adapted BPM model at these positions and a slightly worse fit at the remaining four (position 1: 3.8%; position 2: -0.2% ; position 3: 1.4%; position 4: 1.7%; position 5: -0.2% ; position 6: 0.6%; position 7: 0.5%; position 8: -0.1% ; position 9: -0.2% ; absolute values see Tab. 2). While the BPM yielded an average log likelihood across the 3×3 item positions of -1921 , the adapted BPM yielded an average log likelihood of -1908 , indicating a better fit of the recorded data by the adapted BPM model.

3.4 Effect of the diagonals

Visual inspection of the distribution and mean of participants' response positions suggests two additional effects that were not accounted for by the models tested so far:

First, the mean response positions were shifted away from their corresponding item position relative to the closest wall. For most response positions, the mean response position was shifted relative to the two closest walls. In other words, there seems to be a general tendency for the mean response position to be shifted from the cued item position towards the arena's center. Furthermore, for those item positions where the mean response position appears to only be affected by the closest wall, the mean response position seems to move towards the diagonal between the two closest walls instead. In other words, there seems to be a general tendency for the mean response position to be shifted away from their corresponding item positions both towards the center of the arena and toward the diagonal between the two closest walls.

Second, not only the mean response position, but also the direction of spread of response positions appears to be influenced by the diagonal. The two principal axes of the response positions' distributions do not always stretch along the arena's cardinal directions (i.e., parallel to the walls), as implicated by the BPM. Instead, the long axis is tilted towards the diagonal between the two closest walls. This effect seems to become stronger, the farther away from the closest wall, and the closer to that diagonal an item position is located.

To quantify this we needed a measure of the distribution of response positions. The histograms of the response positions, i.e. the response density maps (RDM), that were considered for our analyses so far, do not allow for quantification of the response positions' spatial extent and orientation. Instead, we calculated the eigenvalues and eigenvectors of the response positions, which characterize both

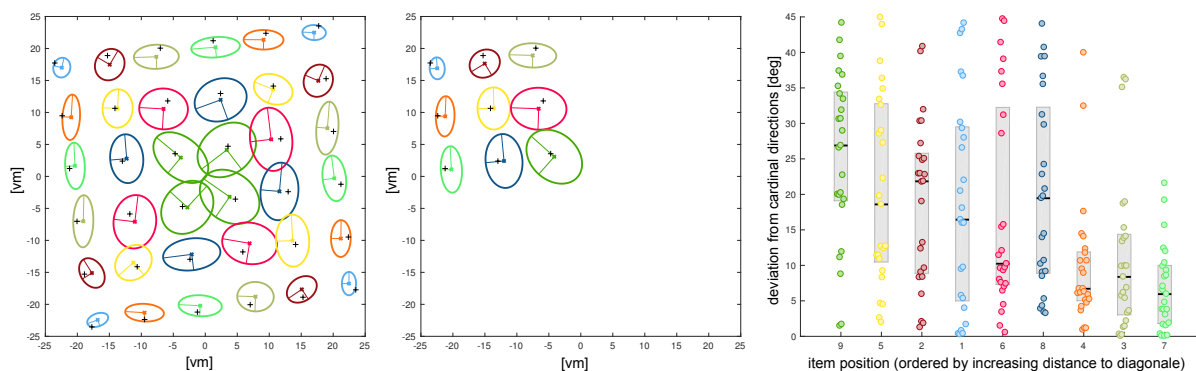


Figure 6: Eigenvectors and their deviation from arena's cardinal directions. Left and middle panels show the distribution of drop positions for all participants at each item position represented by the distributions' eigenvectors and the ellipses spanned by them. Ellipses at item positions in the 6×6 configuration that collate to the same position in the 3×3 configuration are shown in identical colors. The right panel shows the eigenvectors' deviation angles at the 3×3 item positions for each participant, with item positions ordered on the X axis by increasing distance to the closest diagonale. Each dot represents the deviation angle of one participant at the respective item position (color-coded according to left-most panels); median and the 25 through 75 percentile range at each item position are indicated by black lines and gray boxes, respectively.

the spread and the direction of the underlying response positions, and determined their deviation from the arena's cardinal directions at each item position (Fig. 6).

We found a statistically significant correlation between the eigenvectors' deviation angle and the distance to the closest diagonale for the 3×3 item positions across participants (Pearson correlation coefficient $r = -0.39$, $p < .001$), suggesting that the closer the item position was to the diagonale, the more the main direction of variance of the response positions was along the direction of the diagonale (i.e. 45 degrees away from parallel to the closest wall).

3.5 Viewing angles

Because we did not have any a priori assumptions about the viewing angles, we concede that this part of the results becomes more exploratory. However not only position, but also orientation, or the viewing angle, of the participants, may provide us with relevant information about how memory about geometric spaces is stored. To examine this, we extracted participants' viewing direction at the moment when they collected an item and when they dropped (i.e., returned) it. The histogram of viewing angles can be seen in Fig. 7.

We compared the number of trials for which participants were facing the two closest walls (that is, viewing angles ranging counterclockwise from NE to SW) to those where they were facing mostly the two farthest walls (that is, viewing angles ranging clockwise from NE to SW) and found that participants tended to face one or both of the two closest walls, both when collecting and when returning an item (position 1: 88%/89%; position 2: 83%/87%; position 3: 80%/86%; position 4: 84%/87%; position 5: 83%/87%; position 6: 74%/79%; position 7: 74%/80%; position 8: 71%/77%; position 9: 63%/69% of collection and return trial phases, respectively). This result indicates that participants,

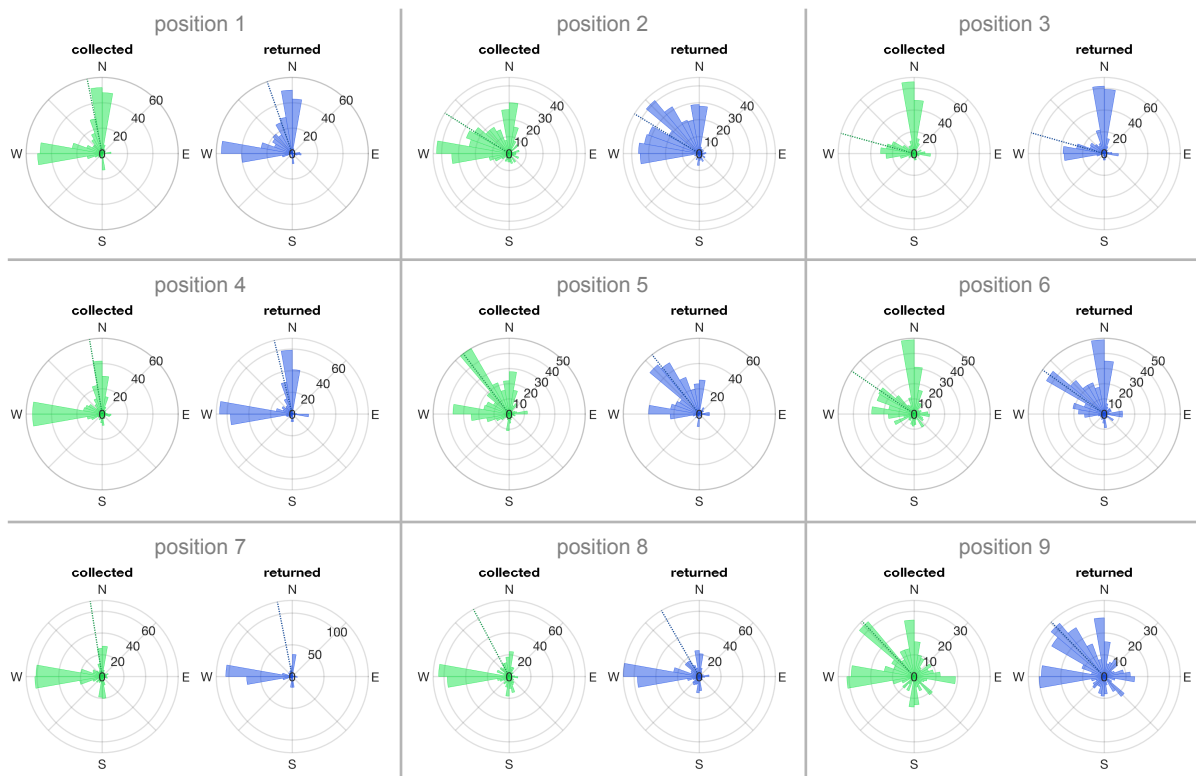


Figure 7: Participants' viewing angle when collecting and dropping an item. Viewing angles are depicted as separate polar histograms for trials' collection (green) and return (blue) phases across all participants and trials at each of the 3×3 item positions. The viewing angles exactly facing the corner between the two closest walls at each item position and corresponding mean response position are also indicated for reference (dashed green and blue lines, respectively). Labels indicate viewing angles in terms of cardinal directions anchored at the arena's center (N and W thus represent the closest two walls).

when collecting or dropping an item, inferred their current location in the arena from their estimated distance towards the two closest walls. It is possible that they match the visual image at a particular viewing angle at the return location to their memory of the view from the item position. Considering the observed shift of mean response positions away from the corresponding item position towards the arena's center, this suggests that participants tend to underestimate their distance towards the closest walls. Furthermore, this underestimation effect seems to be stronger for item positions close to a wall, since for these positions we found larger offsets between item position and participants' mean response compared to item positions farther away from any wall; and to decrease towards the arena's center (for item position 9 we did not observe a significant difference between cued position and participants' mean response). Though this suggests a systematic effect, we did not find a statistically significant correlation between distance from an item position to the closest wall and the corresponding mean distance error (Pearson correlation coefficient; $p = 0.0721$).

Interestingly, the polar histograms of participants' viewing angles further show a tendency for participants to face the wall closest to an item position at item positions close to the walls; and to face the corner between the two closest walls at item positions close to the diagonal between these walls.

This effect is consistent across both the collection and the return phases. This provides a potential explanation for the observed tendency of eigenvectors to deviate towards the diagonal at item positions closest to the diagonal, and further underlines an influence of the diagonals on participants' representation of the arena's space.

4 Discussion

The current study measured the accuracy and precision of participants' spatial representation for the first time systematically across the whole space of a large, purely geometrically defined open-field VE, and explored the underlying geometric determinants. We found that the amount of rotational errors and outliers (approx. 1% for both) was similar in our data to what has been described previously (Cheng et al., 2013). There were no systematic effects of one quadrant of a square arena, such that data could be collapsed into one quadrant. Participants tended to reproduce item positions that were closer to the nearest walls with higher accuracy, suggesting that the geometry of the environment was important for behavior. Additionally, the mean return position was significantly different from the item position for all locations in a quadrant except the most central point, suggesting a systematic shift of the remembered item position towards the centre of the arena. We showed that the previously described boundary proximity model Hartley et al. (2004) fits to participants' responses in a fixed arena geometry and across the whole space of an open-field VE. Adding the deviation between item position and return position improved the model fit. Finally, in addition to the proximity to boundaries, we showed that proximity to the arena's diagonals affects both participants' orientation and the mean and variability of their responses.

4.1 Models of geometric determinants

This study was designed to systematically assess participants' representation of a large-scale open-field VE. Such open-field setups are often used to investigate spatially tuned neurons both in animals and humans (e.g. Doeller et al., 2010; Hafting et al., 2005; Jacobs et al., 2013; Lee et al., 2018; Lever et al., 2009; O'Keefe and Burgess, 1996; Solstad et al., 2008). Despite the importance of open-field setups for the investigation of these cells, no comprehensive and systematic description of participants' spatial representation of such environments has been reported so far. Importantly, even studies intended to investigate the geometric determinants of subjects' spatial representation did not solely consist of proximal geometric boundaries but provided additional distant landmarks (Hartley et al., 2004; O'Keefe and Burgess, 1996) that likely affects location memory. The current study is the first to assess participants' representation of space within a purely geometrically determined virtual environment, in the absence of landmark information.

In their study on geometric determinants of human spatial memory, Hartley et al. (2004) tested and modeled participants' representation of three locations across varying boundary geometries. They found that their Boundary Proximity Model (BPM) best explained the distribution of participants' responses (Hartley et al., 2004). In contrast to their study, we (1) only used a single, quadratic boundary

configuration throughout the whole experiment; (2) assessed participants' spatial representation at nine locations, arranged at the intersections of a regularly spaced grid, that covered the VE's whole space; and (3) provided no landmarks other than the four colored walls that enclosed the virtual arena. We sought to assess how the geometry-based models explain participants' representation of space in a fixed arena geometry. However, most models proposed by [Hartley et al. \(2004\)](#) only differ across changing boundary configurations, but are identical when arena geometry is not modified. Only one additional model, the Absolute Distances Model (ADM; [Hartley et al., 2004](#)), remains different from the BPM for our fixed boundary configuration.

The ADM formulates the simple hypothesis that participants can reproduce each cued location within the arena with equal accuracy and precision, or, in other words, that participants' internal representation of locations is uniform across space. The BPM is derived from electrophysiological recordings that show an increasing influence of a particular boundary on place cells' firing fields with increasing proximity to that boundary ([Hartley et al., 2000, 2004](#); [O'Keefe and Burgess, 1996](#)). In contrast to the ADM, the BPM accounts for the elongated response density along the direction of the closest wall, because it weights each wall by how close it is to the item position. We found the BPM to outperform the ADM at all nine item positions tested, thereby confirming the supremacy of the BPM over the ADM reported by [Hartley et al. \(2004\)](#). In addition, while [Hartley et al. \(2004\)](#) based their conclusion on an across-geometry comparison only, we explicitly tested the memory of locations that cover the entire arena space. We found that the BPM could reproduce the elongated spread in the return positions close to the boundaries of the arena, and the more uniform spread of responses for item positions towards the middle of the arena.

The BPM was formulated based on electrophysiological recordings that showed a systematic boundary proximity-dependent distortion of place cell firing with changing boundary configuration ([Hartley et al., 2000, 2004](#); [O'Keefe and Burgess, 1996](#)). Similar distortion effects on place fields have been reported for rodent place cells recorded on a linear track when the track's end walls were moved such that its long axis was either stretched or squeezed in length ([Huxter et al., 2003](#)). One report directly investigated firing field characteristics of place cells across an environment with fixed boundaries. It shows that, in rats, place cells' field size increased with increasing distance from the end walls along a linear track ([Odobescu, 2010](#)). This correlation can be well explained by a model that uses firing field size as a measure of location uncertainty, with location uncertainty being a linear function of boundary distance, similar to the BPM ([Madl et al., 2014](#)). These studies provide some evidence that place cells' firing field size in an environment might correlate with the behaviorally relevant spatial representation of that environment, thereby supporting the notion that such spatially tuned neurons serve as a neural correlate of behavior.

4.2 Accuracy and precision of participants' responses

The BPM was designed to explain changes in location memory across two different boundary configurations; it does not make explicit predictions about the precision (i.e., the spatial distribution) nor the accuracy (i.e., the mean) of participants' responses at a particular location if the environment does

not change. Yet when we compared the cued item positions with the corresponding mean response positions, we found a statistically significant difference for all item positions but the one closest to the arena's center. This indicates a systematic offset between cued item position and participants' actual representation of that position which the BPM does not account for.

Visual inspection of the offset's magnitude and direction strongly suggests an influence of wall proximity: the mean response position tends to be located closer to the arena's center than the corresponding cued item position, and the magnitude of this offset seems to correlate with an item position's distance to the walls. This effect, however, is not consistent across all item positions. Particularly for positions 3, 5, and 6, the corresponding mean response positions also move towards the diagonal between the two closest walls, indicating that both distance from boundaries and proximity to the arena's diagonals critically influence the offset between cued item position and mean response position. We suggest that both effects are important geometric determinants of participants' representation of space if only geometric information about the environment is available. The design of our experiment, in particular nine item locations and the rotation we used, did not allow us to systematically assess effects such as the influence of the diagonal or the distance to the two closest walls on a continuous scale.

It was possible to evaluate if the offset of the mean response position affects how well the BPM explains participants' responses. We fitted the BPM again, but this time at the mean response locations instead of the cued item positions. On average, this increased the model's log likelihood, suggesting that accounting for the difference between item positions and corresponding mean response positions, i.e. participants' response accuracy, in fact increases the model's fit. However, closer inspection of the log likelihood values for each item position revealed that only five out of the nine item positions show a better fit, while participants' responses at four item positions are explained slightly worse when fitting the BPM at the mean response positions compared to when the BPM is modeled at the cued item positions. This result indicates that simply adjusting the BPM to account for the accuracy in participants' responses might not be sufficient, at least not for all item positions. We suggest that additional effects not considered in the BPM model also play a role in participants' representation of the VE's space.

The BPM in a static environment implicitly reproduces the elongation of participants' responses parallel to the arena's boundaries that we find in our data. In other words, the closer the item position is to one of the boundaries of the VE the more the distribution of participants' responses tends to stretch towards the second closest wall, as seen in our data and predicted by the BPM model (Fig. 4). Visual inspection of the response density maps suggests, however, that the orientation of participants' responses does not always align with the arena's boundaries. Instead, for item positions farther away from their respective closest walls, particularly positions 6 and 9, the orientation of the corresponding response positions distribution seems to tilt away from the arena's cardinal directions defined by its boundaries. When we analyzed the response distributions in terms of their eigenvectors and calculated the deviation of eigenvectors from the arena's cardinal directions, we found this deviation to correlate with item positions' proximity to the arena's diagonals. This suggests that, in a purely

geometry-bound, rectangular VE like ours, participants' representation of space is not only shaped by boundary proximity, as proposed by the BPM, but also by proximity to diagonals.

When participants are given conflicting local landmark and local boundary information, boundary information is preferred to landmark information in spatial learning (Doeller and Burgess, 2008). The phenomenon of "rotational errors", observed when subjects search for a previously learned position in a wrong yet geometrically equivalent location while ignoring available disambiguating non-geometric cues, further indicates a strong prevalence of geometrical information over landmark configuration in subjects' spatial representation of an environment (for a comprehensive review see Cheng et al., 2013). We therefore speculate that the diagonals proximity effect on participants' representation of space observed in our VE should also be seen in rectangular open-field environments that provide additional landmarks information (such as Hartley et al., 2004; Jacobs et al., 2013; Lee et al., 2018), though maybe to a lesser extent in cases where (distal) landmarks allow for a significantly better distance estimation than local boundaries (see below).

4.3 Viewing angles

The analysis of participants' viewing angle at the moments of collection or return of an item offers additional information about participants' behavior. We found a tendency for participants to directly face the closest wall at item positions close to a wall (positions 3, 4, 7, 8); and to face the corner between the two closest walls at item positions farther away from the arena's walls (positions 5, 6, 9). If we assume that participants estimate their current location primarily based on their distance towards the boundary they are facing, then we would expect to see the variance of response positions to spread primarily along that viewing direction. Since the eigenvectors capture the directions of highest variance, this provides a potential explanation for the observed deviation of eigenvectors direction away from the arena's cardinal directions at item positions farther away from the arena's boundaries. Furthermore, considering that the mean response positions show a tendency to shift away from the two closest walls and towards the arena's center, and that participants predominantly orient towards the closest walls when collecting and dropping an item, this indicates that participants, when estimating their location based on the boundaries they are currently facing, systematically underestimate their distance from these boundaries.

4.4 Limitations

This study was designed to systematically measure accuracy and precision of participants' internal representation of an open-field VE at equidistantly located positions across the whole space within the VE's boundaries in order to assess how models of geometric determinants on spatial memory fit participants' behavior. Beyond that, we provide evidence for a role of the arena's boundaries and diagonals on participants' responses that we did not anticipate when designing this study. Because there was a lack of previous literature on the subject, we decided to design and analyze the data in a more exploratory fashion. The observed inconsistencies of boundary proximity and diagonal proximity

on accuracy and precision of participants' responses across item positions might thus be explained by the limited capability of our study design to systematically investigate these effects. To comprehensively assess these effects, a study tailored to specifically investigate their role on participants' representation of space would be required.

4.5 Conclusion

We found that modeling navigators' internal representation of space as a function of proximity to local boundaries (Barry et al., 2006; Hartley et al., 2000, 2004; Madl et al., 2014) generally matches participants' behavior across a virtual quadratic open-field environment. While such models explain the precision of an environment's spatial representation, our results suggest that additionally accounting for the accuracy in the representation of locations could further improve their explanatory power. Importantly, we propose that participants' representation of space in the typical quadratic open-field environment often used to record activity of spatially tuned neurons (Hafting et al., 2005; Jacobs et al., 2013; Lee et al., 2018; Lever et al., 2009; O'Keefe and Burgess, 1996; Solstad et al., 2008) is not solely shaped by a location's boundary proximity but also by a location's proximity to the diagonals spanned by the environment's boundaries. If these spatially tuned neurons do provide a neural substrate for the internal representation of space, we would expect to see similar effects of local boundaries and the corresponding diagonals also in the firing patterns of these neurons.

Acknowledgements

The authors thank Maurizio Pimentel Pierini for assistance with data collection, and Andreas V. Herz for helpful discussion on the study design. Support and funding for this study were provided by the German Federal Ministry of Education and Research (grants: BMBF IFB 01 EO 0901; BMBF BCCN 01 GQ 0440) and the German Research Foundation (grant: DFG GSC 82-3). The authors declare no competing financial interests.

References

- Banino, A., Barry, C., Uria, B., Blundell, C., Lillicrap, T., Mirowski, P., Pritzel, A., Chadwick, M. J., Degris, T., Modayil, J., and et al. (2018). Vector-based navigation using grid-like representations in artificial agents. *Nature*, 557(7705):429–433.
- Barry, C., Lever, C., Hayman, R., Hartley, T., Burton, S., O'Keefe, J., Jeffery, K., and Burgess, N. (2006). The boundary vector cell model of place cell firing and spatial memory. *Reviews in the Neurosciences*, 17(1-2):71–98.
- Cheng, K., Huttenlocher, J., and Newcombe, N. S. (2013). 25 years of research on the use of geometry in spatial reorientation: a current theoretical perspective. *Psychonomic Bulletin & Review*, 20(6):1033–1054.

- Doeller, C. F., Barry, C., and Burgess, N. (2010). Evidence for grid cells in a human memory network. *Nature*, 463(7281):657–661.
- Doeller, C. F. and Burgess, N. (2008). Distinct error-correcting and incidental learning of location relative to landmarks and boundaries. *Proceedings of the National Academy of Sciences*, 105(15):5909–5914.
- Hafting, T., Fyhn, M., Molden, S., Moser, M.-B., and Moser, E. I. (2005). Microstructure of a spatial map in the entorhinal cortex. *Nature*, 436(7052):801–806.
- Hardcastle, K., Ganguli, S., and Giocomo, L. M. (2015). Environmental boundaries as an error correction mechanism for grid cells. *Neuron*, 86(3):827 – 839.
- Hartley, T., Burgess, N., Lever, C., Cacucci, F., and O’Keefe, J. (2000). Modeling place fields in terms of the cortical inputs to the hippocampus. *Hippocampus*, 10(4):369–379.
- Hartley, T., Trinkler, I., and Burgess, N. (2004). Geometric determinants of human spatial memory. *Cognition*, 94(1):39–75.
- Huxter, J., Burgess, N., and O’Keefe, J. (2003). Independent rate and temporal coding in hippocampal pyramidal cells. *Nature*, 425(6960):828–832.
- Jacobs, J., Weidemann, C. T., Miller, J. F., Solway, A., Burke, J. F., Wei, X.-X., Suthana, N., Sperling, M. R., Sharan, A. D., Fried, I., and et al. (2013). Direct recordings of grid-like neuronal activity in human spatial navigation. *Nature Neuroscience*, 16(9):1188–1190.
- Keinath, A. T., Julian, J. B., Epstein, R. A., and Muzzio, I. A. (2017). Environmental geometry aligns the hippocampal map during spatial reorientation. *Current Biology*, 27(3):309–317.
- Krupic, J., Bauza, M., Burton, S., Barry, C., and O’Keefe, J. (2015). Grid cell symmetry is shaped by environmental geometry. *Nature*, 518(7538):232–235.
- Lee, S. A., Miller, J. F., Watrous, A. J., Sperling, M. R., Sharan, A., Worrell, G. A., Berry, B. M., Aronson, J. P., Davis, K. A., Gross, R. E., Lega, B., Sheth, S., Das, S. R., Stein, J. M., Gorniak, R., Rizzuto, D. S., and Jacobs, J. (2018). Electrophysiological signatures of spatial boundaries in the human subiculum. *The Journal of Neuroscience*, 38(13):3265–3272.
- Lever, C., Burton, S., Jeewajee, A., O’Keefe, J., and Burgess, N. (2009). Boundary vector cells in the subiculum of the hippocampal formation. *Journal of Neuroscience*, 29(31):9771–9777.
- Lever, C., Wills, T., Cacucci, F., Burgess, N., and O’Keefe, J. (2002). Long-term plasticity in hippocampal place-cell representation of environmental geometry. *Nature*, 416(6876):90–94.
- Madl, T., Franklin, S., Chen, K., Montaldi, D., and Trappl, R. (2014). Bayesian integration of information in hippocampal place cells. *PLoS ONE*, 9(3):e89762.
- Odobescu, R. I. (2010). *Exteroceptive and interoceptive cue control of hippocampal place cells*. PhD thesis, UCL (University College London).

- O'Keefe, J. and Burgess, N. (1996). Geometric determinants of the place fields of hippocampal neurons. *Nature*, 381(6581):425–428.
- O'Keefe, J. and Dostrovsky, J. (1971). The hippocampus as a spatial map. preliminary evidence from unit activity in the freely-moving rat. *Brain Res*, 34(1):171–5.
- O'Keefe, J. and Nadel, L. (1978). *The hippocampus as a cognitive map*. Oxford: Clarendon Press.
- Savelli, F., Luck, J., and Knierim, J. J. (2017). Framing of grid cells within and beyond navigation boundaries. *eLife*, 6.
- Solstad, T., Boccara, C. N., Kropff, E., Moser, M.-B., and Moser, E. I. (2008). Representation of geometric borders in the entorhinal cortex. *Science*, 322(5909):1865–1868.
- Stensola, T., Stensola, H., Moser, M.-B., and Moser, E. I. (2015). Shearing-induced asymmetry in entorhinal grid cells. *Nature*, 518(7538):207–212.

Supplement

participant	effect of quadrant	effect of item position	interaction
M01	$F(3, 108) = 0.07, p = 0.975$	$F(8, 108) = 4.70, p = 0.000$	$F(24, 108) = 0.94, p = 0.548$
M02	$F(3, 108) = 0.26, p = 0.853$	$F(8, 108) = 1.52, p = 0.157$	$F(24, 108) = 0.92, p = 0.574$
M03	$F(3, 104) = 0.77, p = 0.513$	$F(8, 104) = 5.79, p = 0.000$	$F(24, 104) = 0.85, p = 0.668$
M04	$F(3, 106) = 0.04, p = 0.990$	$F(8, 106) = 5.28, p = 0.000$	$F(24, 106) = 1.43, p = 0.113$
M05	$F(3, 108) = 0.20, p = 0.899$	$F(8, 108) = 2.43, p = 0.019$	$F(24, 108) = 0.62, p = 0.909$
M06	$F(3, 108) = 0.09, p = 0.968$	$F(8, 108) = 2.65, p = 0.011$	$F(24, 108) = 0.90, p = 0.596$
M07	$F(3, 104) = 3.89, p = 0.011$	$F(8, 104) = 5.91, p = 0.000$	$F(24, 104) = 0.85, p = 0.666$
M08	$F(3, 105) = 0.70, p = 0.552$	$F(8, 105) = 11.61, p = 0.000$	$F(24, 105) = 1.27, p = 0.201$
M10	$F(3, 106) = 0.55, p = 0.646$	$F(8, 106) = 3.54, p = 0.001$	$F(24, 106) = 0.88, p = 0.623$
M12	$F(3, 108) = 0.39, p = 0.762$	$F(8, 108) = 3.92, p = 0.000$	$F(24, 108) = 0.55, p = 0.952$
M13	$F(3, 107) = 2.97, p = 0.035$	$F(8, 107) = 7.78, p = 0.000$	$F(24, 107) = 0.81, p = 0.722$
M15	$F(3, 106) = 1.44, p = 0.236$	$F(8, 106) = 4.54, p = 0.000$	$F(24, 106) = 0.86, p = 0.648$
M16	$F(3, 108) = 0.44, p = 0.724$	$F(8, 108) = 3.89, p = 0.000$	$F(24, 108) = 1.03, p = 0.441$
M17	$F(3, 107) = 1.11, p = 0.348$	$F(8, 107) = 4.97, p = 0.000$	$F(24, 107) = 0.84, p = 0.680$
M18	$F(2, 104) = 0.38, p = 0.682$	$F(7, 104) = 7.33, p = 0.000$	$F(23, 104) = 1.21, p = 0.257$
M19	$F(3, 107) = 1.26, p = 0.290$	$F(8, 107) = 1.91, p = 0.066$	$F(24, 107) = 1.19, p = 0.264$
M20	$F(3, 107) = 1.36, p = 0.259$	$F(8, 107) = 2.57, p = 0.013$	$F(24, 107) = 1.07, p = 0.386$
M21	$F(3, 106) = 0.77, p = 0.513$	$F(8, 106) = 16.95, p = 0.000$	$F(24, 106) = 1.11, p = 0.341$
M22	$F(3, 105) = 0.12, p = 0.949$	$F(8, 105) = 5.64, p = 0.000$	$F(24, 105) = 0.51, p = 0.971$
M24	$F(3, 107) = 1.54, p = 0.209$	$F(8, 107) = 9.84, p = 0.000$	$F(24, 107) = 1.17, p = 0.287$
M25	$F(3, 107) = 1.11, p = 0.349$	$F(8, 107) = 7.07, p = 0.000$	$F(24, 107) = 1.09, p = 0.373$
M26	$F(3, 107) = 1.81, p = 0.150$	$F(8, 107) = 2.41, p = 0.020$	$F(24, 107) = 0.47, p = 0.983$
M27	$F(3, 107) = 0.77, p = 0.511$	$F(8, 107) = 2.56, p = 0.013$	$F(24, 107) = 1.20, p = 0.258$
M28	$F(3, 104) = 1.12, p = 0.343$	$F(8, 104) = 5.33, p = 0.000$	$F(24, 104) = 0.88, p = 0.631$
M29	$F(3, 107) = 1.24, p = 0.299$	$F(8, 107) = 5.35, p = 0.000$	$F(24, 107) = 0.50, p = 0.973$

Table 3: Effects of item position and quadrant on observed distance errors. Main effect for item position quadrant (four levels: NE, NW, SW, SE; 2nd column) item position (nine levels, one for each of the 3x3 item positions; 3rd column), and interaction between both (4th column) as estimated by a two-way repeated measures ANOVA are listed for each participant.

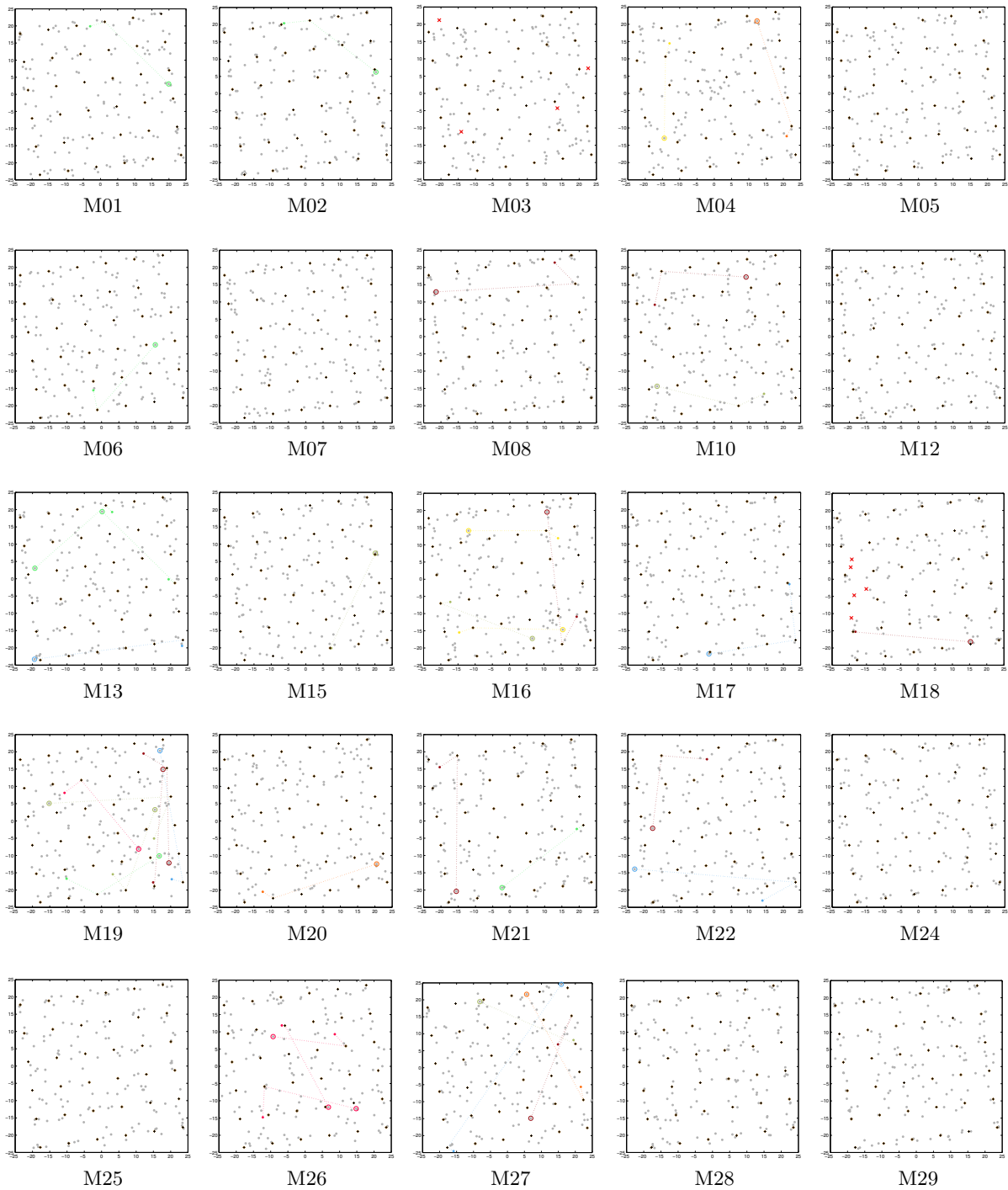


Figure 8: Overview of adjusted drop positions. Panels show indicated participants' drop positions (grey dots). Adapted drop positions are circled and graphically connected by a dotted line with their corresponding item position (black +); the adjusted position after optimal rotation is also connected with the item position by a dotted line and indicated by a colored dot.

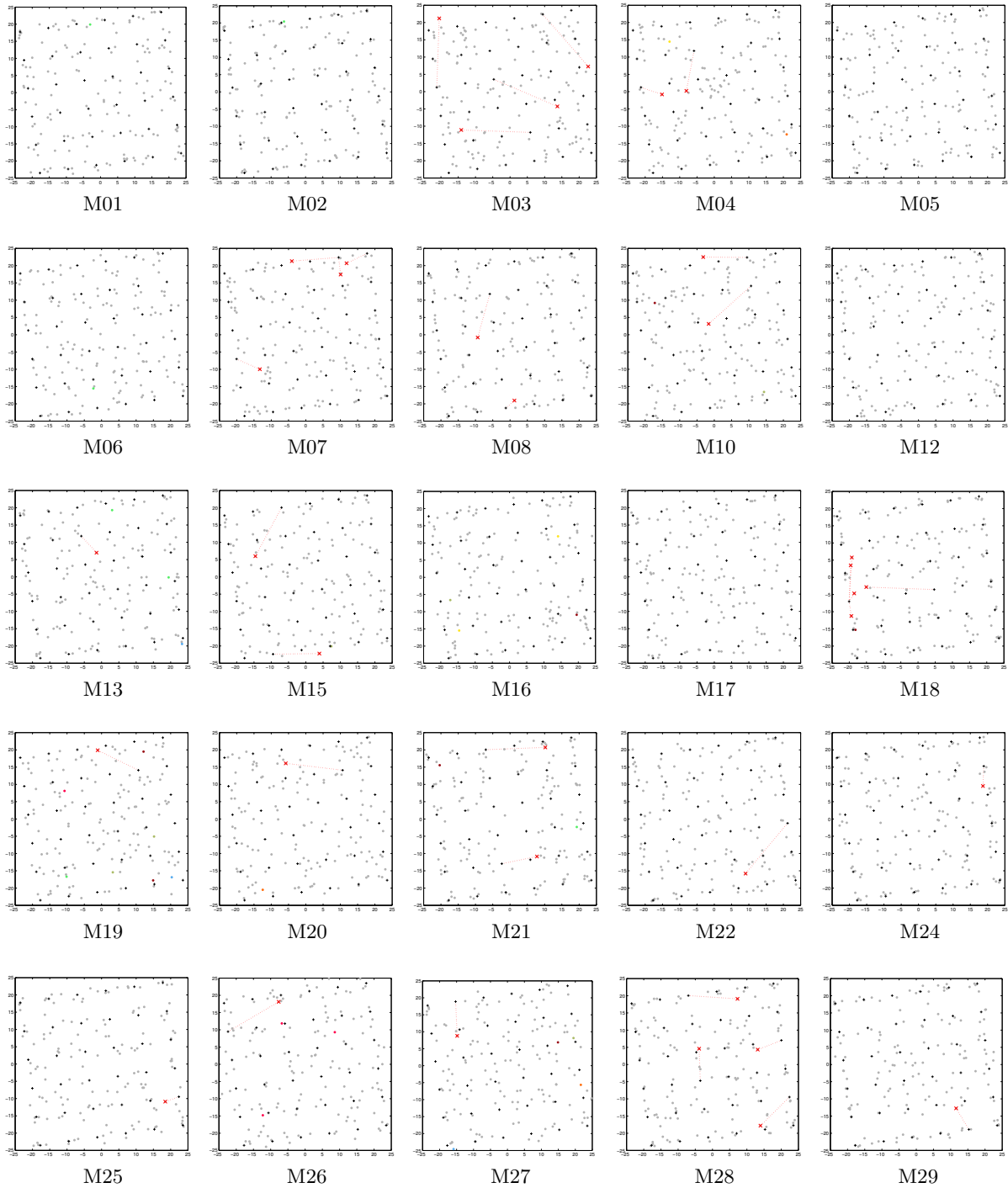


Figure 9: Overview of drop positions considered to be outliers. Panels show indicated participants' drop positions (grey dots) and adjusted drop positions (colored dots). Drop positions considered outliers are crossed out (red crosses) and connected with their corresponding item position (black +) by a dotted red line. (Note that adjusted drop positions that are still considered outliers are not displayed.)

General Discussion

The aim of the studies presented in this thesis was to extend our understanding of how neural processes and behavior relate to each other in the service of human navigation. To achieve this, we adopted the classic open-field setup used to record place-encoding neurons in rodents and translate them into visually sparse virtual environments that human participants can travel using a joystick. This type of setup distinguishes these studies from most other human navigation studies in three decisive ways. First, participants have full control over both their movement speed and direction in an open, obstacle-free space, thus minimizing the restrictions imposed on their navigation behavior by the environment or the control of movement. Second, the virtual environments used here provide only a minimum of landmark cues to limit the cognitive and mnemonic demands introduced by surface textures and salient landmarks. This is particularly important to effectively control the impact of spatial memory on participants' behavior and brain activity. Finally, keeping the experimental paradigm close to rodent setups helps translate findings across species.

Within this framework, the first study tested which regions in the human brain respond to changes in navigational and spatial memory demands during a foraging-like exploration task. It was found that variation in the navigational demands correlates with activity in the brain's central attention hubs and regions of the scene-selective cortex, while participants' anterior hippocampal region was activated depending on their overall task success and spatial memory usage (Chpt. 2). The second study deployed a location recognition task to measure accuracy and precision of participants' spatial representation of this open-field setup, and explored environmental factors that potentially shape the internal representation of space. Participants' location memory was well explained by proximity of a location to the environment's boundaries (walls). The results also suggest that other geometric determinants exert additional influence on participants' behavior and location memory in a quadratic open-field environment (Chpt. 3).

In the final chapter of this thesis I will discuss the implications of the key findings reported in Chpts. 2 and 3 on the 'bigger picture': what can we learn about the scene-elective regions in the human cortex and their role during active navigation (Chpt. 4.1); how does the human hippocampus support navigation and how is this related to its mnemonic functions (Chpt. 4.2); and, finally, how do we represent space in an open-field environment and how does this fit to firing properties of place-encoding neurons believed to underlie our cognitive map of the environment (Chpt. 4.3)?

4.1 Human scene-selective regions contribute to active navigation

In the first study, we found activity in the occipital place area (OPA), the medial place area (MPA), the parahippocampal place area (PPA), all scene-selective regions. As their name suggests, activation in these brain regions is commonly found when participants are presented with visual stimuli of scenes,¹ or navigationally relevant aspects of scenes such as landmarks (for a recent review, see [Epstein and Baker, 2019](#)).

The vast majority of studies that investigated scene-selective regions focused on the different low-level (e.g. contrast, texture, line orientation) and high-level (e.g. scene category, familiarity, viewpoint angles) visual properties of stimuli suitable to activate these regions ([Groen et al., 2017](#)) in tasks where test stimuli are presented to participants as static images on a screen. Few studies have investigated scene-selective regions during navigation-like scenarios ([Kamps et al., 2016](#)) or an actual navigation task ([Julian et al., 2016](#)). My work, in the first study, shows that scene-selective regions are involved in active navigation. When compared to passive movement, the two active navigation conditions activated both the OPA and MPA and long active passive navigation additionally activated the PPA region.

The role of scene-selective regions is difficult to understand in the broader context of human spatial cognition for several reasons. Scene-selective regions are thought to process all kinds of navigationally relevant visual aspects of scenes, sometimes with contradicting findings (e.g. [Dilks et al., 2011](#); [Persichetti and Dilks, 2016](#)). Frequently more than one scene-sensitive region is active during a single task, making it difficult to differentiate between their specific functionalities. Despite attempts to sketch some coarse divisions of labor between scene-selective regions (e.g. [Epstein et al., 2017](#); [Marchette et al., 2017](#)), no clear pattern of their relative contributions to spatial cognition and human navigation has emerged ([Lescroart et al., 2015](#); [Mitchell et al., 2018](#)).

An additional level of complexity comes from the fact that the three scene-selective regions are not anatomically distinct brain structures. Instead they are functionally defined areas from overlapping anatomically adjacent brain regions. Functionally defining anatomically overlapping regions is an error-prone process that can falsely assign, or fail to assign, activation to these regions. Most studies that wish to focus on one or more scene-selective regions use a functional localizer based on the experiment that established the human PPA ([Epstein and Kanwisher, 1998](#)) to circumvent this problem. However, no functional localizer has been able to distinguish between the scene-selective regions. The localizers that have been used do not reliably detect scene-selective regions

¹Adopting the definition by [Henderson and Hollingworth \(1999\)](#), a *scene*, in this context, is defined as a “view of a real-world environment comprising background elements and multiple discrete objects arranged in a spatially licensed manner. Background elements are taken to be larger-scale, immovable surfaces and structures, such as ground, walls, floors, and mountains, whereas objects are smaller-scale discrete entities that are manipulable (e.g. can be moved) within the scene.” ([Henderson and Hollingworth, 1999](#), p. 244)

in all participants (e.g. [Park et al., 2011](#); [Persichetti and Dilks, 2016](#)). Visual comparison to the previously published literature is still commonly used to define these regions (e.g. [Silson et al., 2015, 2016](#)). As a result, a high degree of variability in both the reported size and location of scene-selective regions remains across studies.

The retrosplenial cortex is a prime example of these issues. The human retrosplenial cortex proper is an anatomically defined region comprising of Brodmann Areas 29 and 30 ([Mitchell et al., 2018](#); [Morris et al., 2000](#)). However, neuroimaging studies reporting activation in this region frequently found peak activation to lie significantly more posterior, sometimes not even covering the retrosplenial cortex proper. To differentiate the functional from the anatomical region, the term ‘retrosplenial complex’ was introduced, however it is typically abbreviated ‘RSC’ as is the retrosplenial cortex. The term ‘medial place area’ (MPA) was alternatively proposed for this region ([Silson et al., 2016](#)), since scene-sensitive activity (or its corresponding peak activation) is consistently reported in the medial parietal cortex, largely outside the retrosplenial cortex proper (e.g. [Marchette et al., 2014, 2015](#); [Nasr et al., 2011](#); [Silson et al., 2016](#); [Sulpizio et al., 2016](#); [Watson et al., 2017](#))

Functional heterogeneity within scene-selective regions may also contribute to the difficulty in segregating these regions. This heterogeneity is thought to be caused by functional subfields or gradients, reminiscent of the functional organization in the hippocampus ([Poppenk et al., 2013](#); [Strange et al., 2014](#)). Evidence for differentiation has already been shown in the PPA ([Aminoff and Tarr, 2015](#); [Baldassano et al., 2013, 2016](#); [Baumann and Mattingley, 2016](#); [Nasr et al., 2013, 2014](#)), and RSC/MPA ([Silson et al., 2016](#)).

Based on meta-analyses and a functional connectivity analysis, [Baldassano et al. \(2016\)](#) proposed a framework that proposes how the different visual and navigation-related processes can be ascribed to scene-selective brain regions. They divide scene-sensitive regions into two networks, a posterior ‘visual network’ and an anterior ‘memory and navigation network’ ([Baldassano et al., 2016](#)). The posterior network comprises the OPA, posterior PPA, and other visual areas such as the early visual cortex (EVC) and the lateral occipital cortex (LOC). These regions all have retinotopic maps and process different visual features. The anterior network is composed of the RSC, anterior PPA, and the caudal inferior parietal lobule (cIPL). These regions show strong functional connections with the hippocampus, and are recruited by a broad set of tasks that relate to navigation and memory. Hence, while the posterior network is involved in low-level visual processing, the anterior network processes higher-level contextual and navigational scene information ([Baldassano et al., 2016](#)).

The results of our first study are in line with this framework, particularly with regard to the proposed anterior network. The long active condition – which reveals brain regions involved in active navigation and long-term spatial memory during our foraging task – resulted in activity in the right OPA, right aPPA, right cIPL, and in the RSC/MPA, all regions of the anterior network. Though this is not direct proof for the functionality of

the anterior scene-processing network, it provides further evidence in support of this framework.

This framework still proposes a subdivision of scene-selective regions into individual functional units. An alternative notion was recently outlined in the context of egocentric (i.e., body-centered) and allocentric (i.e., world-centered) representations of space (Ekstrom et al., 2014, 2017). The authors argue rather that navigation behaviour is an inherently network-based phenomenon precluding the simple attribution of specific function to individual brain regions. Evidence for this comes from lesion studies and neuroimaging. Lesions to individual brain areas do not usually impair a single aspect of behavioral function, resulting instead in subtle impairments in navigation. The brain regions involved in navigation are active across a wide variety of navigation tasks instead of for individual behaviors. The authors' proposal would take 'the onus off of unique brain regions with highly specialized neural machinery as central to navigation' and 'reconceive of this function in a more distributed fashion based on highly connected and interacting "hubs" of brain areas.' (Ekstrom et al., 2017, p. 3334f).² These areas then become more or less active, depending on the particular demands of the task at hand.

The results of our first study support this theory. With increasing navigational task demand – from passive transportation to active navigation to active navigation with long-term memory requirements – we observed a corresponding increase in the hemodynamic response in scene-selective regions. These regions thus appear to activate in parallel, and in a task-dependent manner, lending general support to the notion of navigation being a 'fundamentally network-based phenomenon' (Ekstrom et al., 2017, p. 3334). More specifically, they suggest that the three scene-selective regions OPA, RSC/MPA, and PPA are in fact three such network hubs.

In conclusion, while most experiments investigating human scene-selective regions focus on the presentation of static images of scenes on a screen, our study is amongst the few that provide insight into the processing taking place in these regions during an actual navigation task. Our results generally support the notion of a causal role for human scene-selective regions in active navigation that goes beyond the commonly accepted concept of feature processing of visual scenes in these regions (Persichetti and Dilks, 2016). They are in line with a recent proposal (Baldassano et al., 2016) suggesting that scene-selective regions are part of two complementary information processing networks. Our results enhance the range of functions ascribed to these regions in the literature. Finally, following the concept of navigation relying on the demand-based parallel interaction of highly interconnected network hubs (Ekstrom et al., 2014, 2017), our results suggest that human scene-selective regions OPA, RSC/MPA, and PPA show such hub-like behavior during active navigation. A more thorough hypothesis-driven confirmation would be necessary to test these ideas for the scene-selective cortex, but it

²It should be mentioned that Ekstrom et al. (2017) do not argue against the idea of specialization between brain regions whereby particular brain areas host specific neural processes. They rather suggest more parallel and redundant processing to take place in these brain regions than recognized in previous models (Ekstrom et al., 2017).

seems promising to investigate these brain regions in more real-world-like navigation tasks in the future.

4.2 The human hippocampus' role in spatial memory

A second key finding reported in our first study tackles the role of the human hippocampus during navigation, a question that has been heavily investigated and is still hotly debated (Eichenbaum, 2017; Lisman et al., 2017). The hippocampus has turned out to be a particularly versatile brain region. It has been attributed to a wide range of seemingly diverse cognitive functions, including virtually all forms of long-term and short-term memory (Ranganath, 2018), spatial navigation (O'Keefe and Nadel, 1978), visual recognition (Lee et al., 2012), mind-wandering (Karapanagiotidis et al., 2017; McCormick et al., 2018), and decision making (Shohamy and Wimmer, 2011). Many theories and concepts have been proposed that explain the hippocampus' role in this variety of different functions. So far, however, no unifying model exists that incorporates all of the hippocampus' proposed functions.

Treating 'the hippocampus' as a single entity may not be appropriate to sufficiently model the range of cognitive functions attributed to the hippocampus. The hippocampus' complex anatomical architecture comprises several cellular layers and multiple different processing circuits, all of which are connected to different cortical structures and receive different neuronal input. It therefore seems likely that distinct hippocampal components are engaged, depending on the particular demands of the task at hand (Dalton et al., 2018). Recent years has brought increased recognition of the anatomical and cellular differentiation within the hippocampus (Poppenk et al., 2013; Strange et al., 2014), and hippocampal functions are ascribed to specific subunits (e.g. Brunec et al., 2018; Collin et al., 2015; Zeidman and Maguire, 2016).

One such model targets the role of the medial banks of the anterior human hippocampus (amHipp) in human navigation (Zeidman and Maguire, 2016). Several studies suggest the amHipp forms a distinct functional subregion within the human hippocampus (Blessing et al., 2016; Robinson et al., 2015; Zeidman et al., 2015). Based on a review of neuroimaging, anatomical, and neuropsychological literature, this region may be essential whenever a mental representation of an environment is required (Zeidman and Maguire, 2016). Their conceptualization of this mental representation is as follows: 'We can vividly re-experience past events, simulate future events and imagine fictitious scenarios, in addition to experiencing the environment we currently inhabit. To achieve this, we must be able to construct internal representations of environments on the basis of incoming sensory information and/or prior experience.' (Zeidman and Maguire, 2016, p. 175). They argue that this process accounts for the hippocampus' contribution to many of the cognitive functions associated with the hippocampus such as visual perception, imagination and episodic recall. All of these processes require that a model of the world is creates

and this model is then actively used for planning and memory. The authors predict that ‘amHipp should be engaged when a spatially coherent representation of a scene needs to be constructed or used for simulating events.’³ (Zeidman and Maguire, 2016, p. 180)

We found a significant positive correlation between BOLD activity in the amHipp and the proportion of the environment that participants were traversed, measured by the once-to-total viewed area (OVA) ratio. We argue that the OVA ratio is a measure of how well participants were able to construct a coherent spatial representation of the virtual arena space, because in our paradigm participants cannot increase their score by revisiting previously viewed sites. The OVA ratio hence assesses participants’ ability to track and circumvent already visited areas in the environment. This ability requires participants to have a coherent internal representation of already visited locations. The positive correlation of participants’ OVA ratio and their BOLD response in the amHipp region therefore supports the notion that this hippocampal subregion constructs a coherent internal representation of space (Zeidman and Maguire, 2016).

The OVA ratio can also be considered a measure of participants’ object location memory, or spatial memory in broader terms. During our active navigation task this spatial memory must be built and utilized to efficiently search for hidden items in the arena. We argue that participants who are better at this task achieve a higher OVA ratio. Considering that the OVA ratio positively correlates with the BOLD response measured in the amHipp across participants, and that the amHipp is suggest to link ‘elements of scenes in a coherent spatial representation’ (Zeidman and Maguire, 2016, p. 177), our results provide an example of how the human hippocampus may link memory processes with navigational computations for effective navigation.

In conclusion, our results support the model of the anterior medial Hippocampus as a distinct functional region that supports the modeling of spatial scenes (Zeidman and Maguire, 2016). More generally, they help to further elucidate the functional role of the anterior human hippocampus and, thus, to bridge the gap between hippocampal function and corresponding anatomical architecture. High-resolution functional MRI, facilitated by the increasing availability of 7T MRI scanners, has the potential to further break down which regions combine to what Zeidman and Maguire (2016) termed the ‘anterior medial hippocampus’. It will also help to more precisely attribute cognitive functions to anatomical structures in the human Hippocampus. First promising attempts in this direction have already been made (Dalton et al., 2018).

4.3 Spatial memory in an open-field environment

In our second study we shifted the focus from different brain regions and how they contribute to spatial perception and navigational processes towards the nature of our cognitive representation of space.

³The authors define ‘scenes’ as ‘coherent object-containing spaces within which we can potentially operate’ (Zeidman and Maguire, 2016, p. 180), and explicitly include navigation into the set of cognitive functions that rely on the use of scene processing provided by the amHipp.

As discussed above, the results of our first study suggest a positive correlation of the coherence of participants' internal representation of visited locations in the virtual arena with the BOLD response in the anterior medial Hippocampus. There we quantified spatial coherence as the ratio of once to total viewed area across the entire viewable area at the end of a test condition. With this approach we were able to approximate the 'general' coherence of a participant's spatial representation of the virtual arena across the duration of a particular test condition. The method used to assess the OVA ratio averages across the entire area and neglects differences that might occur at different locations within the arena. The result cannot tell us whether or not there are any significant local changes in the accuracy of participants' internal representation of the arena's space. In fact, in the post-experimental interviews most participants reported that they had trouble keeping track of visited locations particularly at the arena's center and when farthest away from the cue card. This suggests that local differences exist within participants' internal representation of the arena's space that cannot be captured with the OVA ratio.⁴

With our second study, we confirmed this notion by quantifying participants' precision and accuracy of remembered locations across the entire area of an open-field environment. Our results indicate a tendency for participants' response precision to decrease towards the arena center, or, in other words, a 'boundary proximity effect' on participants' response density as has been described previously (Hartley et al., 2004). In their study, participants' responses across rectangular open-field environments of different wall lengths are best explained by a model that is based on the observation that rodent place cells' response properties can be well described as a function of their corresponding place fields' boundary proximity (Burgess and O'Keefe, 1996; Hartley et al., 2000; O'Keefe and Burgess, 1996). That study only tested participants' spatial memory at a limited number of locations across varying boundary configurations. In contrast we measured participants' responses at 36 locations (regularly arranged across all four quadrants so that they could be collated to a set of nine locations that all differ in their distances to their two closest walls) within one fixed boundary configuration. This way we were able to demonstrate the general validity of a boundary proximity effect on participants' spatial memory of locations across the entire space of a rectangular open-field environment. The larger number of tested locations, and the responses collected from participants at each of these locations, allowed us, furthermore, to characterize accuracy and precision of participants' responses in more detail. In particular, our results suggest that effects of an environment's boundary configuration on participants' spatial representation might exist that current models do not account for so far.

To our knowledge ours is the first study to systematically and comprehensively assess systematic changes in spatial accuracy across an open-field environment. This is surprising because spatially tuned neurons are typically investigated in open field environments, both in rodents and humans (Doeller et al., 2010; Hafting et al., 2005; Jacobs et al., 2013;

⁴This is not a design flaw: in our first study we were interested in a single value that quantifies the coherence of participants' spatial representation in general terms so that it could then be used as an additional covariate for the group level model.

Lee et al., 2018; Lever et al., 2009; O'Keefe and Burgess, 1996; Solstad et al., 2008). In order to investigate how the firing properties of these neurons relate to the cognitive representation of an environment, it is important to have, in addition to the neural firing rates recorded in this environment, the corresponding internal representation of this environment as measured through behavior.

There is strong evidence suggesting that, in an open-field environment, the geometrical configuration of its boundaries significantly influences the firing properties of spatially tuned neurons in the rodent brain. For example, in square enclosures, the grid pattern expressed by grid cells is systematically rotated and distorted by the environment's geometric features (Stensola et al., 2015). Furthermore, highly polarized environments such as trapezoids that are characterized by non-parallel walls introduce significant asymmetry in grid cells' firing patterns (Krupic et al., 2015). Several studies have also shown that changes in the environment's boundary configuration significantly and persistently affect the firing behavior of rodent place and grid cells (Barry et al., 2007; Hardcastle et al., 2015; Huxter et al., 2003; Krupic et al., 2018; Lever et al., 2002; O'Keefe and Burgess, 1996). Testing whether and how these effects on the neural level are reflected on a cognitive level seems challenging. To do so, one would ideally combine a behavioral task that assesses a navigator's spatial representation in sufficient detail with simultaneous recordings of its place-encoding neurons. To our knowledge this has not been done in rodents so far, and the time and effort required to conduct an experiment similar to our second study in rodents seem considerable. Humans, on the other hand, can relatively easily perform such behavioral tasks, yet electrophysiological recordings in humans are rarely possible and limited to hospitalized patients (Jacobs and Kahana, 2010).

We intended to combine our task with parallel electrophysiological recordings in the human medial temporal lobe region of patients diagnosed with nontractable epilepsy. Unfortunately, we were not able to collect sufficient data from these recordings. We therefore lack the corresponding electrophysiological data that might have allowed us to directly compare patients' neuronal firing properties with their internal spatial representation of our open-field environment. I will therefore, instead, compare our findings with the few already published firing rate maps of neurons that exhibited significant place- or grid cell-like activity in humans (Ekstrom et al., 2003; Jacobs et al., 2013; Miller et al., 2013; Nadasdy et al., 2017).

Two studies so far have published firing rate maps (FRM) of human neurons that show grid cell-like activity while patients navigated an open-field environment: Jacobs et al. (2013) show nearly 20 FRMs of different grid-like cells; Nadasdy et al. (2017) present FRMs of 20 to 30 cells with spatially periodic activity that potentially qualify as grid cells.⁵ Upon visual inspection, most of the depicted FRMs show less regularity in place fields and less well-defined place fields than typically seen in FRMs of rodent grid cells. This may in

⁵The FRMs reported to show grid cell-like firing patterns in Nadasdy et al. (2017) do not always indicate the corresponding gridness score (a measure of spatial periodicity used to characterize the 'hexagonality' of a grid cell's firing pattern; see, e.g., Sargolini et al., 2006), therefore the exact number of potential grid cells cannot be determined.

part be explained by the low number of spikes (compared to the rodent literature) used to calculate the FRM: a higher number of spikes per FRM should allow to determine the location of the firing rate peaks and the shape of the firing fields more precisely. Visual comparison of FRMs with our results is furthermore complicated by the uneven coverage of the test environment by patients' tracks (Jacobs et al., 2013), sometimes leaving substantial amount of the area uncovered (Nadasdy et al., 2017).

Data from human place cells is also scarce and does not provide the information necessary to compare the firing properties of these cells to the participants' location memory that we measured. In the first report of place-encoding neurons in humans, the authors show exactly one FRM of a purely place-responsive cell (that is, a neuron that exclusively shows place selectivity, as compared to view- or goal-responsive neurons that are also reported in this study; Ekstrom et al., 2003). The virtual environment used during their navigation task was not an open field but a simplified virtual town with a wealth of landmark information such as shop fronts. Both their arena's spatial layout and the landmark information introduces an additional level of complexity to the environment, and it is therefore no longer possible to relate the firing patterns just to the geometry of the environment. This is also the case for a second paper that investigated place-responsive cells in humans, that too uses a landmark-rich town-like virtual environment (Miller et al., 2013). Finally, firing rates for human place cells were also reported in the paper that reported the existence of grid-like cells in humans (Jacobs et al., 2013). In the supporting material, the FRMs of four neurons, which the authors consider to be place cells, are shown. While the environment was similar to ours, the published plots do not show the patient's track and spike locations and therefore do also not provide enough information to compare with our results.

A meaningful comparison of the distribution of participants' location memory reported in our second study with firing properties of place or grid-like cells in humans solely based on visual inspection of the FRMs published so far is not possible. However, this does not rule out the possibility that the neural recordings collected in these studies, were they accessible, might already be detailed enough to allow for an informative comparison with our results. An open-field environment with quadratic boundary configuration provided (as, e.g., in Jacobs et al., 2013), the spatial distribution of spikes comprising a particular place field field could then be compared with the distribution of participants' response collected at similar, in terms of boundary proximity relative to arena size, item positions in our setup.

Evidence that boundary proximity has an effect on place-encoding neurons' field sizes that is similar to its effect on participants' location memory observed in our second study is provided by an investigation of hippocampal place cells in rats (Madl et al., 2014; Odobescu, 2010). On a linear track, place field size of rat place cells increases with increasing distance from the track's end walls (Odobescu, 2010). This correlation is well explained when modeling place field size as a function of location uncertainty, with location uncertainty being driven by boundary distance (Madl et al., 2014). Taken

together, these results are in line with the notion that place-encoding neurons provide a neural correlate of navigation behavior.

In conclusion, we quantified accuracy and precision of human participants' location memory across an entire open-field environment for the first time. This is a first step to bridge the gap between the firing properties of place-encoding neurons such as place and grid cells and the corresponding internal representation of space. We showed that the boundary proximity model that was derived from rodent place cell firing behavior in an open-field environment (Hartley et al., 2004; O'Keefe and Burgess, 1996) is generally suitable to describe human participants' location memory in an open-field environment, although a location's proximity to the diagonals spanned by the environment's boundaries also seems relevant. The wealth of behavioral data that we collected allows for a detailed comparison of our cognitive representation of space with the neuronal activity recorded in such an environment. Unfortunately neuronal recordings from humans currently still lack the detailed information about location that would be necessary for comparison. If these neuronal recordings were to be made openly available, it might already be possible to provide valuable insights about the behavioral relevance of these neurons, when combined with the results of our second study. As our paradigm requires participants to travel relatively close to all walls and corners and cover a large proportion of the environment, performing our experiment in epilepsy patients with implanted depth electrodes would allow for the most direct comparison of place-encoding neurons' firing behavior with the corresponding cognitive spatial representation so far.

4.4 Concluding remarks

Much of what is currently known about the neuronal processes that are thought to enable navigation, derives from rodent navigation studies. The cognitive processes associated with navigation, on the other hand, are predominantly investigated in human studies. To understand how these processes on the cognitive and the neural level are causally connected requires knowledge of how findings from rodent and human studies transfer across species. The studies presented within this thesis help to bridge this gap with two experiments that combine two different location recognition tasks with free, joystick-controlled navigation in open-field virtual environments that closely resemble the common experimental environments and conditions used to investigate spatially tuned neurons in rodents.

In the first study we unraveled the impact of different cognitive tasks on brain activity during navigation tasks. In the context of the ongoing discussion about contribution of the hippocampus to human navigation – a discussion that reflects the gap between findings from rodent and human studies – the paradigm from the first study can be used to investigate the influence of navigationally relevant spatial memory on hippocampal activity. This paradigm is ideally combined with imaging techniques that allow for higher spatial and temporal resolution, to further investigate regions that support navigation in

the absence of salient landmarks. Candidate regions could, for instance, include those comprising the scene-selective cortex, where determining the overlap in activity during actual navigation and viewing of static sceneries that typically trigger those regions might provide a starting point for better understanding the (sub-) regions of the scene-selective cortex involved in different aspects of spatial information processing.

The second study demonstrated that this framework can furthermore be used to investigate the effect of environmental features, such as its boundaries, on the human perception of space in the absence of distinct landmarks. Our results suggest that the relationship between participants' memory of locations within the virtual arena, and the arena's boundaries, is more complex than a linear combination of proximity to the arena's four walls. Eliminating non-geometric landmarks from the environment may thus help reveal navigational cues and their impact on human navigation that otherwise might be too subtle to detect, or 'overshadowed' by the effect of salient landmarks on our perception of space. This is particularly relevant with view on spatially tuned neurons found in rodents, whose firing properties are influenced by the configuration of walls and boundaries in open-field setups. Using this framework to quantify and compare the impact of geometric determinants on both the cellular firing properties and the internal representation of space may help to gain a better understanding of how neural activity eventually causes navigation behavior.

Finally, this framework may be a useful tool to investigate different kinds of navigation behavior and, when combined with neuroimaging or single-cell recordings, to directly relate it to brain activity. In both studies presented here, participants were given full control over their movement speed and direction through the virtual environment, and the recorded positional data from both experiments showed recognizable differences in navigation behavior across participants. Further investigating this data could help to better understand what drives human navigation behavior in the absence of distinct landmarks. In the second study, for instance, it may be promising to further analyze whether (and when) participants apply dead reckoning or a view-matching strategy, or a combination of both, to navigate to a previously learned target location, and how this affects task success. Relating different navigation behavior to neural activity could then provide new insights into the relationship between the two, as demonstrated by the correlation of the once viewed area ratio with participants' hippocampal activity shown in our first study.

Taken together, the two studies presented in this thesis helped to better understand the brain regions involved in human navigation and their potential contribution to it, and the influence of environmental geometry on human navigation behavior. This was achieved with a framework that allows detailed analyses of human navigation behavior and to disentangle the cognitive components associated with it, and that facilitates the comparison of findings between rodents and humans. Combined with suitable recording methods, this framework may provide new and substantial insights into the causal relationship between neural activity and human navigation behavior.

4.5 References

- Aminoff, E. M. and Tarr, M. J. (2015). Associative processing is inherent in scene perception. *PLoS ONE*, 10(6):e0128840.
- Baldassano, C., Beck, D., and Fei-Fei, L. (2013). Differential connectivity within the parahippocampal place area. *NeuroImage*, 75:228–237.
- Baldassano, C., Esteva, A., Fei-Fei, L., and Beck, D. M. (2016). Two distinct scene-processing networks connecting vision and memory. *eNeuro*, 3(5).
- Barry, C., Hayman, R., Burgess, N., and Jeffery, K. J. (2007). Experience-dependent rescaling of entorhinal grids. *Nat Neurosci*, 10(6):682–4.
- Baumann, O. and Mattingley, J. B. (2016). Functional organization of the parahippocampal cortex: Dissociable roles for context representations and the perception of visual scenes. *The Journal of Neuroscience*, 36(8):2536–2542.
- Blessing, E. M., Beissner, F., Schumann, A., Br nner, E., and B r, K.-J. (2016). A data-driven approach to mapping cortical and subcortical intrinsic functional connectivity along the longitudinal hippocampal axis. *Human Brain Mapping*, 37(2):462–476.
- Brunec, I. K., Bellana, B., Ozubko, J. D., Man, V., Robin, J., Liu, Z.-X., Grady, C., Rosenbaum, R. S., Winocur, G., Barense, M. D., and Moscovitch, M. (2018). Multiple scales of representation along the hippocampal anteroposterior axis in humans. *Current Biology*, 28(13):2129 – 2135.e6.
- Burgess, N. and O’Keefe, J. (1996). Neuronal computations underlying the firing of place cells and their role in navigation. *Hippocampus*, 6(6):749–762.
- Collin, S. H. P., Milivojevic, B., and Doeller, C. F. (2015). Memory hierarchies map onto the hippocampal long axis in humans. *Nature Neuroscience*, 18(11):1562–1564.
- Dalton, M. A., Zeidman, P., McCormick, C., and Maguire, E. A. (2018). Differentiable processing of objects, associations, and scenes within the hippocampus. *The Journal of Neuroscience*, 38(38):8146–8159.
- Dilks, D. D., Julian, J. B., Kubiľius, J., Spelke, E. S., and Kanwisher, N. (2011). Mirror-image sensitivity and invariance in object and scene processing pathways. *Journal of Neuroscience*, 31(31):11305–11312.
- Doeller, C. F., Barry, C., and Burgess, N. (2010). Evidence for grid cells in a human memory network. *Nature*, 463(7281):657–661.
- Eichenbaum, H. (2017). The role of the hippocampus in navigation is memory. *J Neurophysiol*, 117(4):1785–1796.
- Ekstrom, A. D., Arnold, A. E. G. F., and Iaria, G. (2014). A critical review of the allocentric spatial representation and its neural underpinnings: toward a network-based perspective. *Frontiers in Human Neuroscience*, 8.

- Ekstrom, A. D., Huffman, D. J., and Starrett, M. (2017). Interacting networks of brain regions underlie human spatial navigation: a review and novel synthesis of the literature. *J Neurophysiol*, 118(6):3328–3344.
- Ekstrom, A. D., Kahana, M. J., Caplan, J. B., Fields, T. A., Isham, E. A., Newman, E. L., and Fried, I. (2003). Cellular networks underlying human spatial navigation. *Nature*, 425(6954):184–188.
- Epstein, R. and Kanwisher, N. (1998). A cortical representation of the local visual environment. *Nature*, 392(6676):598–601.
- Epstein, R. A. and Baker, C. I. (2019). Scene perception in the human brain. *Annual Review of Vision Science*, 5(1):373–397.
- Epstein, R. A., Patai, E. Z., Julian, J. B., and Spiers, H. J. (2017). The cognitive map in humans: spatial navigation and beyond. *Nature Neuroscience*, 20(11):1504–1513.
- Groen, I. I. A., Silson, E. H., and Baker, C. I. (2017). Contributions of low- and high-level properties to neural processing of visual scenes in the human brain. *Philosophical Transactions of the Royal Society B: Biological Sciences*, 372(1714):20160102.
- Hafting, T., Fyhn, M., Molden, S., Moser, M.-B., and Moser, E. I. (2005). Microstructure of a spatial map in the entorhinal cortex. *Nature*, 436(7052):801–806.
- Hardcastle, K., Ganguli, S., and Giocomo, L. M. (2015). Environmental boundaries as an error correction mechanism for grid cells. *Neuron*, 86(3):827 – 839.
- Hartley, T., Burgess, N., Lever, C., Cacucci, E., and O’Keefe, J. (2000). Modeling place fields in terms of the cortical inputs to the hippocampus. *Hippocampus*, 10(4):369–379.
- Hartley, T., Trinkler, I., and Burgess, N. (2004). Geometric determinants of human spatial memory. *Cognition*, 94(1):39–75.
- Henderson, J. M. and Hollingworth, A. (1999). High-level scene perception. *Annual Review of Psychology*, 50(1):243–271.
- Huxter, J., Burgess, N., and O’Keefe, J. (2003). Independent rate and temporal coding in hippocampal pyramidal cells. *Nature*, 425(6960):828–832.
- Jacobs, J. and Kahana, M. J. (2010). Direct brain recordings fuel advances in cognitive electrophysiology. *Trends in Cognitive Sciences*, 14(4):162–171.
- Jacobs, J., Weidemann, C. T., Miller, J. E., Solway, A., Burke, J. F., Wei, X.-X., Suthana, N., Sperling, M. R., Sharan, A. D., Fried, I., and et al. (2013). Direct recordings of grid-like neuronal activity in human spatial navigation. *Nature Neuroscience*, 16(9):1188–1190.
- Julian, J. B., Ryan, J., Hamilton, R. H., and Epstein, R. A. (2016). The occipital place area is causally involved in representing environmental boundaries during navigation. *Current Biology*, 26(8):1104 – 1109.
- Kamps, F. S., Lall, V., and Dilks, D. D. (2016). The occipital place area represents first-person perspective motion information through scenes. *Cortex*, 83:17 – 26.

- Karapanagiotidis, T., Bernhardt, B. C., Jefferies, E., and Smallwood, J. (2017). Tracking thoughts: Exploring the neural architecture of mental time travel during mind-wandering. *NeuroImage*, 147:272–281.
- Krupic, J., Bauza, M., Burton, S., Barry, C., and O’Keefe, J. (2015). Grid cell symmetry is shaped by environmental geometry. *Nature*, 518(7538):232–235.
- Krupic, J., Bauza, M., Burton, S., and O’Keefe, J. (2018). Local transformations of the hippocampal cognitive map. *Science*, 359(6380):1143–1146.
- Lee, A. C. H., Yeung, L.-K., and Barense, M. D. (2012). The hippocampus and visual perception. *Frontiers in Human Neuroscience*, 6.
- Lee, S. A., Miller, J. F., Watrous, A. J., Sperling, M. R., Sharan, A., Worrell, G. A., Berry, B. M., Aronson, J. P., Davis, K. A., Gross, R. E., and et al. (2018). Electrophysiological signatures of spatial boundaries in the human subiculum. *The Journal of Neuroscience*, 38(13):3265–3272.
- Lescroart, M. D., Stansbury, D. E., and Gallant, J. L. (2015). Fourier power, subjective distance, and object categories all provide plausible models of bold responses in scene-selective visual areas. *Frontiers in Computational Neuroscience*, 9.
- Lever, C., Burton, S., Jeewajee, A., O’Keefe, J., and Burgess, N. (2009). Boundary vector cells in the subiculum of the hippocampal formation. *Journal of Neuroscience*, 29(31):9771–9777.
- Lever, C., Wills, T., Cacucci, F., Burgess, N., and O’Keefe, J. (2002). Long-term plasticity in hippocampal place-cell representation of environmental geometry. *Nature*, 416(6876):90–94.
- Lisman, J., Buzsáki, G., Eichenbaum, H., Nadel, L., Ranganath, C., and Redish, A. D. (2017). Viewpoints: how the hippocampus contributes to memory, navigation and cognition. *Nature Neuroscience*, 20(11):1434–1447.
- Madl, T., Franklin, S., Chen, K., Montaldi, D., and Trapp, R. (2014). Bayesian integration of information in hippocampal place cells. *PLoS ONE*, 9(3):e89762.
- Marchette, S. A., Ryan, J., and Epstein, R. A. (2017). Schematic representations of local environmental space guide goal-directed navigation. *Cognition*, 158:68–80.
- Marchette, S. A., Vass, L. K., Ryan, J., and Epstein, R. A. (2014). Anchoring the neural compass: coding of local spatial reference frames in human medial parietal lobe. *Nature Neuroscience*, 17(11):1598–1606.
- Marchette, S. A., Vass, L. K., Ryan, J., and Epstein, R. A. (2015). Outside looking in: Landmark generalization in the human navigational system. *Journal of Neuroscience*, 35(44):14896–14908.
- McCormick, C., Rosenthal, C. R., Miller, T. D., and Maguire, E. A. (2018). Mind-wandering in people with hippocampal damage. *The Journal of Neuroscience*, 38(11):2745–2754.

- Miller, J. F., Neufang, M., Solway, A., Brandt, A., Trippel, M., Mader, I., Hefft, S., Merkow, M., Polyn, S. M., Jacobs, J., and et al. (2013). Neural activity in human hippocampal formation reveals the spatial context of retrieved memories. *Science*, 342(6162):1111–1114.
- Mitchell, A. S., Czajkowski, R., Zhang, N., Jeffery, K., and Nelson, A. J. D. (2018). Retrosplenial cortex and its role in spatial cognition. *Brain and Neuroscience Advances*, 2:239821281875709.
- Morris, R., Paxinos, G., and Petrides, M. (2000). Architectonic analysis of the human retrosplenial cortex. *The Journal of Comparative Neurology*, 421(1):14–28.
- Nadasdy, Z., Nguyen, T. P., Török, Á., Shen, J. Y., Briggs, D. E., Modur, P. N., and Buchanan, R. J. (2017). Context-dependent spatially periodic activity in the human entorhinal cortex. *Proceedings of the National Academy of Sciences*, 114(17):E3516–E3525.
- Nasr, S., Devaney, K. J., and Tootell, R. B. (2013). Spatial encoding and underlying circuitry in scene-selective cortex. *NeuroImage*, 83:892 – 900.
- Nasr, S., Echavarria, C. E., and Tootell, R. B. H. (2014). Thinking outside the box: Rectilinear shapes selectively activate scene-selective cortex. *Journal of Neuroscience*, 34(20):6721–6735.
- Nasr, S., Liu, N., Devaney, K. J., Yue, X., Rajimehr, R., Ungerleider, L. G., and Tootell, R. B. H. (2011). Scene-selective cortical regions in human and nonhuman primates. *Journal of Neuroscience*, 31(39):13771–13785.
- Odobescu, R. I. (2010). *Exteroceptive and interoceptive cue control of hippocampal place cells*. PhD thesis, UCL (University College London).
- O’Keefe, J. and Burgess, N. (1996). Geometric determinants of the place fields of hippocampal neurons. *Nature*, 381(6581):425–428.
- O’Keefe, J. and Nadel, L. (1978). *The hippocampus as a cognitive map*.
- Park, S., Brady, T. F., Greene, M. R., and Oliva, A. (2011). Disentangling scene content from spatial boundary: Complementary roles for the parahippocampal place area and lateral occipital complex in representing real-world scenes. *Journal of Neuroscience*, 31(4):1333–1340.
- Persichetti, A. S. and Dilks, D. D. (2016). Perceived egocentric distance sensitivity and invariance across scene-selective cortex. *Cortex*, 77:155 – 163.
- Poppenk, J., Evensmoen, H. R., Moscovitch, M., and Nadel, L. (2013). Long-axis specialization of the human hippocampus. *Trends in Cognitive Sciences*, 17(5):230 – 240.
- Ranganath, C. (2018). Time, memory, and the legacy of howard eichenbaum. *Hippocampus*, 29(3):146–161.
- Robinson, J. L., Barron, D. S., Kirby, L. A. J., Bottenhorn, K. L., Hill, A. C., Murphy, J. E., Katz, J. S., Salibi, N., Eickhoff, S. B., and Fox, P. T. (2015). Neurofunctional topography of the human hippocampus. *Human Brain Mapping*, 36(12):5018–5037.

- Sargolini, F., Fyhn, M., Hafting, T., McNaughton, B. L., Witter, M. P., Moser, M.-B., and Moser, E. I. (2006). Conjunctive representation of position, direction, and velocity in entorhinal cortex. *Science*, 312(5774):758–762.
- Shohamy, D. and Wimmer, G. E. (2011). The striatum and beyond: Contributions of the hippocampus to decision making. *Decision Making, Affect, and Learning: Attention and Performance XXIII*, 23:281.
- Silson, E. H., Chan, A. W.-Y., Reynolds, R. C., Kravitz, D. J., and Baker, C. I. (2015). A retinotopic basis for the division of high-level scene processing between lateral and ventral human occipitotemporal cortex. *Journal of Neuroscience*, 35(34):11921–11935.
- Silson, E. H., Steel, A. D., and Baker, C. I. (2016). Scene-selectivity and retinotopy in medial parietal cortex. *Frontiers in Human Neuroscience*, 10.
- Solstad, T., Boccara, C. N., Kropff, E., Moser, M.-B., and Moser, E. I. (2008). Representation of geometric borders in the entorhinal cortex. *Science*, 322(5909):1865–1868.
- Stensola, T., Stensola, H., Moser, M.-B., and Moser, E. I. (2015). Shearing-induced asymmetry in entorhinal grid cells. *Nature*, 518(7538):207–212.
- Strange, B. A., Witter, M. P., Lein, E. S., and Moser, E. I. (2014). Functional organization of the hippocampal longitudinal axis. *Nature Reviews Neuroscience*, 15(10):655–669.
- Sulpizio, V., Boccia, M., Guariglia, C., and Galati, G. (2016). Functional connectivity between posterior hippocampus and retrosplenial complex predicts individual differences in navigational ability. *Hippocampus*, 26(7):841–847.
- Watson, D. M., Hartley, T., and Andrews, T. J. (2017). Patterns of response to scrambled scenes reveal the importance of visual properties in the organization of scene-selective cortex. *Cortex*, 92:162 – 174.
- Zeidman, P., Lutti, A., and Maguire, E. A. (2015). Investigating the functions of subregions within anterior hippocampus. *Cortex*, 73:240 – 256.
- Zeidman, P. and Maguire, E. A. (2016). Anterior hippocampus: the anatomy of perception, imagination and episodic memory. *Nature Reviews Neuroscience*, 17(3):173.

List of publications

C. Roppelt, S. Glasauer, V. L. Flanagin: "The Impact of Varying Navigational and Spatial Memory Demands on Human Brain Activity during Spatial Exploration", *in preparation*

C. Roppelt, V. L. Flanagin: "Human Spatial Accuracy in an Open-Field Virtual Environment", *in preparation*

Selected conference contributions

C. Roppelt, V. L. Flanagin (2016) "Human Spatial Accuracy in an Open Field Virtual Environment", *1st Interdisciplinary Navigation Symposium*, Bad Gastein, Austria

C. Roppelt, S. Glasauer, V. L. Flanagin (2015) "Human Behavior and Brain Activity in Spatial Exploration", *25th Ocular Motor Meeting*, Munich, Germany

C. Roppelt, S. Glasauer, V. L. Flanagin (2014) "Behavioural Strategies and Brain Activity in Human Spatial Exploration", *9th FENS Forum of Neuroscience*, Milan, Italy

A. Ries, A. Nayerova, C. Roppelt, A. Gatz, A. Loebel, K. Thurley, V. L. Flanagin (2014) "A general substrate of magnitude estimation: cerebral contributions for distance and time", *Bernstein Conference 2014*, Göttingen, Germany

C. Roppelt, S. Glasauer, V. L. Flanagin (2013) "Human behavior during spatial exploration", *Society for Neuroscience Conference*, San Diego, CA, USA

V. L. Flanagin, C. Roppelt, S. Glasauer (2013) "Neurons with place-field like properties describe exploratory behavior", *Society for Neuroscience Conference*, San Diego, CA, USA

C. Roppelt, S. Glasauer, V. L. Flanagin (2013) "Human exploration in virtual environments", *Bernstein Center for Computational Neuroscience Workshop on Spatial Cognition*, Seon, Germany

Curriculum Vitae

Christopher Franz Kurt Roppelt

born in Ingolstadt, Germany

Research Experience

04/2011 – 12/2016

German Center for Vertigo and Balance Disorders, München
Graduate Researcher

09/2010 – 01/2011

University Hospital Ludwig-Maximilians-Universität, München
Student Research Assistant in Clinical Neurology

10/2007 – 12/2008

Dept. of Informatics, Albert-Ludwigs-Universität Freiburg
Student Research Assistant in Bioinformatics

08/2007 – 09/2007

Dept. of Bioinformatics, Albert-Ludwigs-Universität Freiburg
Research Internship

Education

10/2011 – present

Graduate School for Systemic Neurosciences
Ludwig-Maximilians-Universität München
PhD Candidate

10/2006 – 01/2011

Albert-Ludwigs-Universität Freiburg
Diploma in Biology

10/2004 – 08/2006

Friedrich-Alexander-Universität Erlangen-Nürnberg
Intermediate Degree in Biology (“Vordiplom”)

06/2003

Leibniz-Gymnasium Altdorf b. Nürnberg
General qualification for university entrance (“Allgemeine Hochschulreife”)

Eidesstattliche Versicherung/ Affidavit

Hiermit versichere ich an Eides statt, dass ich die vorliegende Dissertation *Maps and Memories of Space in the Human Brain* selbstständig angefertigt habe, mich außer der angegebenen keiner weiteren Hilfsmittel bedient und alle Erkenntnisse, die aus dem Schrifttum ganz oder annähernd übernommen sind, als solche kenntlich gemacht und nach ihrer Herkunft unter Bezeichnung der Fundstelle einzeln nachgewiesen habe.

München, den 25th of October 2019

Christopher Roppelt

I hereby confirm that the dissertation *Maps and Memories of Space in the Human Brain* is the result of my own work and that I have only used sources or materials listed and specified in the dissertation.

Munich, 25th of October 2019

Christopher Roppelt

Declaration of author contributions

“The Impact of Varying Navigational and Spatial Memory Demands on Human Brain Activity during Spatial Exploration” (in prep.)

C. Roppelt, S. Glasauer, V. L. Flanagin

Authors' contributions: CR, SG, and VLF designed the study; CR and VLF conducted the pilot studies; CR and SG programmed the task and virtual environment; CR and VLF conducted the data collection; CR and VLF designed and programmed the MRI data analysis; CR designed and programmed the behavioural data analysis; CR and VLF interpreted the data; CR wrote the manuscript and designed the figures; VLF critically revised the manuscript; VLF supervised the project.

“Human Spatial Accuracy in an Open-Field Virtual Environment” (in prep.)

C. Roppelt, V. L. Flanagin

Authors' contributions: CR and VLF conceived and designed the study; CR programmed the task and virtual environment; CR supervised the data collection; CR designed and programmed the analyses; VLF contributed to modeling of the data; CR and VLF interpreted the data; CR wrote the paper manuscript and designed the figures; VLF critically revised the paper manuscript; VLF supervised the project.

Munich, 25th of October 2019

Christopher Roppelt

Dr. Virginia L. Flanagin

